HYDROLYSIS OF REFINED PALM OIL TO FATTY ACIDS USING $ZnAl_2O_4$ CATALYST

KAMONWAN SITANON

A THESIS SUBMITTED IN PARTIAL FULFILLMENT

OF THE REQUIRMENTS FOR THE DEGREE OF

MASTER OF SCIENCE IN PETROCHEMICALS AND HYDROCARBON CHEMISTRY

FACULTY OF SCIENCE

KING MONGKUT'S INSTITUTE OF TECHNOLOGY LADKRABANG

2012

KMITL-2012-SC-M-015-003

หัวข้อวิทยานิพนธ์	**ปฏิกิริยาไฮโดรลิซิสน้ำมันปาล์มสกัดเป็นกรดไขมันโดยใช้ตัวเร่งปฏิกิริยาซิงค์อะลูมิเนต**
นักศึกษา	**นางสาวกมลวรรณ สิตานนท์**
รหัสประจำตัว	50068003
ปริญญา	**วิทยาศาสตรมหาบัณฑิต**
สาขาวิชา	**ปิโตรเคมีและเคมีของไฮโดรคาร์บอน**
พ.ศ.	2555
อาจารย์ที่ปรึกษาวิทยานิพนธ์	ผศ.ดร. วันฉัตร ชื่นชม

บทคัดย่อ

วัตถุประสงค์ของงานวิจัยนี้ คือ การสังเคราะห์ผลิตภัณฑ์กรดไขมันโดยปฏิกิริยาไฮโดรลิซิสของน้ำมันปาล์มสกัดกับน้ำ ด้วยตัวเร่งปฏิกิริยาของแข็งออกไซด์ คือ อะลูมินา และซิงค์อะลูมิเนต ในเครื่องปฏิกรณ์แบบกะ นอกจากนี้ยังได้มีการศึกษาถึงอุณหภูมิที่ใช้ในการเผาตัวเร่งปฏิกิริยาในอากาศและปัจจัยต่างๆ ที่มีผลต่อเปอร์เซนต์การเปลี่ยนแปลงของสารตั้งต้น รวมถึงเปอร์เซนต์ผลผลิตที่ได้ พบว่าอุณหภูมิที่เหมาะสมในการเผาตัวเร่งปฏิกิริยาในอากาศของอะลูมินาคือ 500 องศาเซลเซียส เป็นเวลา 5 ชั่วโมง และของซิงค์อะลูมิเนตคือ 600 องศาเซลเซียส เป็นเวลา 5 ชั่วโมง และยังพบว่าเมื่ออุณหภูมิในการทำปฏิกิริยา เวลาในการทำปฏิกิริยา อัตราส่วนโดยโมลของน้ำต่อน้ำมัน และปริมาณของตัวเร่งปฏิกิริยาเพิ่มขึ้นจะทำให้เปอร์เซนต์การเปลี่ยนแปลงของสารตั้งต้นและเปอร์เซนต์ผลผลิตที่ได้เพิ่มขึ้นตามไปด้วย โดยสภาวะที่เหมาะสมในงานวิจัยนี้คือ อัตราส่วนโดยโมลของน้ำต่อน้ำมันปาล์มเท่ากับ 54:1 ที่อุณหภูมิ 240 องศาเซลเซียส เป็นเวลา 60 นาที โดยใช้ 3.0 เปอร์เซนต์โดยน้ำหนักของซิงค์อะลูมิเนตเป็นตัวเร่งปฏิกิริยา ซึ่งเปอร์เซนต์การเปลี่ยนแปลงของสารตั้งต้นได้เท่ากับ 100.0 % และเปอร์เซนต์ผลผลิตที่ได้เท่ากับ 100.0 % และยังพบอีกว่าตัวเร่งปฏิกิริยาชนิดซิงค์อะลูมิเนตให้เปอร์เซนต์ผลผลิตที่มากกว่าตัวเร่งปฏิกิริยาชนิดอะลูมินา เนื่องจากมีพื้นที่ผิวที่สูงกว่า นอกจากนั้นแล้วตัวเร่งปฏิกิริยาชนิดอะลูมินาเป็นตัวเร่งปฏิกิริยาที่มีลักษณะชอบน้ำ ซึ่งไม่เหมาะสมกับปฏิกิริยานี้ เพราะน้ำจะถูกดูดซับบนพื้นผิวของตัวเร่งปฏิกิริยา และไปยับยั้งการทำปฏิกิริยากับไตรกลีเซอไรด์ ดังนั้นซิงค์อะลูมิเนตจึงเป็นตัวเร่งปฏิกิริยาที่เหมาะสมมากกว่าในการทำปฏิกิริยาไฮโดรลิซิสของน้ำมันปาล์มสกัดกับน้ำ โดยเมื่อมีการนำเอาซิงค์อะลูมิเนตกลับมาใช้อีกครั้งที่สภาวะเดิมพบว่าเปอร์เซนต์การเปลี่ยนแปลงของสารตั้งต้นและเปอร์เซนต์ผลผลิตที่ได้หลังจากผ่านการใช้งาน 5 ครั้งใกล้เคียงกับตัวเร่งปฏิกิริยาที่ยังไม่ผ่านการใช้งาน

Thesis Title	Hydrolysis of Refined Palm Oil to Fatty Acids Using $ZnAl_2O_4$ Catalyst
Student	Ms. Kamonwan Sitanon
Student ID.	50068003
Degree	Master of Science
Program	Petrochemicals and Hydrocarbon Chemistry
Year	2012
Thesis Advisor	Asst. Prof. Dr. Vanchat Chuenchom

ABSTRACT

The aim of this research was to synthesise fatty acids via hydrolysis reaction of refined palm oil with water in a batch reactor using solid oxide catalysts, namely alumina and zinc aluminate. Effect of the calcination temperature of catalysts and variables that affect the percent conversion and yield were studied. It was found that an appropriate calcination temperature in air for 5 hours was at 500 °C for alumina, and at 600 °C for zinc aluminate. The percent yield of fatty acids was increased when reaction temperature, reaction time, molar ratio of water to oil, and the amount of catalyst were raised. The optimum condition in this research was 54:1 molar ratio of water to oil at 240 °C for 60 minutes using 3.0 wt.% of zinc aluminate as catalyst. Percent conversion of triglycerides for this condition was 100.0 % and percent yield of fatty acids was 100.0 %. Zinc aluminate was shown to be more effective than alumina due to the reason that zinc aluminate has higher surface area. In addition, alumina is hydrophilic catalyst. It was not appropriate for this reaction because the water was easily absorbed to the surface, blocking the access of the triglycerides. Therefore, zinc aluminate was more suitable than alumina as catalyst for hydrolysis reaction of refined palm oil with water. Furthermore, the used zinc aluminate was reused, and it was found that it exhibited slightly change in percent conversion and yield after the fifth use compared to the fresh catalyst.

ACKNOWLEDGEMENT

For the thesis completion, the author would like to express her profound gratitude to my advisor, Asst. Prof. Dr. Vanchat Chuenchom for helpful suggestion and encouragement throughout this research. She is also grateful to Assoc. Prof. Dr. Tawan Sooknoi, Asst. Prof. Dr. Patchanee Charoenying and Asst. Prof. Dr. Apanee Luengnaruemitchai for serving as the chairman of committee and the committees, and their valuable comments.

The author would like to extend her sincere appreciation to Asst. Prof. Dr. Patchanee Charoenying for their helpful of the testing product using Nuclear Magnetic Resonance spectrometer.

Sincere thanks to the department of Chemistry, Faculty of Science, King Mongkut's Institute of Technology Ladkrabang for equipment, chemicals and facilitates.

Unforgettable, the author would like to thank all teachers, her friend and her research group for their constant guidance advice, support and encouragement.

Finally, the author would like to thanks his parents and her family for their constant supports and encouragements.

Kamonwan Sitanon

CONTANTS

CONTENTS (Continued)

CONTENTS (Continued)

LIST OF TABLES

LIST OF TABLES (Continued)

Table **page**

LIST OF FIGURES

LIST OF FIGURES (Continued)

LIST OF FIGURES (Continued)

LIST OF FIGURES (Continued)

Figure **page**

CHAPTER 1

INTRODUCTION

1.1 Motivation

Hydrolysis reactions are important in the processing of fats and oils by the chemical industry. Fatty acids which are produced from these reactions are major components used in the preparation of a wide variety of products, such as soaps, cosmetics, pharmaceuticals, surfactants, lubricants, plasticizers, paints, foods and agriculture. These industries can now be considered environmental friendly due to the development of green processes driven by the need to prevent pollution, to be publicly acceptable and to eliminate hazardous by-products. Processes that utilize biomass (such as vegetable oils, animal fats and spent yeast) for energy resources are also considered to be green and have associated economic and social advantages. [1-3].

Triglycerides (main component of vegetable oils and fats) can be hydrolyzed with water/steam to produce 3 mol of free fatty acids and 1 mol of glycerol by the following consecutive reactions:

$$\text{Triglyceride} + H_2O \rightleftharpoons \text{Diglyceride} + \text{Fatty acid} \quad \text{(I)}$$

$$\text{Triglyceride} + H_2O \rightleftharpoons \text{Diglyceride} + \text{Fatty acid} \quad \text{(II)}$$

$$\text{Triglyceride} + H_2O \rightleftharpoons \text{Diglyceride} + \text{Fatty acid} \quad \text{(III)}$$

The Colgate-Emery method has been used for the industrial hydrolysis of triglyceride. This method requires high temperature (250-330 °C) and high pressure (50-60 bar), and has the disadvantages of high energy consumption as well as thermally damaging the products [15].

A conventional method for oil hydrolysis usually uses an enzyme catalyzed process. The advantages of the enzyme hydrolysis technique are that the reaction can be performed under a mild temperature and a simple operational process. Lipases have been successfully employed as biocatalysts in solvent media [16]. But the drawbacks are that the using solvents are expensive, flammable, toxic and involves higher investment costs to meet safety requirements and this process is of doubtful importance because of its high cost and long reaction time. There are still

major problems to be solved in the further development of this process before it becomes commercially viable.

Heterogeneous catalysts are more beneficial than homogenous catalysts because of chemical reaction advantages and easy catalyst separation from the product. Solid catalysts are the important classes of catalysts widely investigated in different fields of application and need to be very stable as well as active in order to compete with the homogeneous processes. Standards are very strict on fuels quality and particularly the amount of impurities (especially metal impurities) has to be very low. A literature survey shows that it is hard to obtain fuels totally free of impurities coming from both homogeneous and heterogeneous catalysts. Studies of heterogeneous catalyst stability, when performed, generally shows that leaching of active species occurs in the effluent which is not acceptable for an industrial process [46-48].

However, Veronique Pugnet developed a novel process for the production of biodiesel from vegetable oil using zinc aluminate catalyst. The experimental conditions of the reaction have been extensively studied. The leaching of active species has been thoroughly studied with zinc oxides and zinc aluminates at 200 °C in a stainless steel (SS) reactor. Zinc aluminate has been proven to be stable and active in the transesterification reaction of oil by methanol in a batch process [5].

Zinc aluminate can be used for the acetylation reaction that occur at lewis acid sites on the surface of the catalyst [30] and it has a hydrophobic behavior in this important organic reactions such as transesterification, esterification. Hydrophobic surfaces are preferable for conducting organic reactions in water, because water covers the surface of solid acids and prevents the adsorption of organic material [45].

There are not many reports in the journal or patent literature where solid catalyst has been used successfully for the hydrolysis of oils and fats to fatty acids. Kanokwan Ngaosuwan reported the mechanistic pathways in hydrolysis and transesterification at a relatively high temperature (100–130 °C) and moderate pressures (120–180 psi) with tricaprylin and water for hydrolysis or methanol for transesterification using a tungstated zirconia catalyst in a batch reactor. It was found that upon increasing the concentration of TCp, the reaction rates for both hydrolysis and transesterification increased at all conditions [38].

In this research, the hydrolysis of palm oil with water using solid oxide catalysts, namely alpha alumina and zinc aluminate, was carried out. As the fact that Thailand is an agricultural

country, palm oil can be found in high quantity, therefore, it will be used as a starting material for hydrolysis into fatty acids in this work. Another starting material for hydrolysis is water. The effect type of catalysts, amount of catalyst, reaction time, reaction temperature, molar of water to oil ratio and reuse of catalyst on hydrolysis reaction were also investigated.

1.2 Objectives

The specific objectives of the study are as follows:

1.2.1 To investigate the preparation of fatty acids from refined palm oil and water by hydrolysis reaction using solid oxides, namely alpha alumina and zinc aluminate as catalysts.

1.2.2 To study the effect of reaction parameters; namely the type of catalysts, calcinations temperature, amount of catalyst, the water to oil ratio, reaction temperature, reaction time, and reuse of catalyst on hydrolysis reaction.

1.3 Scope of study

1.3.1 Literature survey, the design and preparation of the experimental procedure.

1.3.2 Preparation of fatty acids from palm oil by hydrolysis reaction with water, both with and without the use of solid oxides as catalysts. The appropriate conditions are determined by varying the following parameters.

1.3.2.1) Effect of the calcination temperature; 400, 500, 600, 700 °C

1.3.2.2) Effect of the amount of catalysts; 0, 1, 2, 3, 4, 5 wt.%

1.3.2.3) Effect of the water to oil ratio; 13:1, 48:1, 54:1, 81:1 and 108:1

1.3.2.4) Effect of the type of catalyst; alpha alumina (α-Al_2O_3) and zinc aluminate ($ZnAl_2O_4$)

1.3.2.5) Effect of the reaction temperature; 220, 230, 240 °C

1.3.2.6) Effect of the reaction time; 30, 60, 90, 120 and 150 minutes. (The reaction time will be started to count after the temperature of the reaction mixture is raised to the set-point)

1.3.2.7) Effect of reuse of catalyst

1.3.3 Characterization of catalyst using X-ray diffractometer, Gas Adsorption Analyzer, Atomic Absorption Spectrophotometer, Scanning Electron Microscopy.

1.3.4 Comparison of the percent yield obtained between the reaction using fresh catalysts and used catalysts.

1.3.5 Characterization of fatty acid product using Nuclear Magnetic Resonance spectroscopy and High Performance Liquid Chromatography.

1.4 Expected result

This research would provide a process for high yield fatty acids production from the hydrolysis of palm oil which could be developed into an industrial scale process.

CHAPTER 2

THEORY AND LITERATURE REVIEWS

2.1 Palm oil

2.1.1 Introduction

The sources of oils and fats are various vegetable and animal raw materials (e.g., tallow, lard) with the vegetable raw materials soybean, palm, rapeseed and sunflower oil being the most important ones regarding the amounts involved. Triglycerides are the main constituents of vegetable oils and animal fats. The chemical formula is

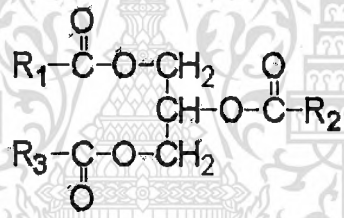

Hydrolysis vegetable oil is an important industrial operation. The products, fatty acids and glycerol are basic raw materials for a wide range of applications. The fatty acids are used as a feed stock for the production of oleochemicals such as fatty alcohols, fatty amines and fatty esters. These oleochemicals are used as lubricant grease, anti-block agent, plastisizers, and emulsifiers. Depending upon climate and soil conditions, different nations are looking into different vegetable oils, for example, soybean oil in the United States, rapeseed and sunflower oils in Europe, palm oil in Thailand, Indonesia and Malaysia [1-3].

2.1.2 Composition and physical properties

The oil palm (*Elaies gunenesis*) produces two distinct oils-palm oil from the fleshy endosperm and palm kernel oil from the kernels. Palm oil is orange-red color contributed by a high carotene content; 0.03 to 0.15 %, of which 90 % consists of alpha- and betacarotene. Palm oil has saturated and unsaturated fatty acids which palmitic and oleic acids are the main

components. The fatty acids distribution of the oil is given in Table 2.1 the oil melts over a range of temperatures from 25 °C to 50 °C. The physical properties of palm oil are shown in Tables 2.2, respectively.

Table 2.1 Fatty acids distribution of palm oil

Name	Structure	% w/w	Formula	Molecular weight
Lauric	C12:0	0.2	$CH_3(CH_2)_{10}COOH$	200.31
Myristic	C14:0	1.1	$CH_3(CH_2)_{12}COOH$	228.36
Plamitic	C16:0	44.0	$CH_3(CH_2)_{14}COOH$	256.42
Stearic	C18:0	4.5	$CH_3(CH_2)_{16}COOH$	284.47
Oleic	C18:1	39.2	$C_{17}H_{33}COOH$	282.44
Linoleic	C18:2	10.1	$C_{17}H_{31}COOH$	280.43
Others		0.9		

Table 2.2 Physical properties of palm oil

Characteristic	Palm oil for food	Palm oil for industry
Relative density @ 40/25 °C	0.900 - 0.907	0.900 - 0.907
Refractive index @ n_D 40 °C	1.45 - 1.46	1.45 - 1.46
Iodine value, Wijs	45 - 60	45 - 60
Saponification value (mg KOH/g oil)	190 - 209	190 - 209
Acid value (max mg KOH/g oil)	0.6	10
Water and volatile matter @ 105 °C (max %wt)	0.2	0.5

2.1.3 The reaction of fats and oils [17-19]

2.1.3.1 Oxidation

In this process, the unsaturated fatty acids are subjected to oxidation. The more double bonds there are, the greater the opportunity for addition of oxygen to double bonds, increasing the

risk that the fat or oil will become rancid. Oxidation is complex and is promoted by heat, light, certain metals (iron and copper), and enzymes known as lipoxygenases. The reaction can be separated into three stages: initiation, propagation, and termination.

The initiation stage of the reaction involves formation of a free radical. The hydrogen on a carbon atom adjacent to one carrying a double bond is displaced to give a free radical, as shown in Figure 2.1

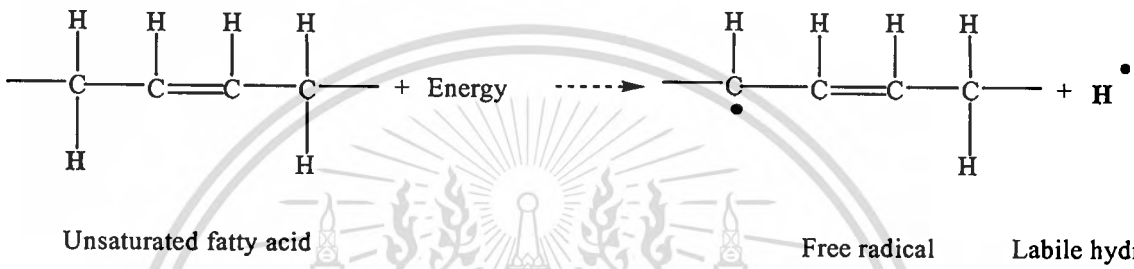

Figure 2.1 The initiation stage of autoxidation.

There is chemical activity around and in the double bonds. (The bold type indicates the atoms or groups of atoms involved in the reactions.) As previously mentioned, this reaction is catalyzed by heat, light, certain metals such as copper and iron, and lipoxygenases. The free radicals that form are unstable and very reactive.

The propagation stage follows the initiation stage and involves oxidation of the free radical to yield activated peroxide. This in turn displaces hydrogen from another unsaturated fatty acid, forming another free radical. The liberated hydrogen unites with the peroxide to form a hydroperoxide and the free radical can be oxidized as just described. Thus, the reaction repeats, or propagates, itself. Formation of one free radical, therefore, leads to the oxidation of many unsaturated fatty acids.

Hydroperoxides are very unstable and decompose into compounds with shorter carbon chains, such as volatile fatty acids, aldehydes, and ketones. These are responsible for the characteristic odor of rancid fats and oils. The two reactions of the propagation stage of autoxidation are shown in Figure 2.2

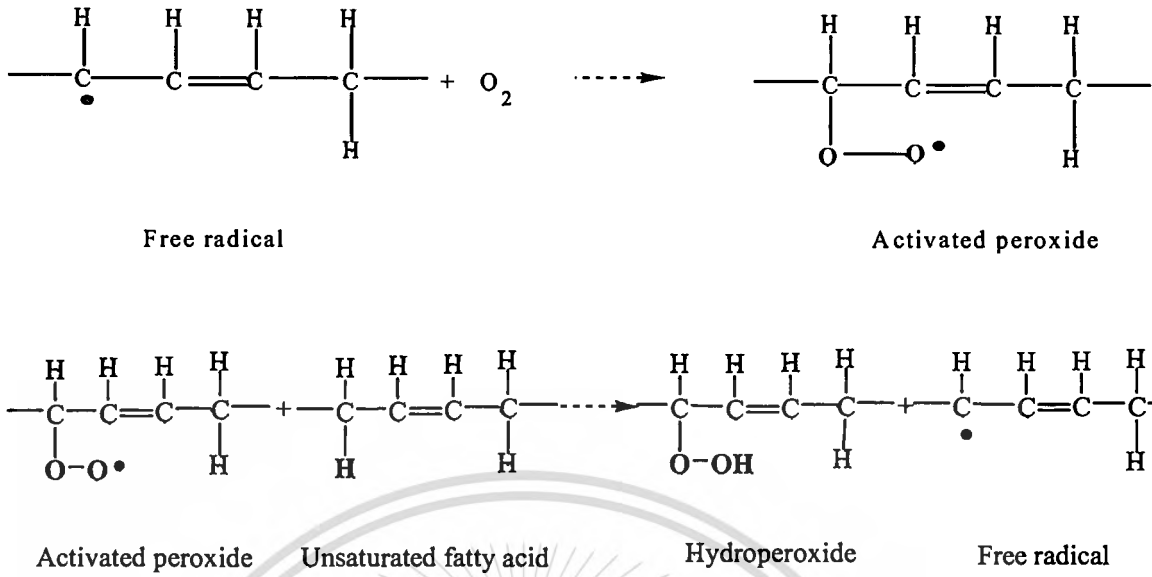

Figure 2.2 The two reactions of the propagation stage of autoxidation.

The termination stage of the reaction involves the reaction of free radicals to form nonradical products. Elimination of all free radicals is the only way to halt the oxidation reaction [18, 19].

2.1.3.2 Hydrogenation

Hydrogenation of unsaturated fatty acid occurs when hydrogen gas is reacted with oil under controlled conditions of temperature and pressure, and in the presence of a nickel, copper, or other catalyst. The reaction is carefully controlled and stopped when the desired extent of hydrogenation has been reached. As the reaction progresses, there is a gradual production of trans fatty acids that increases the melting point of the fat or oil and creates a more solid product. Shortening is hydrogenated oil.

The extent of the hydrogenation process is controlled to achieve stability and the physical properties required in the finished food. If the reaction is taken to completion, a saturated fat is obtained and the product is hard and brittle at room temperature. However, this is not usually the aim of hydrogenation, as partial hydrogenation normally is desired, providing an intermediate degree of solidification, reducing the number but not eliminating all double bonds. In fact, approximately 50 % of the total fatty acids present in partially hydrogenated vegetable shortening products are monounsaturated and about 25 % are polyunsaturated [18].

2.1.3.3 Halogen addition

The reaction which is used to measure the proportion of unsaturated constituents present in a fat, is addition of halogen such as chlorine, bromine and iodine to the double bonds of the unsaturated fatty acids. Reaction of bromine with a triglyceride is shown in Figure 2.3

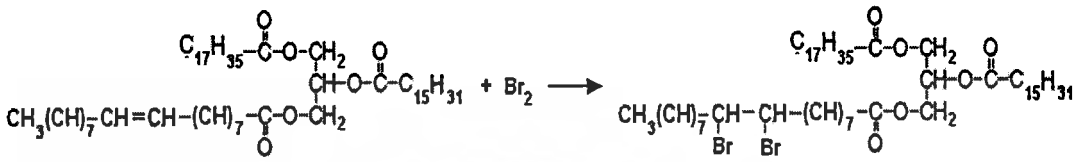

Figure 2.3 Reaction of bromine with a triglyceride.

The quantity of halogen taken up is expressed in terms of iodine so called the "iodine value", which is the number of grams of iodine absorbed per 100 g. fat [20].

2.1.3.4 Hydrolysis

Under the proper condition of fat/water miscibility, the triglyrides of fats and oils are hydrolyzed to free fatty acids and glycerol. The reaction is not a simple one; it proceeds in stages, and it is reversible. If reactants and product are not removed from the sphere of the reaction, an equilibrium depending on the concentration of the former eventually is reached. In several methods of industrial fat splitting, a high degree of hydrolysis is ensured by using a large excess of water, repeatedly withdrawing the aqueous glycerol rich phase and replacing it with water. High temperature and high pressure accelerate aqueous hydrolysis. The temperature selected is determined by the content of polyunsaturated and particularly, conjugated polyunsaturated fatty acids in the fat because if polymerization is permitted to interfere with the hydrolysis as a competing reaction, splitting is troublesome. Hydrolysis can be either autocatalysis in the presence of water by metals, or be brought about by the action of the enzyme lipase. The latter is, of course, the fat splitting enzyme of animal digestion, but it is also found in palm fruit, fungi and other organisms which gain access to fats. One of the most important tasks of the palm oil producer is to prevent hydrolysis by reducing to a minimum the amount of water and impurities present in the oil, and by the destruction of the enzyme. Hydrolysis in alkali is distinguished as "saponification" and gives rise to soaps and glycerol [18].

2.2 Fatty acids

Fatty acids are almost entire straight chain aliphatic carboxylic acids. Most natural fatty acids contain from 4 to 22 carbon atoms and most contain an even number of carbon atoms in the chain. For example, butyric acid is the smallest fatty acid, having four carbon atoms, and it is found in butter; lard and tallow contain longer fatty acids. Fatty acids may be saturated or unsaturated.

Saturated fatty acids contain only single carbon-to-carbon bonds and have the general formula $CH_3(CH_2)_n COOH$. They have a linear shape, as shown in Figure 2.4

Figure 2.4 "Ball and stick" models of stearic acid.

Unsaturated Fatty acids, containing one or more carbon-to-carbon double bonds. Monounsaturated fatty acids such as oleic acid contain only one double bond; polyunsaturated fatty acids, such as linoleic acid, contain two or more double bonds, as shown in Figure 2.5

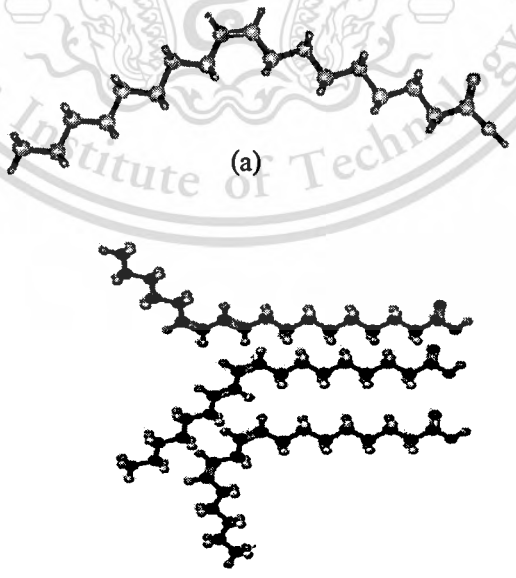

(a)

(b)

Figure 2.5 "Ball and stick" models of (a) oleic acid; (b) linoleic acid.

The melting point increases with chain length and decreases with increased unsaturation (Table 2.3). Among saturated acids, odd chain acids are lower melting than adjacent even chain acids. The presence of cis-double bonds markedly lowers the melting point, the bent chains packing less well. Trans-acids have melting points much closer to those of the corresponding saturates. Polymorphism results in two or more solid phases with different melting points. Methyl esters are lower melting than fatty acids but follow similar trends.

Fatty acid salts and many polar derivatives of fatty acids are amphiphilic, possessing both hydrophobic and hydrophilic areas within the one molecule. These are surface-active compounds that form monolayers at water/air and water/surface interfaces and micelles in solution. Their surface-active properties are highly dependent on the nature of the polar head group and, to a lesser extent, on the length of the alkyl chain. Most oleochemical processes are modifications of the carboxyl group to produce specific surfactants [19, 20].

Table 2.3 Melting points of some fatty acids and methyl esters illustrating the effect of chain length and unsaturation.

Fatty acid	Melting point (°C)	Fatty acid	Melting point (°C)
16:0	62.9 (30.7)		
17:0	61.3 (29.7)		
18:0	70.1 (37.8)		
18:1 9*c*	16.3, 13.4	18:1 9*t*	45
18:2 9*c*12*c*	-5	18:2 9*t*12*t*	29
19:0	69.4 (38.5)		
20:0	76.1 (46.4)		

2.3 Hydrolysis reaction

The world production of fatty acids is from the hydrolysis of triglycerides in fats or biological oils with the removal of glycerol.

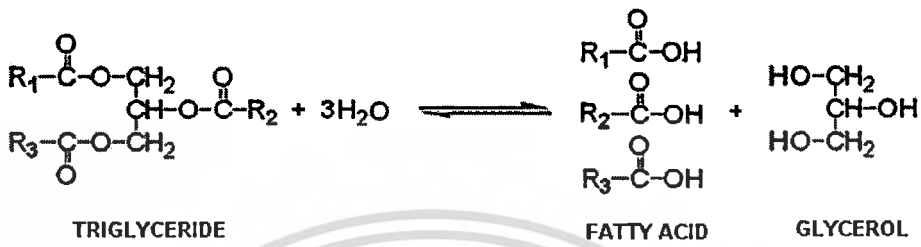

This reaction occurs as three stepwise reactions: one molecule of triglycerides is hydrolyzed to one molecule of diglycerides to produce one molecule of fatty acids, and is repeatedly hydrolyzed to which is further hydrolyzed to glycerol, producing three molecule of fatty acids in total. In general, there are two methods of hydrolysis reaction. One method simply uses a catalyst and the other is without a catalyst [18].

2.3.1 Catalyst for hydrolysis reaction [21-25]

2.3.1.1 Homogeneous catalysts

Alkaline catalyzed hydrolysis

Historically, soaps were produced by alkaline hydrolysis of oils and fats, and this process is still referred to as saponification. Soaps are now produced by neutralization of fatty acids produced by fat splitting, but alkaline hydrolysis may still be preferred for heat-sensitive fatty acids.

On a laboratory scale, alkaline hydrolysis is carried out with only a slight excess of alkali, typically 1M potassium hydroxide in 95% ethanol, refluxing for one hour, and the fatty acids recovered after acidification of the reaction mixture. This is a sufficiently mild procedure that most fatty acids, including polyunsaturates, epoxides, and cyclopropenes, are unaltered.

The mechanism of base catalyzed hydrolysis is described in Figure 2.6. The first step involves the attack of the hydroxide ion to the carbonyl carbon of the triglyceride molecule, breaking the π-bond and creating the tetrahedral intermediate. The reaction of this intermediate

with a water produces the alkoxide ion in the second step. In the last step, the rearrangement of the tetrahedral intermediate gives rise to an ester and a diglyceride [21, 22].

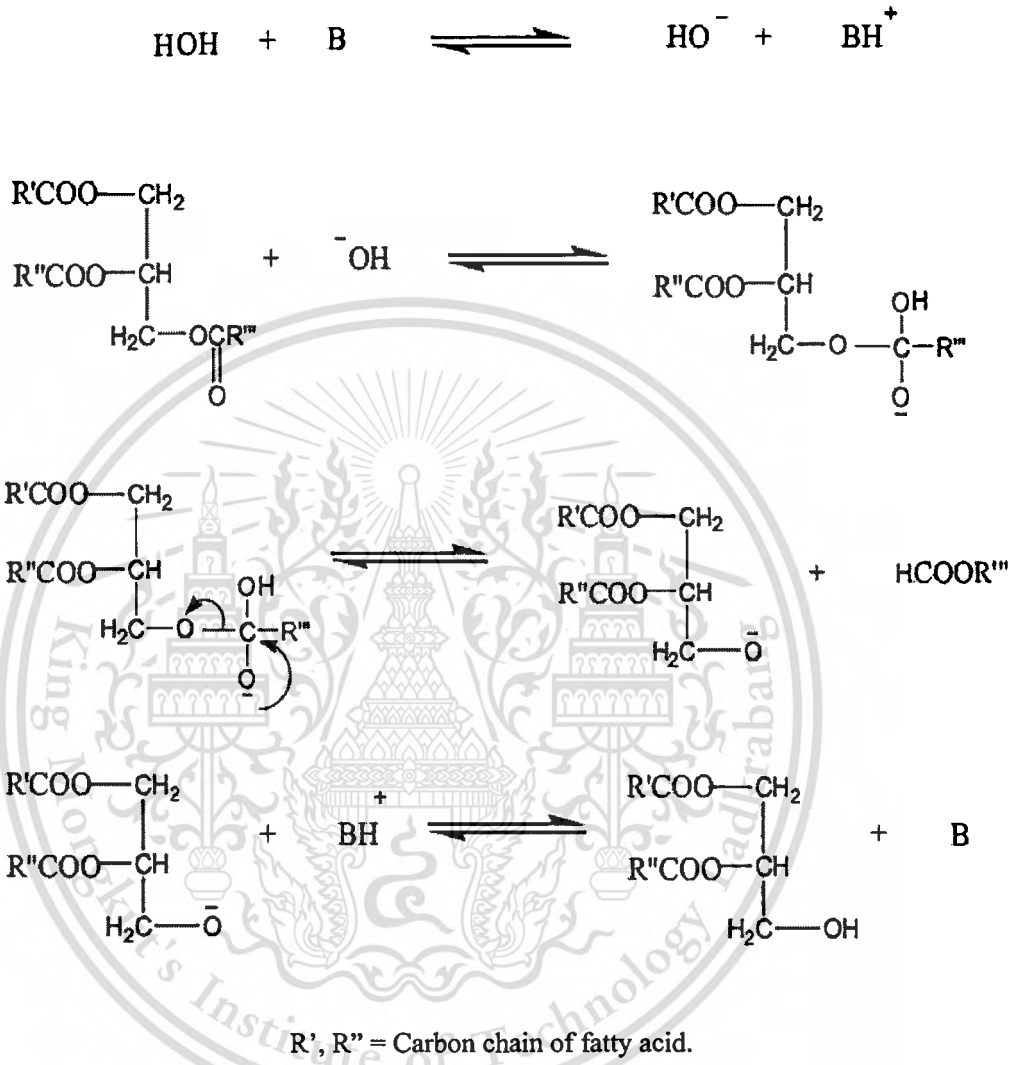

Figure 2.6 Mechanism of the base-catalyzed hydrolysis of triglycerides.

Acid catalyzed hydrolysis

Hydrolysis reaction can be catalyzed by liquid acid catalysts such as sulfuric acids and hydrofluoric acids. These catalysts give very high yields in fatty acids but these liquid acids are corrosive and produce a large amount of waste. The mechanism of acid-catalyzed hydrolysis of vegetable oil for a monoglyceride is shown in Figure 2.7. However, it can be extended to di- and triglycerides. The protonation of carbonyl group of the ester leads to the carbocation, which after

a nucleophilic attack of the alcohol produces a tetrahedral intermediate. This intermediate eliminates glycerol to form a new ester and to regenerate the catalyst [21].

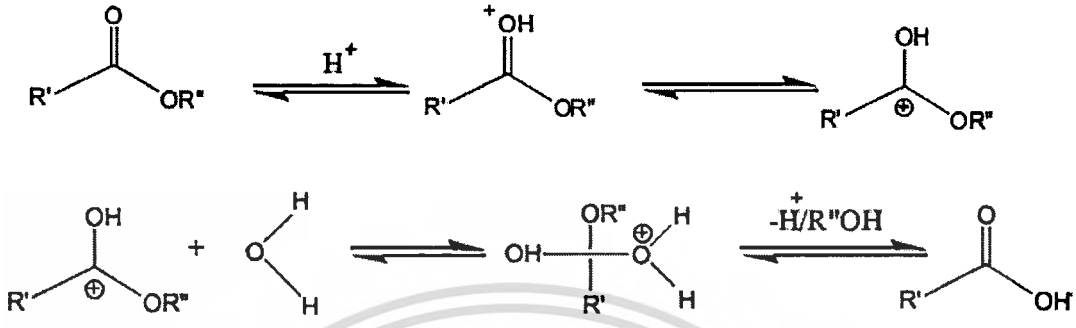

R" = CH_2–
CH –OH
CH_2–OH ; glyceride

R' = carbon chain of the fatty acid

Figure 2.7 Mechanism of the acid-catalyzed hydrolysis of triglycerides.

2.3.1.2 Heterogeneous catalysis

Whereas traditional homogeneous catalysis offers a series of advantages, its major disadvantage is the fact that homogenous catalysts cannot be reused. Moreover, catalyst residues have to be removed from the fatty acids product, usually necessitating several washing steps, which increases production costs. Thus there have been various attempts at simplifying product purification by applying heterogeneous catalysts, which can be recovered by decantation or filtration or are alternatively used in a fixed-bed catalyst arrangement.

Heterogeneous acid and basic catalysts could be classified as Bronsted or Lewis catalysts, though in many cases both types of sites could be present and it is not easy to evaluate the relative importance of the two types of sites in the reaction.

The mechanism of transesterification of glyceride to biodiesel with heterogeneous Lewis acid catalysts in the presence of the formation of a more electrophilic species also occurs with heterogeneous Lewis acid catalysts as the first step is as follows:

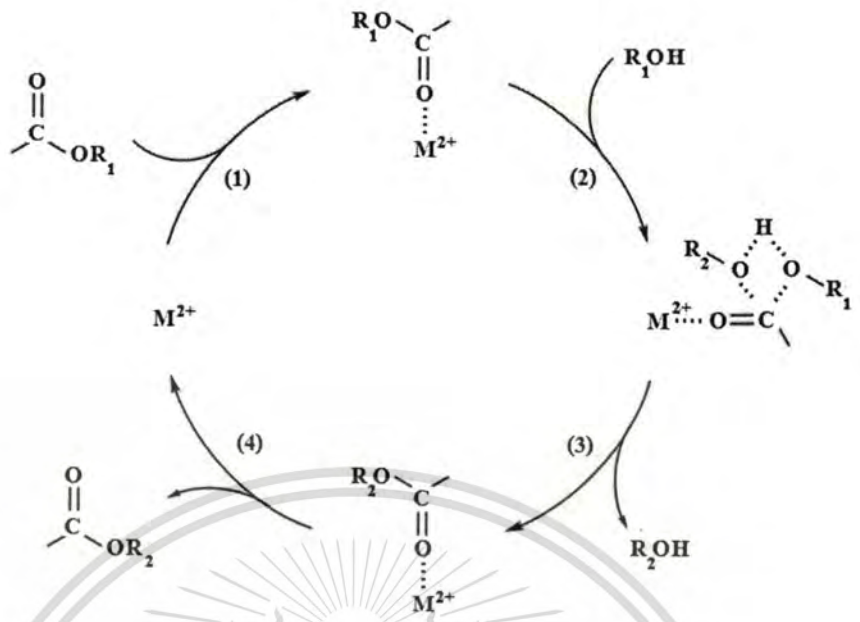

In this case, the rate-determining step depends on the Lewis catalyst's acid strength. After the Lewis complex formation (stage 1), the alcohol nucleophilic bonding (stage 2), and the new ester formation (stage 3), the new ester desorbs from the Lewis site (stage 4) and the cycle is repeated [23].

Hydrolysis and transesterification of triglycerides (TGs) follow similar reaction pathways. Three consecutive and reversible reactions occur to form diglycerides (DG), monoglycerides (MG) and glycerol (GL) accompanied by the formation of a FFA in hydrolysis or a methyl ester in transesterification with each step. For each TG molecule, the net reaction produces three molecules of FFA (hydrolysis) or three molecules of methyl esters (transesterification) and one molecule of glycerol. Solid acid catalysts have the capacity to successfully catalyze TG hydrolysis as well as transesterification [38].

2.3.1.3 Enzymes as catalysts

In addition to the inorganic or metallo-organic catalysts presented so far, also the use of lipases from various microorganisms has become a topic in fatty acids production. Lipases are enzymes which catalyze both the hydrolytic cleavage and the synthesis of fatty acids bonds.

As compared to other catalyst types, biocatalysts have several advantages. They enable conversion under mild temperature-, pressure- and pH-conditions. Neither the fatty acids product nor the glycerol phase has to be purified from basic catalyst residues or soaps. Therefore phase

separation is easier, high-quality glycerol can be sold as a by-product, and environmental problems due to alkaline wastewater are eliminated.

However, lipase-catalyzed hydrolysis reaction also entail a series of drawbacks. As compared to conventional alkaline catalysis, reaction efficiency tends to be poor, so that biocatalysis usually necessitates far longer reaction times and higher catalyst concentrations. The main hurdle to the application of lipases in industrial fatty acids production is their high price, especially if they are used in the form of highly-purified, extra cellular enzyme preparations, which cannot be recovered from the reaction products. One strategy to overcome this difficulty is the immobilization of lipases on a carrier, enabling the removal of the enzymes from the reaction mixture and their reuse for subsequent hydrolysis reaction [16, 24].

2.3.2 Hydrolysis reaction without catalysts

The hydrolysis of triglycerides by subcritical water has proved to be the most promising process and has several notable advantages over the conventional processes. A non-catalytic fatty acids production route with subcritical water has been developed that allows a simple process and high yield because of simultaneous hydrolysis of oil.

The basic idea of subcritical treatment is based on the effect of the relationship between pressure and temperature. It was investigated without using the catalyst. An experiment has been carried out in the batch-type reaction vessel preheated at 270 and 350 ^{o}C and at a pressure of 20 MPa.

This phenomenon with the high temperature conditions seems to be likely to promote hydrolysis reaction of oil. As a result, the reaction was found to be complete in a very short time and with simpler purification procedure [25].

2.4 Oxide minerals [26]

Mineral phases containing only oxide in their structures. By volume, oxide minerals comprise only a small fraction of the Earth's crust. However, their geochemical and petrologic importance cannot be overstated. Oxide minerals are important ores of metals such as iron, aluminum, titanium, uranium, and manganese. Oxide minerals occur in all geological environments. Some form as primary minerals in igneous rocks, while others form as secondary phases during the weathering and alteration of silicate and sulfide minerals. Some oxide minerals

are biogenic; for example, iron (III) and manganese (IV) oxides often result from bacterial oxidation of dissolved Fe^{2+} and Mn^{2+} in low-temperature aqueous solutions.

Iron and manganese oxide minerals often occur as nanocrystalline or colloidal phases with high, reactive surface areas. Adsorption of dissolved aqueous ions onto colloidal iron and manganese oxides plays a major role in the fate of micronutrients and heavy metals in soil and ground water and the trace-element chemistry of the oceans. Much current research is focused on measuring the thermodynamics and kinetics of metal adsorption by colloidal Fe-Mn oxides in the laboratory.

2.4.1 Bonding and crystal chemistry

To a first approximation, the bonding in oxide minerals can be viewed in the ionic model. According to Pauling's rules, the coordination number of a metal cation (such as Mg^{2+}, Al^{3+}, and Ti^{4+}) is determined by the radius of the cation relative to that of the oxide anion (O^{2-}). This allows one to predict the structures of some of the simpler oxide minerals. Cations with similar ionic radii (such as Mg^{2+} and Fe^{2+}) are able to substitute for each other and form a solid solution. The simple ionic radii arguments will fail when electronic configurations preclude the spherical symmetry of the cations. The ions Cu^{2+} and Mn^{3+}, with nine and four d electrons, tend to adopt distorted coordination environments because of the Jahn-Teller effect. Also, d-electron configurations can give rise to large octahedral site-preference energies that cause small cations, such as Mn^{4+}, to always adopt octahedral coordination. The magnetic and semiconducting properties of transition-metal oxide minerals, such as magnetite (Fe_3O_4), give useful geophysical signatures for subsurface exploration.

2.4.1.1 X_2O oxides

The mineral cuprite (Cu_2O) forms during the low-temperature oxidation of primary copper sulfide minerals. It is sometimes an important ore of copper. In the structure of cuprite, Cu^{+} ions are in twofold coordination with oxygen. No other monovalent cations form stable X_2O oxide minerals.

2.4.1.2 XO oxides

Oxides of divalent metals, such as Fe^{2+} and Mg^{2+}, with the formula XO will adopt the NaCl structure (Figure 2.8) in which the metal cation is in sixfold coordination. Fe^{2+} and Mg^{2+}

have nearly identical ionic radii, and a phase made up of the solid solution (Mg,Fe)O, called ferropericlase, is probably the second most abundant mineral in the Earth's lower mantle. Experimental evidence indicates that it maintains the NaCl structure over the pressure range of the Earth's interior. The end member MgO (periclase) is quite rare as a crustal mineral; it occurs in some metamorphosed limestones. Most other XO oxide minerals are also very rare. Not all XO oxides adopt the NaCl structure. Because the ionic radius of Zn^{2+} is somewhat smaller than that of Mg^{2+}, the mineral zincite ZnO has a structure based on the tetrahedral coordination of Zn. The mineral tenorite (CuO) is a secondary alteration phase of copper sulfides and has a structure based on the square planar coordination of Cu^{2+}. This structure results from the Jahn-Teller distortion of the CuO_6 coordination polyhedron. Larger divalent cations, such as Sr and Ba, form oxide structures based on eightfold coordination, but these are not stable minerals.

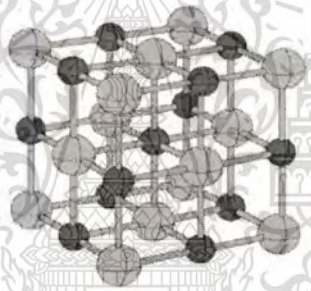

Figure 2.8 NaCl structure adopted by XO oxides such as MgO. Small spheres are divalent cations such as Mg^{2+}. Large spheres are O^{2-} anions.

2.4.1.3 XO_2 oxides

Tetravalent cations, such as Ti^{4+}, Sn^{4+}, and Mn^{4+}, whose ionic radii favor sixfold coordination, adopt the rutile structure (Figure 2.9). Rutile (TiO_2) is a common accessory mineral in felsic igneous rocks, gneisses, and schists. It also has two low-temperature polymorphs, anatase and brookite, but these are less common. Cassiterite (SnO_2) is the only significant ore mineral of tin. Cassiterite occurs mostly in granite-hosted hydrothermal deposits such as those in Cornwall, England. Pyrolusite (β-MnO_2) is found in low-temperature hydrothermal deposits. It is less common then previously supposed. MnO_2 also forms another polymorph (ramsdellite, α-MnO_2) based on double chains of MnO_6 polyhedra. This has a structure similar to that of goethite (α-FeOOH). Like pyrolusite, ramsdellite forms in low-temperature hydrothermal deposits. To

complicate matters, a phase called nsutite (γ-MnO_2) is a disordered intergrowth of pyrolusite and ramsdellite that forms by the oxidation of manganese carbonate minerals. Synthetic nsutite is used in dry-cell batteries.

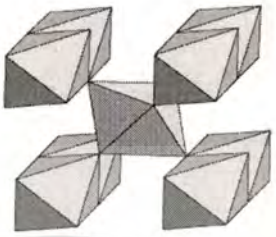

Figure 2.9 Rutile structure adopted by XO_2 oxides.

Large tetravalent cations, such as U^{4+} and Th^{4+}, prefer to be in eightfold coordination with oxygen and form oxides with the fluorite structure (Figure 2.10). Uraninite (UO_2) is the most important ore of uranium and is a primary mineral in granites.

Figure 2.10 Fluorite structure adopted by uraninite (UO_2) and thorianite (ThO_2).

2.4.1.4 X_2O_3 oxides and ilmenite

Trivalent cations, such as Fe^{3+} and Al^{3+}, having radii appropriate for sixfold-coordination with oxygen, will adopt the corundum (α-Al_2O_3) structure (Figure 2.11). Hematite (α-Fe_2O_3) is a common phase in soils and sediments and forms by the oxidation of Fe^{2+} in primary silicates. (Rust is mostly hematite.) Hematite is the most important ore mineral of iron and is the dominant mineral found in Precambrian banded iron formations. These vast deposits formed because of the oxidation of dissolved Fe^{2+} in the oceans when the Earth's atmosphere accumulated oxygen from photosynthetic bacteria. Corundum is a minor accessory mineral in metamorphic rocks and occurs in peraluminous igneous rocks. Partial solid solution is found between corundum and hematite.

The gemstone ruby is Al_2O_3 with minor Cr^{3+}, while sapphire is Al_2O_3 with other chromophores. A modification of the corundum structure is found in the mineral ilmenite ($FeTiO_3$). This is an important accessory mineral in felsic igneous rocks. Above 950 °C (1740 °F), there is complete solid solution between hematite and ilmenite. Bixbyite (Mn_2O_3) is a distorted corundum structure resulting from the Jahn-Teller effect in Mn^{3+}.

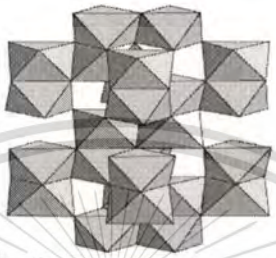

Figure 2.11 Polyhedral representation of Al_2O_3 structure adopted by X_2O_3 oxides. Each octahedron represents an M^{3+} cation surrounded by six O^{2-} anions, which define the vertices of the octahedral.

Alumina (Al_2O_3)

Alumina (Al_2O_3) are widely used in different industrial chemical processes such as hydrodesulfurization, dehydration, cracking, etc. Alumina exhibit wide ranges of acid and base strength. The proton doner groups are usually –OH groups, and the Lewis acid sites are exposed metal ions. The basic groups are usually oxygen ions and –OH groups. As in solution acid-base catalysis, the important elementary steps on the surface involve transfer of protons and hydride ions, and the catalytic activity may be simply related to proton donor strength, although sometime the chemistry is more subtle, involving the concerted action of proton donor and proton acceptor groups.

Many methods can be used to synthesize alumina, such as the co-precipitation, sol–gel, cellulose templating, thermal decomposition, flame spray pyrolysis and so on. Every methods have its own advantages and disadvantages.

Alumina has higher surface area and chemical activity, it has been used extensively as a catalyst or catalyst support because of the excellent properties such as high surface area, good catalytic activity, good mechanical strength, high hardness, and transparency [27].

2.4.1.5 Spinel oxides

The spinel structure (Figure 2.12) is adopted by oxides with the formula $A^{2+}B^{3+}{}_2O_4$. The spinel structure has one tetrahedral cation site and two octahedral cation sites per four oxygens. In a normal spinel (for example $MgAl_2O_4$, Fe_3O_4), the tetrahedral site is occupied by a divalent cation such as Mg^{2+}, Fe^{4+}, while the octahedral sites are occupied by trivalent cations such as Fe^{3+}, Cr^{3+}, or Al^{3+}. The inverse spinel structure is a variation where the tetrahedral sites are occupied by trivalent cations and the octahedral sites are occupied by a mixture of divalent and trivalent cations. A variety of solid solutions are possible within the spinel structure oxides.

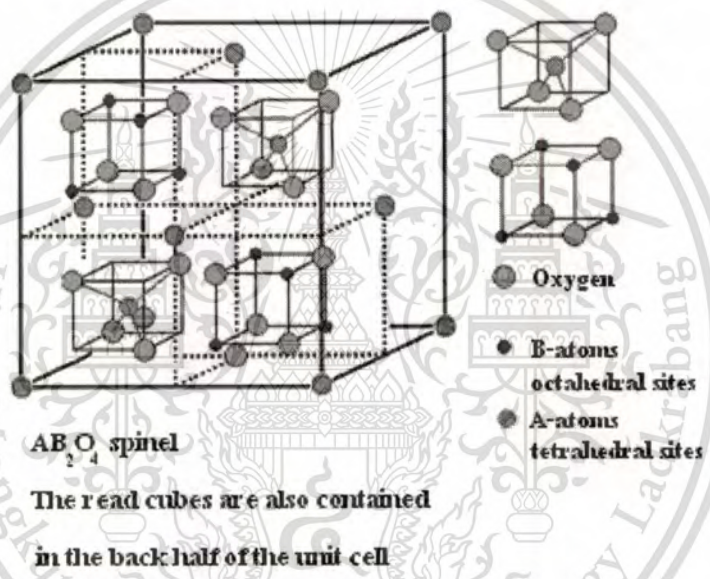

Figure 2.12 Spinel structure adopted by AB_2O_4 oxides.

Spinel oxides are well known for their rich catalytic action. These oxides are non-toxic, inexpensive, very stable materials with strong resistance to acids and alkalis, and they have high melting points and relatively high surface areas. These properties make them suitable for use as solid heterogeneous catalysts for organic transformations.

2.5 Spinel-type zinc aluminate ($ZnAl_2O_4$)

Zinc aluminate ($ZnAl_2O_4$), naturally occurring as the mineral gahnite, is a member of the spinel family. (AB_2O_4) are well known for their rich catalytic action. These oxides are non-toxic, inexpensive, very stable materials with strong resistance to acids and alkalis, and they have high thermal stability, relatively high surface areas and a hydrophobic behavior. These properties make them suitable for use as solid heterogeneous catalysts for organic transformations. Among them, zinc aluminate ($ZnAl_2O_4$) has been used extensively as a heterogeneous catalyst in many reactions, such as cracking, dehydration, hydrogenation, dehydrogenation, dehydrogenative condensation of normal alcohols, methylation of phenolic compounds and N-alkylation of 2-hydroxypyridine with methanol. Finally, zinc aluminate can be used for the acetylation reaction that occur at Lewis acid sites on the surface of the catalyst [30].

2.5.1 Zinc aluminate ($ZnAl_2O_4$) preparation

2.5.1.1 Coprecipitation method

The coprecipitated Zinc aluminate ($ZnAl_2O_4$) were prepared by co-precipitation of $Zn(NO_3)_2{\cdot}6H_2O$ and $Al(NO_3)_2{\cdot}9H_2O$ in an aqueous solution with aqueous ammonia solution at ambient temperature and the mixture was stirred until complete precipitation occurred at a pH between 8 and 9. The precipitate was filtered, washed with distilled water, and dried. The dry precipitate was calcined at 600-700 °C for 5 hours to obtain the $ZnAl_2O_4$ nanoparticles.

Coprecipitation method offers some advantages. They are simple and rapid preparation, easy control of particle size and composition, and various possibilities to modify the particle surface state and overall homogeneity [29-31].

2.5.1.2 Hydrothermal method

The aluminium hydroxide and basic aluminium nitrate with the empirical formula $Al_2(OH)_{6-x}(NO_3)_x$, wherein x was close to 1, were used as aluminium containing precursors for the hydrothermal preparation of $ZnAl_2O_4$. Basic aluminium nitrate was obtained by hydrolysis of powdered aluminium metal in an aqueous solution of aluminium nitrate at elevated temperatures (preferably between 70 and 90 °C) for several days. The mixtures were prepared by the controlled addition (with stirring) of zinc acetate to an aqueous solution of the basic aluminium nitrate,

wherein the molar ratio of Al:Zn was close or equal to 2:1 and the concentration of the aqueous reaction medium was below 10 wt.%. The resulting homogenous mixture was then introduced into a steel autoclave. The reaction mixture was treated hydrothermally for 3 to 6 hours at 150–170 °C with stirring, under static condition. After quenching the autoclave in cold water, the obtained sol was condensed by evaporating, drained, and water washed. The resulting transparent gel was air or freeze-dried, and a portion of the solid was calcined at 300 °C and at higher temperature [32, 33].

2.5.1.3 Sol-gel method

The appropriate amounts of start materials $Al(NO_3)_2 \cdot 9H_2O$, $Zn(NO_3)_2 \cdot 6H_2O$ and glycol were dissolved in ethanol, mixed well with each other, and then slowly adding ethanol solution of oxalic acid at room temperature under constant magnetic stirring, wherein the molar ratio of Al/Zn was 2:1. In this process, oxalic acid is used to chelated with various cationic precursors. Ethylene glycol is used to promote mixed oxalate polymerization by polyesterification reaction, which leads to the formation of organic esters and water by-products. The mixture was then stirred for one day and then evaporated at 80 °C for two hours under constant stirring. When the mixture was heated, the polyesterification occurs and a homogeneous sol was formed. Then the sol was further heated at 120 °C until a gel was formed. Subsequently dried and grinded the gel, thus the gel precursor powder was attained. The resulting material was calcined at 500-700 °C for 5 hours [34, 35].

2.5.2 Zinc aluminate ($ZnAl_2O_4$) synthesis techniques

Zinc aluminate ($ZnAl_2O_4$) was synthesized by a solid–vapour process. In principle, the thermal evaporation technique is a simple process in which condensed or powder source material are vaporized at elevating temperature and then the resultant vapour phase condense under certain conditions (temperature, pressure, atmosphere, substrate etc) to form the desired product. The processes are usually carried out in a horizontal tube furnace, as shown in Figure 2.13 which is composed of a horizontal tube furnace, an alumina tube, a rotary pump system and a gas supply and control system. A viewing window is set up at the left end of the alumina tube, which is used to monitor the growth process.

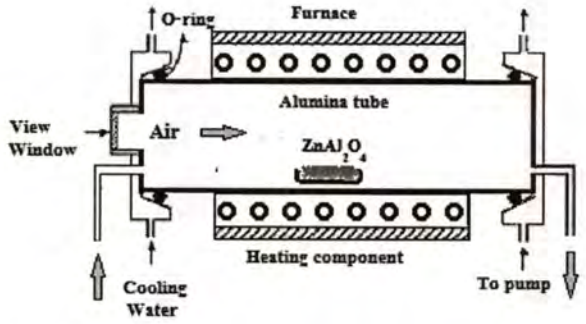

Figure 2.13 A schemetic diagram of the experimental apparatus for grouth of spinel oxides by the solid-vapour phase process.

The right-hand end of the alumina tube is connected to the rotary pump. Both ends are sealed by rubber O-rings. The ultimate vacuum for this configuration is $\sim 2\times10^{-3}$ Torr. The carrying gas comes in from the left end of the alumina tube and is pumped out at the right end. The source material are loaded on an alumina boat and positioned at the centre of the alumina tube, where the temperature is the highest. Alumina substrates were placed downstream for collecting growth products. This simple set-up can achieve high control of the final product.

There are several processing parameters such as temperature, pressure, carrier gas (including gas species and its flow rate), substrate and evaporation time period, which can be controlled and need to be selected properly before and during the thermal vaporization. The source temperature selection mainly depends on the volatility of the source material. Usually, it is slightly lower than the melting point of the source material. The pressure is determined according to the evaporation rate or vapour pressure of the source material. The substrate temperature usually drops with the distance of its location from the position of the source material. The local temperature determines the type of product that will be obtained. It is also noted that the thermal evaporation process is very sensitive to the concentration of oxygen in the growth system. Oxygen influences not only the volatility of the source material and the stoichiometry of the vapour phase, but also the formation of the product. In the present study, after evacuating the alumina tube to $\sim 2\times10^{-3}$ Torr, thermal vaporization was conducted at a designed heating rate and at a pressure of 200–600 Torr and air carrier gas at 60 sccm (standard cubic centimetres per

minute). The on and off times as well as the duration of inlet of the carrier gas could greatly affect the growth kinetics [36].

The as-deposited products were characterized and analysed by means of X-Ray Diffraction (XRD), Scanning Electron Microscopy (SEM), Transmission Electron Microscopy (TEM) and Energy Dispersive X-ray Spectroscopy (EDS).

2.6 Literature Reviews

In 2009, Kanokwan Ngaosuwan et. al. reported the hydrolysis of tricaprylin (TPC) using tungstated zirconia (WZ) and the solid acid composite SAC-13 (Nafion resin nanoparticles supported on mesoporous silica) as catalysts. The hydrolysis of TCp was carried out at 110-150 °C in a semibatch reactor with continuous addition of water at low flow rates capable of achieving 100% selectivity of the carboxylic acid side chains on the triglyceride to HCp [17].

In 2010, Kanokwan Ngaosuwan et. al. reported solvent effects on the nature of the catalytic activity of the solid acid tungstated zirconia (WZ) for hydrolysis and transesterification of tricaprylin (TCp), two reactions that can occur during biodiesel synthesis, at 130 °C and 12.2 atm in a batch reactor using different solvents. It was found that hexane and a mixture of lauric acid (HLa) and hexane resulted in the highest catalytic activities for transesterification and hydrolysis reaction [37].

In 2010, Kanokwan Ngaosuwan et. al. reported the mechanistic pathways in hydrolysis and transesterification at a relatively high temperature (100–130 °C) and moderate pressures (120–180 psi) with tricaprylin and water for hydrolysis or methanol for transesterification using a tungstated zirconia catalyst in a batch reactor. It was found that upon increasing the concentration of TCp, the reaction rates for both hydrolysis and transesterification increased at all conditions [38].

In 2006, P.S. Sreeprasanth, R. Srivastava, D. Srinivas and P. Ratnasamy developed a novel application of Fe–Zn double-metal cyanide (DMC) complexes as solid catalysts in the preparation of fatty acid alkyl esters (biodiesel/biolubricants) from vegetable oils. The catalysts are hydrophobic (no H_2O adsorption at reaction temperatures) and contain only Lewis acidic sites (NH_3 and pyridine adsorption). Bronsted acid sites are absent (absence of 1546 and 1639 cm^{-1} bands on adsorption of pyridine). Basic sites are also absent (no CO_2 adsorption). Unlike the homogeneous or other solid catalysts (like $ZnO–Al_2O_3$, for example), the Fe–Zn, DMC catalysts are highly active even for the simultaneous transesterification of triglycerides and esterification of

the free fatty acids (FFA) present in unrefined and waste cooking oils as well as non-edible oils. They are also tolerant of water, probably, due to their surface hydrophobicity [39].

In 2010, J.K. Satyarthi, D. Srinivas and P. Ratnasamy reported that solid Fe-Zn double-metal cyanide (DMC) complexes exhibit high catalytic activity for hydrolysis of edible and non-edible vegetable oils and animal fat. In a batch reaction, complete conversion of vegetable oil triglycerides to fatty acids with selectivity greater than 73 wt.% was obtained at temperatures as low as 463 K, autogenous pressure and with 5 wt.% of catalyst. Catalytic activity of DMC was superior to Amberlyst™70, SAPO-11, H-β, HY, $MoOx/Al_2O_3$ and sulfated zirconia. Rates of hydrolysis were greatly enhanced when solvents (tetrahydrofuran or N, N-dimethylformamide), phase transfer agents (tetrapropyl ammonium bromide) and products (a mixture of mono, diglycerides and fatty acids) or fatty acid was added to the feed. Surface hydrophobicity which enables high wettability and activation of glycerides on active, acidic sites of reusable DMC is attributed to be the major cause for its superior catalytic activity [40].

In 2010, S. Yan, S.O. Salley and K.Y. Simom Ng investigated a series of zinc and lanthanum mixed oxides catalysts for synthesis of FAME from unrefined and waste oils. A strong interaction between Zn and La species was observed with enhanced catalyst activities. Lanthanum promoted zinc oxide distribution, and increased the surface acid and base sites. The catalyst with 3:1 ratio of zinc to lanthanum was found to simultaneously catalyze the oil transesterification and fatty acid esterification reactions, while minimizing oil and biodiesel hydrolysis. A reaction temperature window of 170–220 °C was found for the biodiesel formation. A high yield (96 %) of fatty acid methyl esters (FAME) was obtained within 3 hours even using unrefined or waste oils [41].

In 2010, V. Pugnet et. al. developed a novel process for the production of biodiesel from rapeseed oil using zinc aluminate catalyst. It was found to be particularly stable as compared to ZnO catalyst. Optimization of the reaction parameters for achieving high yields and obtaining high quality products was performed [42].

In 1997, R.L. Holliday, J.W. King, and G.R. List reported that water, in its subcritical state, can be used as both a solvent and reactant for the hydrolysis of triglycerides. In this study, soybean, linseed, and coconut oils were successfully and reproducibly hydrolyzed to free fatty acids with water at a density of 0.7 g/ml and temperatures of 260-280 °C. Under these conditions the reaction proceeds quickly, with conversion of greater than 97 % after 15-20 minutes. Some geometric isomerization of the linolenic acids was observed at reaction temperatures as low as

250 °C. Reactions carried out at higher temperatures and pressures, up to the critical point of water, produced either degradation, pyrolysis, and polymerization, of the oils and resultant fatty acids [43].

In 2009, R. Alenezi, G.A. Leekea, R.C.D. Santos and A.R. Khan studied the thermal non-catalytic hydrolysis of sunflower oil with subcritical water. A number of experimental runs were conducted in a tubular reactor over a range of temperatures from 270 °C to 350 °C and reaction times (up to 30 minutes) at 20 MPa and was found to be an effective method for producing a fatty acid yield of greater than 90 % without any catalyst [44].

In 2004, D. Kusdiana and S. saka, studied a two-step reaction hydrolysis and methyl esterification for preparation of biodiesel fuel. Hydrolysis was carried out at a subcritical state of water to obtain fatty acids from triglycerides of rapeseed oil, while the methyl esterification of the hydrolyzed products of triglycerides was treated near the supercritical methanol condition to achieve fatty acid methyl esters. Consequently, the two-step preparation was found to convert rapessed oil to fatty acid methyl esters in considerably shorter reaction time and milder reaction condition than the direct supercritical methanol treatment. The optimum reaction condition in this two-step preparation was 270 °C and 20 minutes for hydrolysis and methyl esterification [14].

CHAPTER 3

EXPERIMENTAL DETAILS

3.1 Chemicals

1. Refined palm oil from Lumsung (Thailand) Co, Ltd.
2. Deionized water
3. Alpha aluminum oxide powder from J.T.Baker
4. Aluminium nitrate from Ajax
5. Zinc nitrate from Ajax
6. Sodium sulfate anhydrous from Fisher Scientific
7. Sodium hydroxide from Fisher Scientific
8. Hydrochloric acid 37% (analytical grade) from Lab Scan
9. Deuterochloroform from Sigma Aldrich
10. Methanol (HPLC grade) from Fisher
11. Dichloromethane (HPLC grade) from Fisher
12. Acetonitrile (HPLC grade) from Fisher
13. Acetone (analytical grade) from Lab Scan
14. Hexane (analytical grade) from Lab Scan
15. Benzene (analytical grade) from J.T. Baker
16. Air Zero gas from TIG
17. Nitrogen gas from TIG

3.2 Apparatus and instruments

1. Nuclear Magnetic Resonance Spectrometer: Avance DPX300, Bruker
2. Thermogravimetric Analyzer: Model Pyris 1 TGA, Perkin Elmer
3. High Performance Liquid Chromatography: HP Altima, equipped with Altima HP C-18 column, 5μm, 150 mm x 4.6 mm i.d., from Alltech and Evaporative Light Scattering Detector (ELSD) from Alltech
4. Pump for High Performance Liquid Chromatography: LDC 4100

5. Filter paper 0.45 µm
6. Atomic Absorption Spectrophotometer: 280FS AA, Varian
7. Furnace: Thermolyne 6000
8. Gas Adsorption Analyzer: Autosorb-1, Quantachrome
9. X-ray Powder Diffractometer: D8 Avance, Bruker AG
10. Stainless steel reactor with cylindrical autoclave and PID temperature controller: Parr series 4561
11. Hot plate
12. Supporting stand
13. Laboratory glassware

3.3 Experimental steps

3.3.1 Preparation of catalyst.

3.3.1.1 Co-precipitation of zinc nitrate and aluminum nitrate using ammonia as precipitating agent.

3.3.2 Characterization of catalyst.

3.3.2.1 Determination of the structure of catalyst using X-ray Powder Diffractometer (XRD).

3.3.2.2 Determination of the surface area of catalyst using Gas Adsorption Analyzer (Autosorb-1b).

3.3.2.3 Determination of the Zn/Al ratio of catalyst using Atomic Absorption Spectrophotometer (AAS).

3.3.2.4 Determination of the morphology of catalyst using Scanning Electron Microscopy (SEM).

3.4.2.5 Determination of Acid/Base Strength using Hammett indicators followed by the titration [49, 50].

3.4.2.6 Determination of Acidity/Basicity by the titration method [57].

3.3.3 Catalyst testing in hydrolysis of palm oil.

3.3.3.1 Preparation of fatty acids from refined palm oil by hydrolysis reaction with water, both with and without the use of solid oxides, namely alumina and zinc aluminate as catalysts.

3.3.4 Characterization of fatty acid product.

3.3.4.1 Nuclear Magnetic Resonance Spectrometer (NMR) to determine the yield.

3.3.4.2 High Performance Liquid Chromatography (HPLC) to determine the conversion.

3.4 Experimental procedures

3.4.1 Catalyst preparation

Zinc aluminate catalysts were prepared in aqueous solution from metal nitrates by coprecipitation method using ammonia as a precipitating agent. Zinc nitrate and aluminum nitrate were dissolved in distilled water, mixed well with each other, and then the appropriate amount of aqueous ammonia solution was added to the above solution, and the mixture was stirred until complete precipitation occurred at a pH between 8 and 9, wherein the molar ratio of Al/Zn was 2:1. The precipitate was filtered, washed with distilled water, and dried. The dry precipitate was calcined at 400, 500, 600 and 700 °C for 5 hours, respectively.

3.4.2 Characterization

3.4.2.1 Determination of the structure of catalyst using X-ray Powder Diffractometer (XRD).

The structure of catalyst was determined by X-ray powder Diffractometer (D8 Avance, Bruker, Scientific Instruments Service Centre; KMITL). The sample was prepared by packing catalyst in the sample holder. CuK$\propto$ X-ray beam was used for analysis at 40 kV, 40 mA. The sample was scanned from 2θ angle 20° to 80° with 1 second/step time and 0.05 2θ/step increment. X-ray diffraction pattern of the sample was compared with the pattern of standard metal oxides for structure determination.

3.4.2.2 Determination of the Zn/Al ratio of catalyst using Atomic Absorption Spectrophotometer (AAS).

After chemical attack with microwave digestion in 4 ml of 65 % HNO_3, 3 ml of 37 % HCl and 1 ml of HF 40 % acids at 220 °C, the solution was cooled to room temperature and then 7 ml of 4 % H_3BO_3 was added for the complete removal of HF and fluorides before injecting solution to the flame of a Varian 280FS AA flame spectrometer. For some refractory elements (Zn and Al), a hotter N_2O+C_2H_2 flame was necessary.

3.4.2.3 Determination of the surface area of catalyst using Gas Adsorption Analyzer (Autosorb-1b)

The surface area of catalyst was determined by Gas Adsorption Analyzer (Autosorb-1C, Quantachrome). The sample was prepared by weighing approximately 20 mg of sample into the cleaned and dried sample cell. The sample cell was attached to the out gassing station. Heating mantle was installed and the temperature was raised to 350 °C under vacuum. The sample was out-gassed for 24 hours. The sample cell was then removed from the out gassing station after the nitrogen was filled and was attached to the analysis station. The equilibration time was set to 3 minutes and the nitrogen adsorption was measured at the partial pressure (P/P0) ranged from 10^{-6} to 1.0 at 77.4 K.

3.4.2.4 Determination of the morphology and the surface composition of catalyst using Scanning Electron Microscopy (SEM).

The morphology of catalyst was determined using Scanning Electron Microscopy (SEM) with a Hitachi S-4800 electron microscope operating at 5.0 kV. The sample was prepared by dispersing the catalyst sample on carbon tape of an SEM stup.

3.4.2.5 Determination of Acid/Base Strength [49, 50].

Site strength refers to the relative tendency of an acid or base to donate or accept a proton. The strength of an acid and base can be compared by their reaction with water. Acidic and basic site strengths of each of the metal oxides were determined by basic and acidic Hammett indicators, respectively. Approximately 0.05 g of catalyst sample was shaken with 1 ml of a solution of Hammett indicator diluted in benzene and methanol for basic and acidic tests, respectively, and left to equilibrate for 2 hours. The color of the catalyst was then noted. The

basic Hammett indicator (for acid site strength) used were Neutral red (pK_a = 6.8), Methyl red (pK_a = 4.8), P-dimethylaminoazobenzene (pK_a = 3.3), and Crystal violet (pK_a = 0.8). The acidic Hammett indicator (for base site strength) used were Phenolphthalein (pK_{BH+} = 8.2), Nile blue (pK_{BH+} = 10.1), Tropaeolin (pK_{BH+} = 11), 2,4-dinitroaniline (pK_{BH+} = 15), 4-chloro-2-nitroaniline (pK_{BH+} = 18.2), and 4-chloroaniline (pK_{BH+} = 26.5). The H_0 value of a sample at acid site was determined by the smallest H_0 value among the Hammett indicators, which has been subjected to a color change and has a H_0 value less than 7.0. In addition, the H_0 value of a sample at the base site was determined by the greatest H_0 value among the Hammett indicators, which had been subjected to a color change and having a H_0 value more than 7.0.

3.4.2.6 Determination of Acidity/Basicity [57].

A common method for evaluating the basicity of a base is to report the acidity of the conjugate acid and vice versa for the acidity. In this work, the method of titration was used to determine the acidity/basicity of the catalysts. For basicity, the basic catalyst (0.1 g) was suspended in 20 cm^2 of 0.01M HCl solution for 48 hours. The basic catalyst will neutralize HCl by an equivalent amount to its basicity. As a result, the original concentration of HCl will be reduced. The resultant concentration of HCl was determined by titration with NaOH, and finally, the adsorbed amount of HCl on the catalyst was determined. In retrospect, for acidity determination, an acidic catalyst (0.1 g) was suspended in 20 cm^2 of 0.01M NaOH solution for 48 hours and the amount of NaOH adsorbed to the catalysts was determined via titration with HCl. For amphoteric catalysts, both acidity as well as basicity were determined.

3.4.3 Catalyst testing on hydrolysis of palm oil.

The reactor used to produce fatty acids was a 300 ml Parr series reactor equipped with programmable PID temperature controller and a 300 ml cylindrical autoclave made of stainless steel with internal cooling and a mechanical stirrer. The temperature of the reaction vessel was measured with an iron-constant thermocouple and controlled at ± 2 °C for a set time.

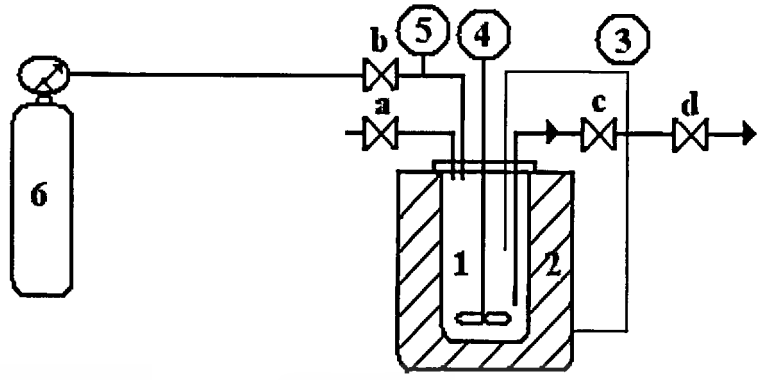

Figure 3.1 Schematic diagram of experimental apparatus. 1) autoclave; 2) oven; 3) temperature control monitor; 4) mechanical stirrer; 5) pressure control monitor; 6) nitrogen gas tank

3.4.3.1 Synthesis of fatty acids without catalyst

1) Refined palm oil (70 g, 0.082 mole) and distillation water (79.75 g, 4.43 mole, water to oil ratio = 54:1) were poured into the autoclave.
2) The autoclave was then placed on the electric furnace. The mixture was stirred with equipped mechanical stirrer to sufficiently keep the system in homogeneity.
3) The mixture was stirred and heated to 230 °C by oven for 60 minutes at a 5 °C/min heating rate. The system pressure was raised to 25 ±1bar.
4) After the pre-set time, the reaction was cooled down to room temperature.
5) The product mixture was then poured into a separatory funnel. The autoclave was rinsed with hexane. The mixture was allowed to stand in separatory funnel for 1 hour to ensure the phase separation between fatty acids and glycerol. The glycerol phase (bottom layer) was removed and stored in a separated container.
6) Afterwards, the water and hexane in the product (upper layer) were removed at 60-80 °C for half an hour.
7) The product was then dried using anhydrous sodium sulfate and was filtered through a Bruchner funnel.
8) Step 1) to 7) were repeated by changing the molar ratio of water to oil from 54:1 to 13:1, 26:1, 84:1 and 108:1.
9) Next, step 1) to 7) were repeated by changing the reaction temperature in step 3) from 230°C to 220 °C and 240 °C using the optimum water to oil ratio from 8).

10) Finally, step 1) to 7) were repeated by changing the time in step 3) from 60 minutes to 30, 90, 120 and 150 minutes using the optimum water to oil ratio from 8) and the reaction temperature from 9).

3.4.3.2 Synthesis of fatty acids using alumina as catalyst

1) Alumina was first calcined in air at 500 °C for 5 hours and was then kept in a dessicator until used.
2) Refined palm oil (70 g, 0.082 mole) was poured into the autoclave.
3) Alumina (2.10 g, 3.0 % by weight of refined palm oil) and distillation water (79.75 g, 4.43 mole, water to oil ratio = 54:1) were added into the autoclave from step 2).
4) The autoclave was then placed on the electric furnace. The mixture was stirred with equipped mechanical stirrer to sufficiently keep the system in homogeneity.
5) The mixture was stirred and heated to 230 °C by oven for 60 minutes at a 5 °C/min heating rate. The system pressure was raised to 25 ±1bar.
6) After the pre-set time, the reaction was cooled down to room temperature.
7) The product mixture was then poured into a separatory funnel. The autoclave was rinsed with hexane. The mixture was allowed to stand in separatory funnel for 1 hour to ensure the phase separation between fatty acids and glycerol. The glycerol phase (bottom layer) was removed and stored in a separated container.
8) Afterwards, the water and hexane in the product (upper layer) were removed at 60-80 °C for half an hour.
9) The catalyst was separated from the product mixture by vacuum filtration, and was washed several times with acetone, dried and then weighed.
10) The product was dried using anhydrous sodium sulfate and was filtered through a Bruchner funnel.
11) The following experimental steps were then carried out using the same procedure as described earlier in section 3.4.3.1.

3.4.3.3 Synthesis of fatty acids using zinc aluminate as catalyst

The synthesis of fatty acids using zinc aluminate was carried out by following the procedure explained in section 3.4.3.2 except alumina was replaced by zinc aluminate calcined in air at 600 °C for 5 hours.

3.4.3.4 Effect of the calcining temperature on the synthesis of fatty acids using alumina and zinc aluminate

1) alumina was first calcined in air at 400 °C for 5 hours and was kept in a dessicator.
2) The following experimental steps were then carried out using the same procedure as described earlier in step 2) to 10) of section 3.4.3.2.
3) The experiment was repeated by changing the calcining temperature from 400 °C to 500 °C, 600 °C and 700 °C, respectively.
4) Step 1) to 3) were repeated by changing alumina to zinc aluminate.

3.4.3.5 Synthesis of fatty acids using reused catalysts

1) Refined palm oil (70 g, 0.082 mole) was poured into the autoclave.
2) The used alumina catalyst from section 3.4.3.2 (2.10 g, 3.0 % by weight of refined palm oil) and distillation water (79.75 g, 4.43 mole, water to oil ratio = 54:1) was added into the autoclave from step 1).
3) The following experimental steps were then carried out using the same procedure as described earlier in step 4) to 10) of section 3.4.3.2.
4) The reused alumina catalyst was washed several times with acetone, dried, weighed, and was then heat in oven at 120 °C for 12 hours. The reused alumina catalyst was then kept in a dessicator.
5) Finally, step 1) to 4) were repeated by changing the catalyst to used zinc aluminate from section 3.4.3.3.

3.4.4 Characterization of fatty acid product.

3.4.4.1 Nuclear Magnetic Resonance Spectrometer (NMR) to determine the yield

The percent yield of fatty acid product was determined using the NMR technique. The fatty acid product was diluted in deuterochloroform. The measurement was performed on a Bruker AVANCE DPX300 NMR spectrometer with 300-MHz proton resonance 40 frequency. The integral spectra were obtained in separated scans from 0 to 10 parts per million (ppm).

The free fatty acids (FFA) from palm oil were quantitatively determined by NMR spectroscopy. Assignments of the ^{1}H NMR peaks are listed in Table 3.1

Table 3.1: Assignment of ^{1}H NMR peaks of oleic acid and palm oil

Proton(s)	Functional group	compound/chemical shift, δ (ppm)	
		oleic acid	**palm oil**
CH_3-C	terminal methyl group	0.88	0.85-0.88
-$(CH_2)_n$-	backbone CH_2	1.14-1.43	1.25-1.30
-CH_2CH_2COOH	β-methylene proton	1.54-1.69	1.61
=CH-CH_2-	α-methylene group to one double bond	1.92-2.11	2.01-2.05
-CH_2COOH	α-methylene group to acid	2.34	-
-CH_2COOR	α-methylene group to ester	-	2.28-2.33
=CH-CH_2-CH=	α-methylene group to two double bonds	-	2.74-2.76
-$COOCH_3$	methyl group of ester	-	-
-CH_2OCOR	methylene group ($C_1$and C_3) of glyceride	-	4.11-4.17
-CHOCOR	methine proton at C_2 of glyceride	-	-

α-CH_2 peaks of fatty acids appear at δ values higher than those of the glyceryl (palm oil) esters when the quantification of FFA content in palm oil is attempted by ^{1}H NMR. The difference in chemical shift between the fatty acids and ester is shown in Figure 3.2a. One of the triplet peaks of FFA shifts out of the α-CH_2 region of the ester with two peaks of the FFA triplet merged with the other two of ester as shown in Figure 3.2b. This can be used to determine the FFA content in palm oil.

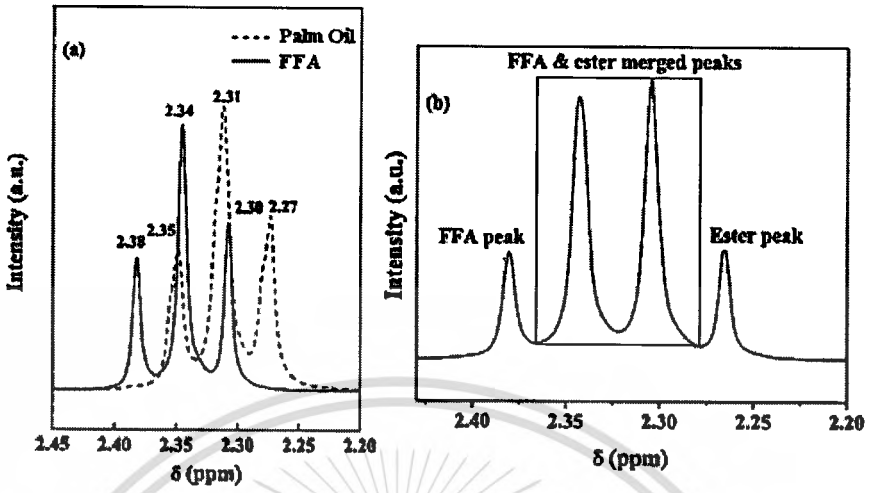

Figure 3.2 ^{1}H NMR spectrum in α-CH_2 region: (a) glyceryl (palm oil) esters and oleic acid (FFA) and (b) mixture of oleic acid and its glyceryl ester.

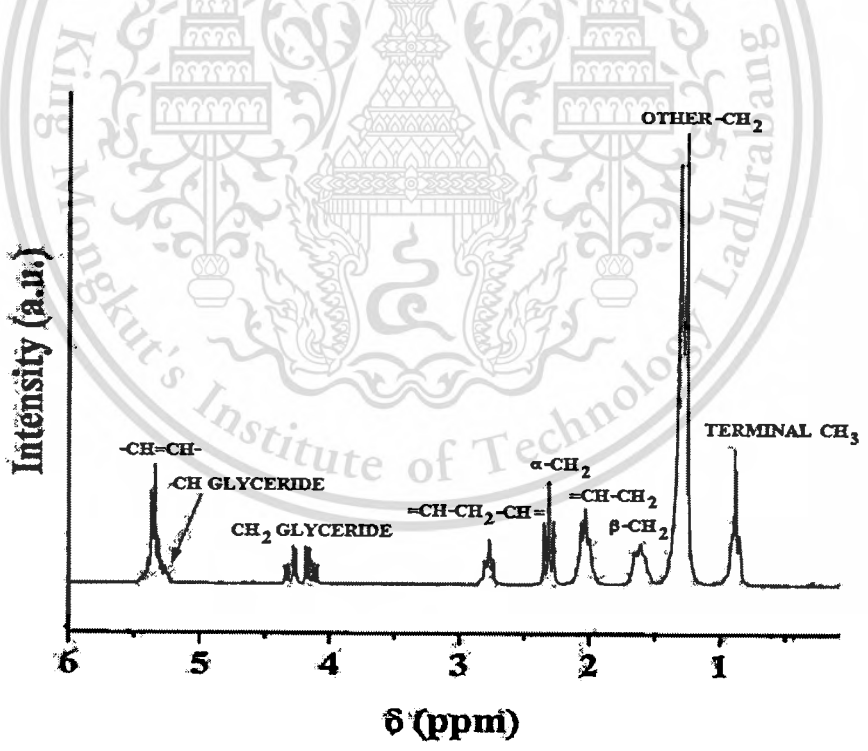

Figure 3.3 ^{1}H NMR spectrum and assignment of palm oil peaks.

The triplet peaks appear with an intensity ratio of 1:2:1. The total area corresponding to α-CH_2 of both FFA and ester can be determined by integrating the spectral region at 2.20-2.41 ppm. The area of the unmerged peak of the FFA triplet can be determined by integration of the spectral region at 2.37-2.41 ppm. The weight percentage of FFA in oil is thus [51]

$$\text{Free fatty acids (FFA), \%} = \frac{4 \times \text{area of umerged peak of } \alpha\text{-}CH_2 \text{ of FFA}}{\text{total area of } \alpha\text{-}CH_2 \text{ of both FFA and ester}} \times 100\%$$

3.4.4.2 High Performance Liquid Chromatography (HPLC) to determine the conversion

The percent conversion of triglyceride can be determined using HPLC. The system used was Altima high liquid chromatography equipped with Evaporative Light Scattering Detector (ELSD). The sample analysis was performed using Altima C18 (5μm) column; 150 mm.x4.6 mm i.d., with a mobile phase of dichloromethane-acetonitrile (gradient), a flow rate of 1 ml/min at ambient, and drift tube temperature of 75 °C with nitrogen. The injector volume was 50 μl of 0.0125 g fatty acid product in 25 ml of 70:30 acetonitrile: dichloromethane.

The weight percentage of refined palm oil calculated from HPLC chromatogram is thus

$$\frac{\text{Concentration of triglycerides from HPLC chromatogram (g/ml)}}{\text{Concentration of product mixture used for HPLC (g/ml)}} = \frac{\text{weight of triglyceride in product mixture (g)}}{\text{weight of product mixture from reaction (g)}}$$

$$\text{\% conversion} = \frac{\text{weight of palm oil (g)} - \text{weight of triglyceride in product (g)}}{\text{weight of palm oil (g)}} \times 100$$

CHAPTER 4

RESULTS AND DISCUSSION

In this research, hydrolysis reactions of refined palm oil to fatty acids were carried out in Parr reactor using alumina and zinc aluminate as catalysts. The results shown in this chapter are from characterization of the catalysts by X-ray Powder Diffractometer (XRD) and Gas Adsorption Analyzer (Autosorb-1C), determination of the chemical composition of catalysts using Atomic Absorption Spectrophotometer, characterization of fatty acid products by Nuclear Magnetic Resonance Spectrometer (NMR) to determine the yield, and characterization of fatty acid products by High Performance Liquid Chromatography (HPLC) to determine the conversion of triglycerides, The variables such as the effect of calcination temperature, the type of catalyst, the amount of catalysts, reaction temperature, reaction time, water to oil ratio and the reuse of catalysts that affect the yield of fatty acids and conversion of triglycerides over the hydrolysis of refined palm oil are discussed.

4.1 Characterization of palm oil

The main compositions of fatty acids in palm oil are myristic acid, palmitic acid, stearic acid, oleic acid and linoleic acid which have general structure as shown in Figure 4.1. Its composition was characterized using Nuclear Magnetic Resonance Spectrometer (NMR) and High Performance Liquid Chromatography (HPLC).

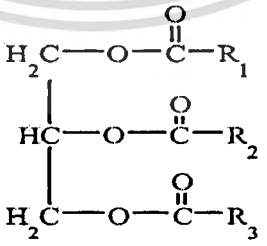

R_1 R_2 and R_3 = CH_3-$(CH_2)_{12}$-(myristic acid), CH_3-$(CH_2)_{14}$- (palmitic acid), CH_3-$(CH_2)_{16}$- (stearic acid), CH_3-$(CH_2)_7$-CH=CH-$(CH_2)_7$- (oleic acid), and CH_3-$(CH_2)_4$-CH=CH-CH_2-CH=CH-$(CH_2)_7$- (linoleic acid)

Figure 4.1 The general structure of fatty acids in palm oil.

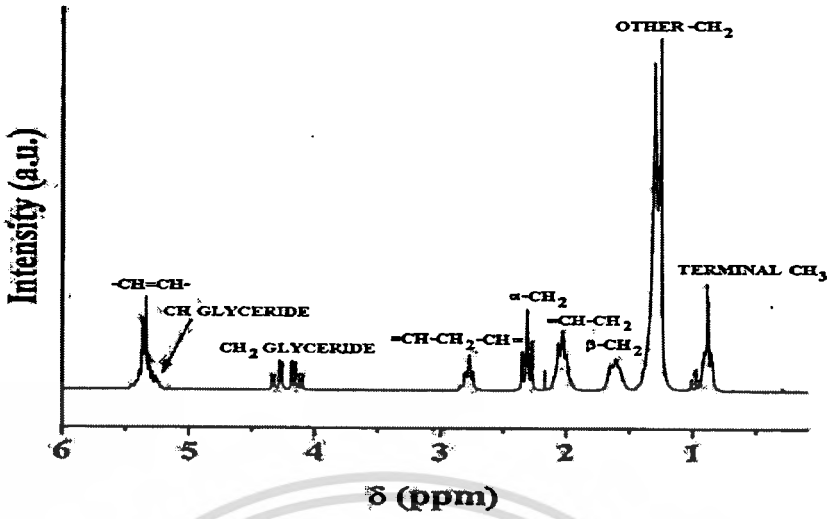

Figure 4.2 ^{1}H-NMR spectrum of refined palm oil in $CDCl_3$.

^{1}H-NMR spectrum of palm oil in $CDCl_3$ (Figure 4.2) shows the signals of methyl protons (CH_3-C-) and methylene protons (-C-CH_2-C-) at δ 0.85-0.88 and 1.25-1.30 ppm, respectively. The signal of –CH_2-C-COO-C– appears at δ 1.61 ppm. The signal of –CH_2-C=C– appears at δ 2.01-2.05 ppm. The signal of –CH_2-COO-C– appears at δ 2.28-2.33 ppm. The signal of –C=C-CH_2-C=C– appears at δ 2.74-2.76 ppm. The signals of –CH_2-OOC-R– and > CH-OOC-R appear at δ 4.11-4.17 and 4.27-4.32 ppm, respectively. The signal of –CH=CH– appears at δ 5.26-5.35 ppm.

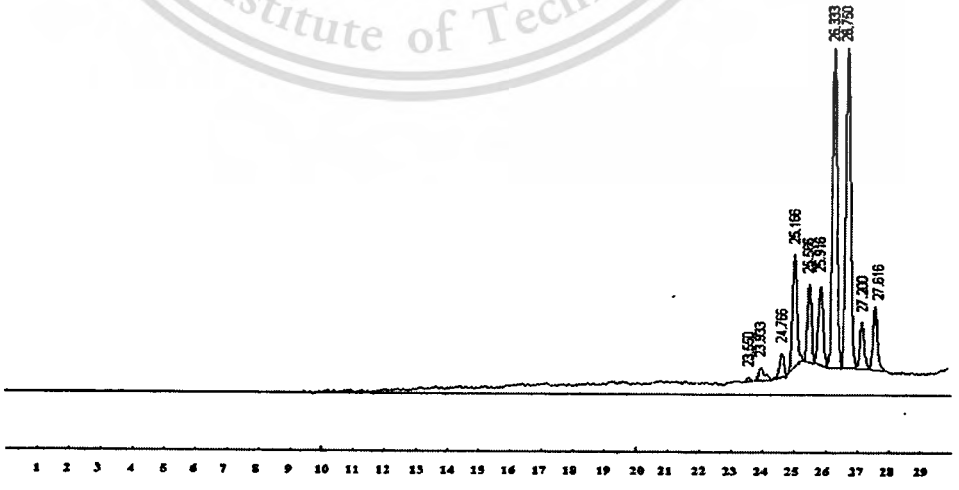

Figure 4.3 High Performance Liquid Chromatogram of refined palm oil.

The chromatogram of refined palm oil from high performance liquid chromatography is illustrated in Figure 4.3. The sample analysis was performed using Altima C18 (5μm) column; 150 mm. x 4.6 mm i.d., with a mobile phase of dichloromethane-acetonitrile (gradient), a flow rate of 1 ml/min at ambient, and drift tube temperature of 75 °C with nitrogen. The injector volume was 50 μl of 0.0125 g fatty acid product in 25 ml of 70:30 acetonitrile : dichloromethane. It shows that the peaks which belong to the triglycerides of refined palm oil appear at the retention time of 23-28 minutes.

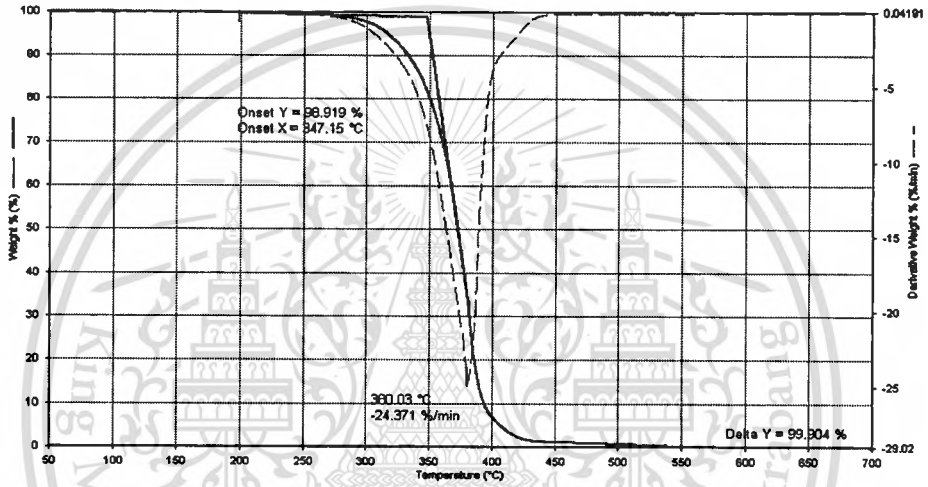

Figure 4.4 Thermal degradation of refined palm oil

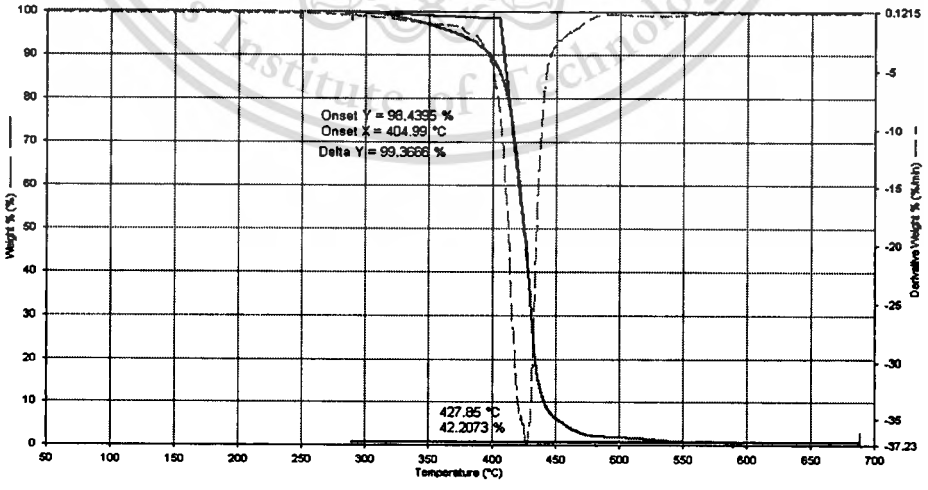

Figure 4.5 Oxidative degradation of refined palm oil

Figure 4.4 and 4.5 indicate that refined palm oil starts to evaporate rapidly from liquid to vapor accompanied by degradation. The thermal and oxidation stabilities were determined from the onset temperatures under nitrogen and oxygen atmospheres, which were found to be 380.03 °C and 427.85 °C, respectively [58].

4.2 Characterization of catalysts

Commercial alumina was calcined in air at 500 °C. The prepared zinc aluminate was characterized by X-ray diffraction methods. The XRD pattern shows that the product has a single phase and that the only peaks detected were the characteristic peaks of the cubic phase zinc aluminate. AAS analysis also showed the presence of Zn and Al in the 1:2 molar ratio confirming the formation of single-phase zinc aluminate particles. Zinc aluminate was then calcined in air at 600 °C for 5 hours. Both catalysts were kept in desiccator before used as catalyst for hydrolysis reactions.

4.2.1 Catalyst structure

Structure of catalysts was determined by X-ray Powder Diffractometer (D8 Avance, Bruker, Scientific Instruments Service Centre; KMITL). CuK∝ X-ray beam was used for analysis. X-ray diffraction patterns of alumina scanned from 2θ angle 20° to 60° after calcinations at 500 °C and zinc aluminate scanned from 2θ angle 20° to 80° after calcinations at 600 °C are shown in Figure 4.6 and 4.7, respectively.

Figure 4.6 shows the XRD pattern of highly crystalline alumina at 2θ = 25.4°, 35.02°, 37.62°, 43.2°, 52.4° and 57.34°. Figure 4.7 shows the XRD pattern of highly crystalline zinc aluminate at 2θ = 31.32°, 36.90°, 44.88°, 49.10°, 55.65°, 59.45°, 65.25°.

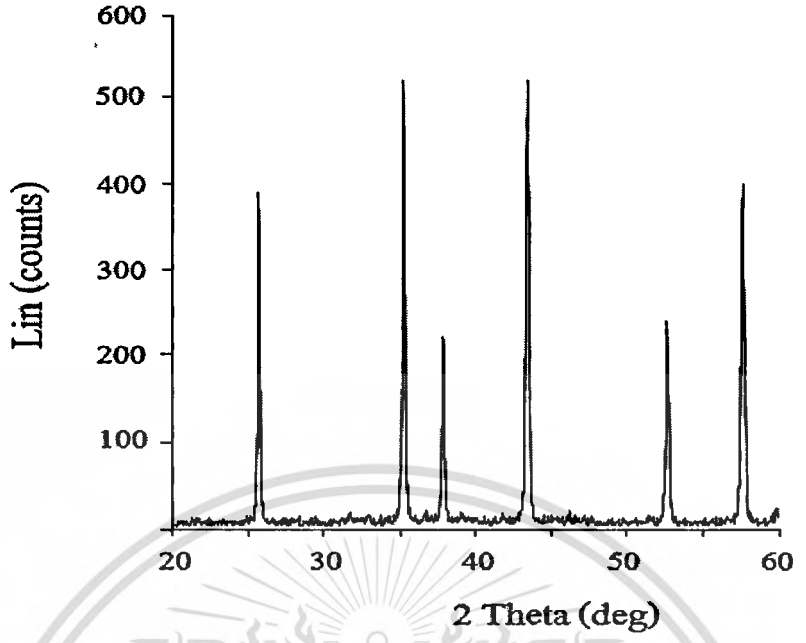

Figure 4.6 X-ray diffraction pattern of alumina.

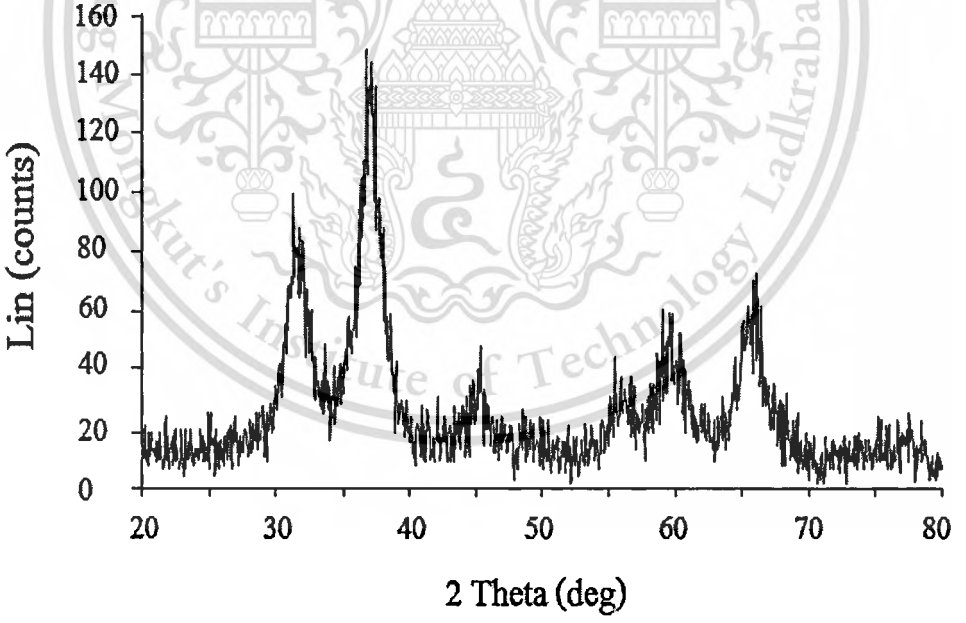

Figure 4.7 X-ray diffraction pattern of zinc aluminate.

4.2.2 Specific surface area

Surface area of solid oxides was determined by Gas Adsorption Analyzer (Autosorb-1C, Quantachrome). The nitrogen adsorption was measured at the partial pressure (P/P0) ranged from 10^{-6} to 1.0 at 77.4 K. The BET surface area analysis of calcined alumina at 500 °C and zinc aluminate at 600 °C are shown in Table 4.1.

Table 4.1 The specific surface areas of catalysts

Catalyst	Specific surface area (m^2/g)
Alumina (500 °C)	21.17
Zinc aluminate (600 °C)	130.19

4.2.3 Acidity/Basicity of the catalysts.

On the basis of the method described in sections 3.4.2.5 and 3.4.2.6 using Hammett indicators followed by the titration, acid/base site strength and acidity/basicity was determined [49,50]. Acidic or basic site strength was estimated according to solution color change. Alumina and zinc aluminate was found to be amphoteric with a site strength (H_0) in the range of 6.8 and 8.2. The benzene solutions from both catalysts gave an orange coloration with Neutral red (pKa strength between 6.8 and 8.2) whereas the methanol solutions from both catalysts were colorless with phenolphthalein (pKa strength between 0.0 and 8.2).

Table 4.2 depicts the type of catalyst with their site strength and acidity/basicity values. The acidity/basicity of catalyst was determined using a titration method [55]. For basicity, the basic catalyst (0.1 g) was suspended in 20 cm^2 of 0.01M HCl solution for 48 hours, then filtered to obtain the solution containing unreacted HCl which to be titrated with NaOH (0.01 mol/dm^3). In retrospect, for acidity determination, an acidic catalyst (0.1 g) was suspended in 20 cm^2 of 0.01M NaOH solution for 48 hours, then filtered to obtain the solution containing unreacted NaOH which to be titrated with HCl (0.01 mol/dm^3). Zinc aluminate was found to be of high acidity than alumina, with a acidity of 0.59 mmol of NaOH/g of zinc aluminate.

Table 4.2 Site strength of the metal oxides and their respective acidity/basicity value

Catalyst	Type	Acid/base site Strength, (H_0)	Acidity (mmol of NaOH/g of catalyst)	Basicity (mmol of HCl/g of catalyst)
Alumina	amphoteric	$6.8 < (H_0) < 8.2$	0.24	0.07
Zinc aluminate	amphoteric	$6.8 < (H_0) < 8.2$	0.59	0.26

4.3 Determination of the conversion and yield from hydrolysis

4.3.1 Nuclear Magnetic Resonance Spectrometer (NMR) to determine the yield

The yield of fatty acids in the reaction mixture at different time intervals determined by ^{1}H Nuclear Magnetic Resonance Spectroscopy. The triplet peaks appear with an intensity ratio of 1:2:1. The total area corresponding to α-CH_2 of both FFA and ester can be determined by integrating the spectral region at 2.20-2.41 ppm. The area of the unmerged peak of the FFA triplet can be determined by integration of the spectral region at 2.37-2.41 ppm. The weight percentage of FFA in oil is thus [51]

$$\text{Free fatty acids (FFA), \%} = \frac{4 \times \text{area of unmerged peak of } \alpha\text{-}CH_2 \text{ of FFA}}{\text{total area of } \alpha\text{-}CH_2 \text{ of both FFA and ester}} \times 100\%$$

The results are shown in Figures 4.8 and 4.9. During the hydrolysis of refined palm oil with water, the decrease of the ester in the reaction mixture was followed, as a function of time, by the ^{1}H NMR method. At the start of the reaction, ^{1}H NMR spectrum in the α-CH_2 region (2.3-2.4 ppm) showed quartetlike spectral pattern of the peaks of the triplet of FFA shifts out of the α-CH_2 region of the ester. The intensity of the triplet signals due to ester decreased and that of the fatty acids increased with the reaction time (Figure 4.9). Finally, at the end of 120 minutes, the peaks corresponding to ester disappeared, and only a triplet corresponding to that of the fatty acids was detected.

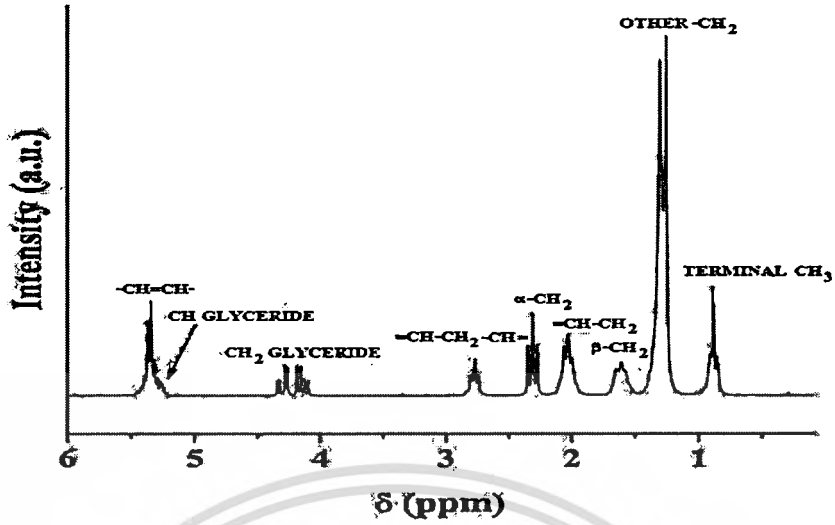

Figure 4.8 ^{1}H-NMR spectrum of refined palm oil.

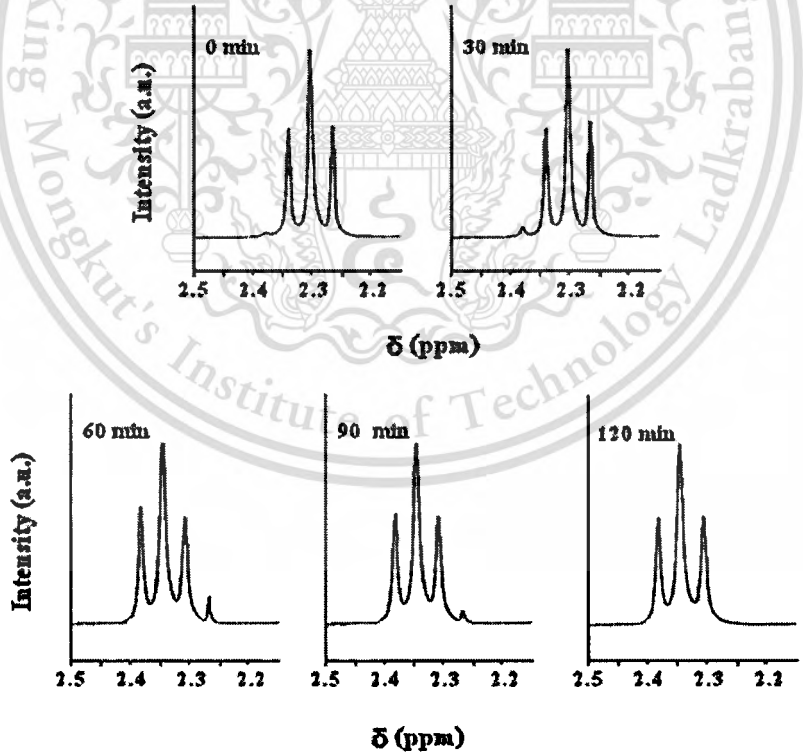

Figure 4.9 ^{1}H NMR spectra in the α-CH_2 region: non-catalytic reaction of refined palm oil with water as a function of time; *reaction condition: molar ratio of water to oil = 54, reaction temperature = 240 °C.*

4.3.2 High Performance Liquid Chromatography (HPLC) to determine the conversion

In this research, the percent conversion of triglycerides was determined using High Performance Liquid Chromatography. These triglycerides separated by high performance liquid chromatography appear at the retention time between 23-28 minutes in chromatograms, while the peaks observed at the retention time of 15-23 minutes are believed to be partially hydrolysed esters such as diglycerides. Monoglycerides appear at the retention time of less than 13 minutes. A similar result has also been reported by Joshi, Toler and Walker [52, 53] which studied the production of biodiesel by transesterification of cottonseed oil. The reaction was carried out using ethanol and potassium hydroxide (KOH). The biodiesel was analyzed for conversion using a HPLC equipped with an ELSD detector. The mobile phase was a mixture of acetonitrile and dichloromethane. During the transesterification process, intermediate glycerols such as monoacylglycerols (MAGs) separated by high performance liquid chromatography appear at the retention time of less than 13 minutes, diacylglycerols (DAGs) appear at the retention time of 15-23 minutes and triglycerides appear at the retention time between 23-28 minutes in the final biodiesel product.

For example, it is found that the HPLC chromatogram of sample 2 (Figure 4.11) is different from that of sample 1 (Figure 4.10) in which the peaks of triglycerides completely disappear due to the complete conversion. The conversion of triglycerides calculated from HPLC chromatogram will be discussed in Appendix A

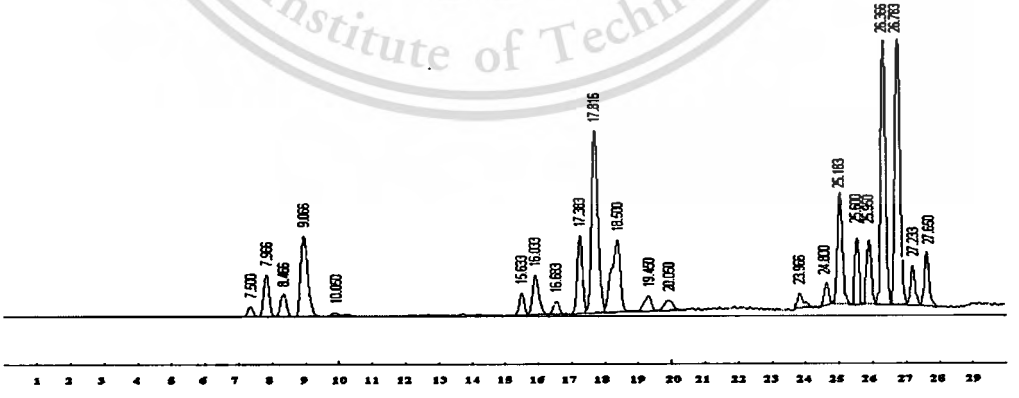

Figure 4.10 High Performance Liquid Chromatogram of non-catalytic reaction of refined palm oil with water; *reaction condition: molar ratio of water to oil = 54, reaction temperature = 230 °C, reaction time 30 min*utes (sample 1).

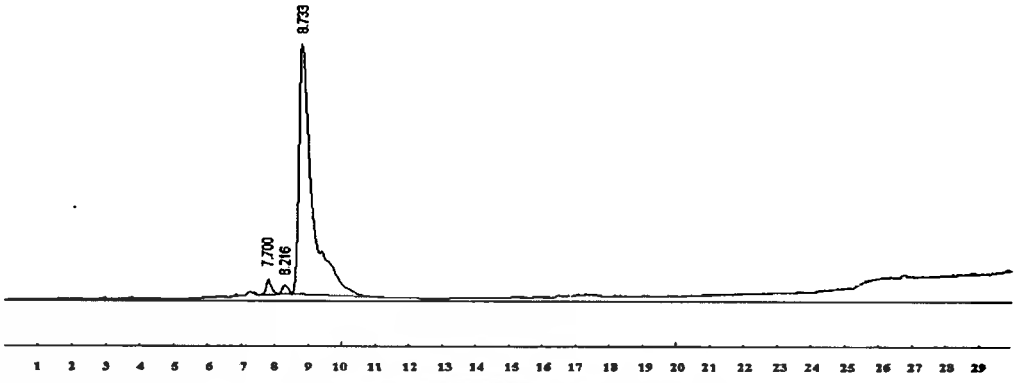

Figure 4.11 High Performance Liquid Chromatogram of non-catalytic reaction of refined palm oil with water; *reaction condition: molar ratio of water to oil = 54, reaction temperature = 230 °C, reaction time 120 min*utes (sample 2).

4.4 Effect of parameters on hydrolysis

The hydrolysis reactions of refined palm oil were carried out in a Teflon-lined stainless-steel autoclave under autogeneous pressure in the non-catalytic and catalytic hydrolysis methods. Solid oxide catalysts, namely alumina and zinc aluminate, were used. The variables affecting the conversion and yield of hydrolysis reaction, such as the type of catalysts, amount of catalyst, reaction temperature, calcination temperature, reaction time and the molar ratio of water to palm oil were investigated. The results were also compared with that from the reaction using no catalyst. Furthermore, the reuse of both catalysts were also investigated in this research.

4.4.1 The effect of the calcination of catalysts

The effect of calcination temperatures on the catalytic properties of alumina and zinc aluminate were investigated with the goal to determine the optimum pretreatment temperature and to understand the nature of active sites for hydrolysis reaction. To activate the catalyst, alumina and zinc aluminate were dehydrated and pretreated for 5 hours in air in a furnace at calcination temperatures from 400 °C to 700 °C. Catalyst total surface area was determined using a multipoint BET method. The individual phase of alumina and zinc aluminate alone was identified at the minimal temperature at 400 °C. As the calcination temperature increased, a decrease in its specific surface area was detected as shown in Table 4.3.

Table 4.3 Properties for catalysts calcined at various temperatures.

Calcination temperature (°C)	BET surface area (m^2/g)	
	Alumina	Zinc aluminate
400	21.58	299.03
500	21.17	194.67
600	18.55	130.91
700	18.02	86.46

Figure 4.12 shows the XRD pattern of highly crystalline alumina at 2θ = 25.4°, 35.02°, 37.62°, 43.2°, 52.4° and 57.34°. It can be deduced that the structure of alumina was not changed, however, the peak intensity was increased with the calcination temperatures due to an increasing in its crystallinity.

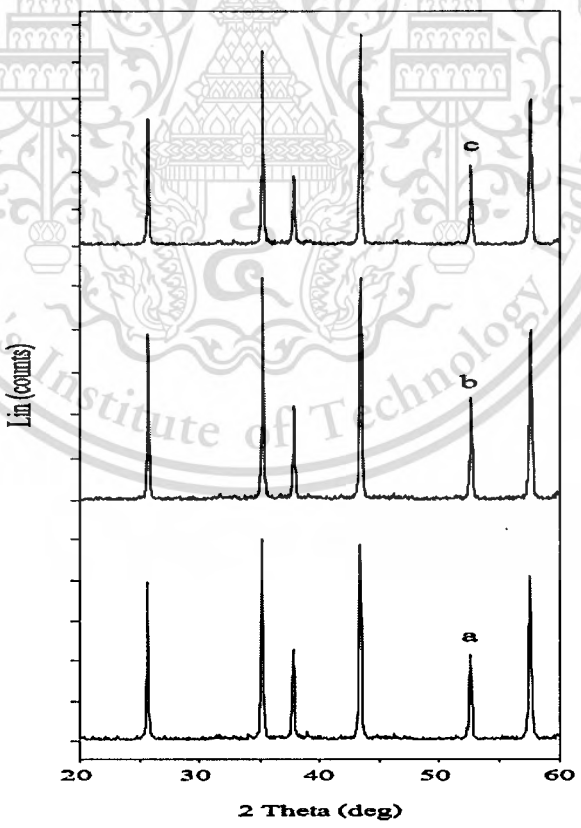

Figure 4.12 XRD diffraction patterns of alumina calcined at various temperatures; (a) calcined at 400 °C; (b) calcined at 500 °C; (c) calcined at 600 °C.

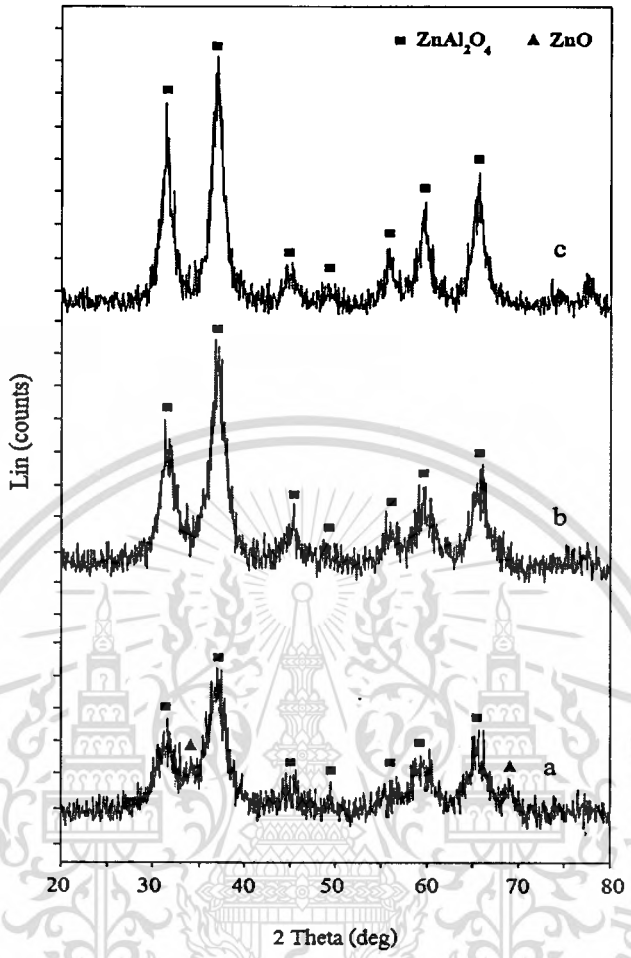

Figure 4.13 XRD diffraction patterns of zinc aluminate calcined at various temperatures; (a) calcined at 500 °C; (b) calcined at 600 °C; (c) calcined at 700 °C.

The purity and crystallinity of the zinc aluminate nanoparticles were examined by using powder X-ray diffraction (XRD), as shown in Figure 4.13. The diffraction peaks are broadened markedly due to the small size effect of the particles. The peaks appearing at 2θ = 31.32°, 36.90°, 44.88°, 49.10°, 55.65°, 59.45°, 65.25°, 74.07°, and 77.35°can be indexed as (2 2 0), (3 1 1), (4 0 0), (3 3 1), (4 2 2), (5 1 1), (4 4 0), (6 2 0), and (5 3 3) crystal planes of the cubic crystalline structure of zinc aluminate, respectively, in accordance with the standard JCPDS card of cubic spinel-type zinc aluminate (JCPDS File No. 05-0669). AAs analysis showed the presence of Zn and Al in the 1:2 molar ratio confirming the formation of single-phase zinc aluminate particles. The catalyst samples calcined for 5 hours from 600 to 700 °C (Figure 4.13 (b) and (c)) showed clear and sharp peaks of a crystalline phase of zinc aluminate. In contrast, the calcined catalyst at 500 °C

(Figure 4.13 (a)) exhibited the mixed crystalline phases between zinc oxide and zinc aluminate. The XRD pattern of the sample shows the value of full width at half maximum (FWHM) for the (3 1 1) diffraction peaks decrease slightly and the intensity of the diffraction peaks increases after the calcinations what is associated with an increase in the degree of crystallinity and in the crystallite size. The sample obtained by calcination of the precursor above 500 °C is a single-phase material, and no impurities are observed in the resulting product. It was consistently reported by X. Wei and D. Chen [34] which showed that the high purity of zinc aluminate can be achieved in the preparation of nanosized $ZnAl_2O_4$ when calcination temperature was raised.

To determine the effect of the calcination temperature of catalysts, the hydrolysis reactions of refined palm oil were carried out with a fixed water molar ratio of 54:1, reaction temperature of 230 °C and 3.0 wt.% of solid oxides pretreated at varied calcination temperature from 400 °C to 700 °C. The results are given in Table 4.4 which shows the relationships between the calcination temperatures of catalysts and yield of fatty acids. The activity-changed profiles indicate that the catalytic activities depend on the calcination temperature. After calcinations at elevated temperatures from 400 to 700 °C, the catalysts exhibited the increased catalytic activity. This suggests that the high temperature pretreatment is indispensable for getting high activities of the catalysts.

Table 4.4 The effect of the calcinations temperature of catalysts on % yield of fatty acid; reaction condition: reaction temperature = 230 °C, molar ratio of water to refined palm oil = 54, 3.0 wt.% of catalysts, reaction time = 60 minutes.

Catalyst / Calcination Temperature (°C)	Alumina	Zinc aluminate
	% yield of fatty acids	% yield of fatty acids
400	54.05	68.23
500	61.56	70.95
600	58.72	77.74
700	61.31	73.57

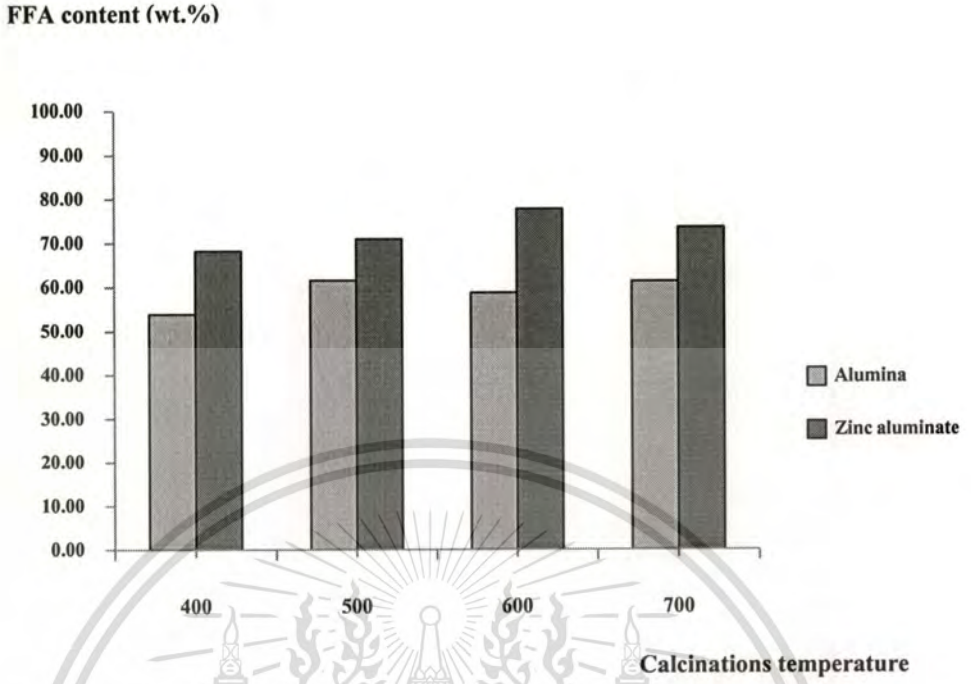

Figure 4.14 Effect of the calcination temperatures of catalysts on % yield of fatty acid; *reaction condition: reaction temperature = 230 °C, 3.0 wt.% of catalysts, reaction time = 60 minutes, molar ratio of water to refined palm oil = 54.*

As shown in Figure 4.14, the yield of fatty acids using alumina and zinc aluminate are gradually increased at first with the rise of calcination temperature from 400 °C. This is because of the increase in crystallinity with no impurities at higher temperatures. For alumina, the yield of fatty acids boosted up to 500 °C before finally becoming almost constant because the sinterability of alumina is very low. This is consistent with previous research by R. Sarkar et. al. [58] which shown that only the high calcination temperature above 1600 °C resulted in greater agglomeration of alumina particles.

The morphology of alumina and the agglomeration of alumina particles were studied by scanning electron microscopy (Figure 4.15). It was found that the catalysts had no significant changes in the crystal morphology and size when calcination temperature rised.

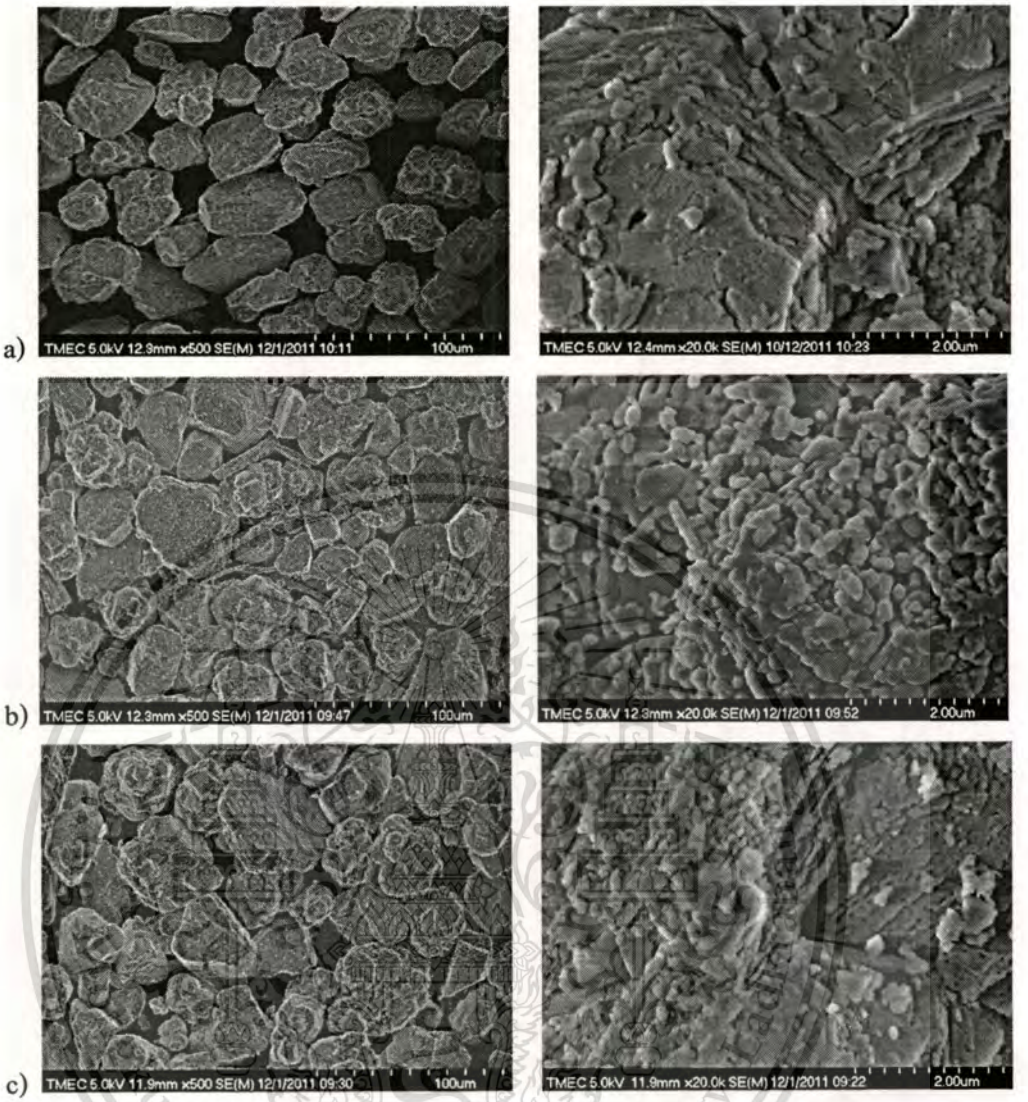

Figure 4.15 SEM images of alumina calcined at various temperatures; (a) calcined at 400 °C; (b) calcined at 500 °C; (c) calcined at 600 °C.

As for zinc aluminate, the obtained yields of fatty acids over the catalyst calcined at 400-500 °C lower than that at 600-700 °C. This was attributed to the complete formation of zinc aluminate calcined at 600-700 °C as suggested by XRD results (Figure 4.13). However the yields of fatty acids over the catalyst calcined at 700 °C lower than that at 600 °C. This is because of a decrease in their specific surface area caused by sintering of the catalyst particles as observed by scanning electron microscopy (Figure 4.16). It has been shown that the agglomerate of zinc aluminate particles size grows with the rise in calcination temperature. M. Zayat and D. Levy [57] reported on the synthesis of cobalt aluminate particles prepared by the sol-gel method. The

particles were calcined to temperatures between 400 and 1000 °C, for the formation of the mixed oxide having spinel structure. The surface properties of the different samples (BET surface area and pore size distribution) were measured. The specific surface areas of cobalt aluminate powders were found to depend strongly on the calcination temperature. All samples showed a remarked tendency to sinter, decreasing in surface area as the temperature was raised.

The optimum calcination temperature was found to be 500 °C for alumina and 600 °C for zinc aluminate which gave the highest catalytic activity for the hydrolysis reaction.

Figure 4.16 SEM images of zinc aluminate calcined at various temperatures; (d) calcined at 500 °C; (e) calcined at 600 °C; (f) calcined at 700 °C.

4.4.2 The effect of the amount of catalyst

In this research, the amount of catalyst was varied from 0.0 to 5.0 wt.% while the calcinations temperature of alumina was fixed at 500 °C and zinc aluminate was fixed at 600 °C, reaction temperature was fixed at 230 °C, water to oil molar ratio of 54, reaction time of 60 minutes, respectively. The effect of the amount of catalyst on percent yield are shown in Table 4.5 and plotted in Figures 4.17, the yield of the reaction increased with the amount of catalyst. It can be assure that alumina and zinc aluminate can evidently accelerate the fatty acids yield even if a small amount was added. When the amount of catalysts increased to 3.0 wt.%, the yields of 58.72 % and 77.74 % were reached using alumina and zinc aluminate, respectively. The hydrolysis rate was significantly improved as the amount of catalysts increased from 0.0 to 5.0 wt.%. However, since the percent yield of fatty acid increased a little when the amount of catalyst was further increased from 3.0 to 5.0 wt.%, therefore 3.0 wt.% of both catalysts was chosen.

Table 4.5 The effect of the amount of catalyst on % yield of fatty acids; reaction condition: reaction temperature = 230 °C, molar ratio of water to refined palm oil = 54, reaction time = 60 minutes.

Catalyst / wt. % of catalyst	Alumina	Zinc alumiante
	% yield of fatty acids	% yield of fatty acids
0.0	42.04	42.04
1.0	47.98	66.67
2.0	54.57	74.98
3.0	58.72	77.74
4.0	58.90	78.91
5.0	59.32	81.25

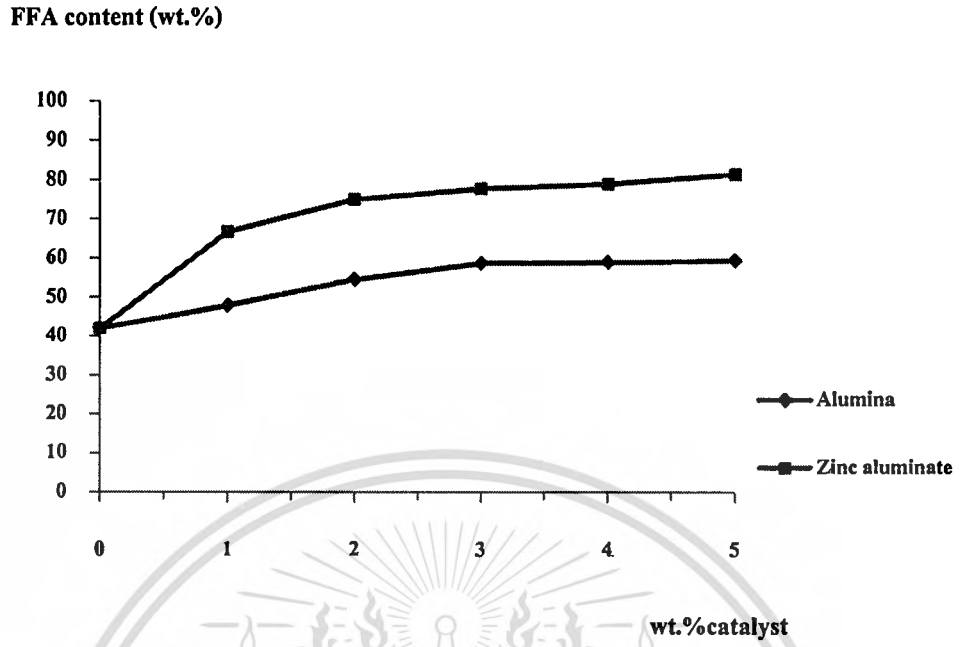

Figure 4.17 Effect of the amount of catalyst on % yield of fatty acids; *reaction condition: reaction temperature = 230 °C, molar ratio of methanol to palm oil = 54, reaction time = 60 minutes.*

4.4.3 The effect of water to oil ratio

The mechanistic for the heterogeneous catalysed hydrolysis was shown to be in principle similar to homogeneous catalyzed hydrolysis. Both triglyceride and water can be adsorbed on the zinc aluminate. The reaction mechanism of acid catalysed hydrolysis is suggested in Figure. 4.18. The interaction of the carbonyl oxygen of fatty acid with the Lewis acidic site (L^+) of the catalyst forms carbocation. The nucleophilic attack of water to the carbocation produces a tetrahedral intermediate, the new ester desorbs from the Lewis site and the cycle is repeated. The reaction mechanism of base catalysed hydrolysis is suggested in Figure. 4.19. Water can be adsorbed on the base site (B^-) of the catalyst and forms oxygen anion. The nucleophilic attack of water to the esters produces a tetrahedral intermediate. Then the hydroxyl group breaks and forms two kinds of esters. In both cases, these cycles are repeated twice to ultimately yield FFAs and glycerol as final product.

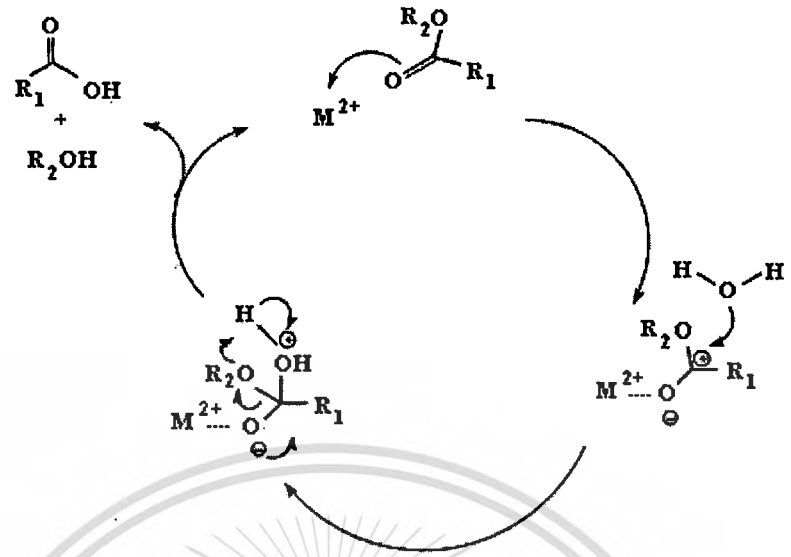

R1, R2: Carbon chain of fatty acid.

Figure 4.18 Proposed catalytic cycle for zinc aluminate in acid catalysed hydrolysis.

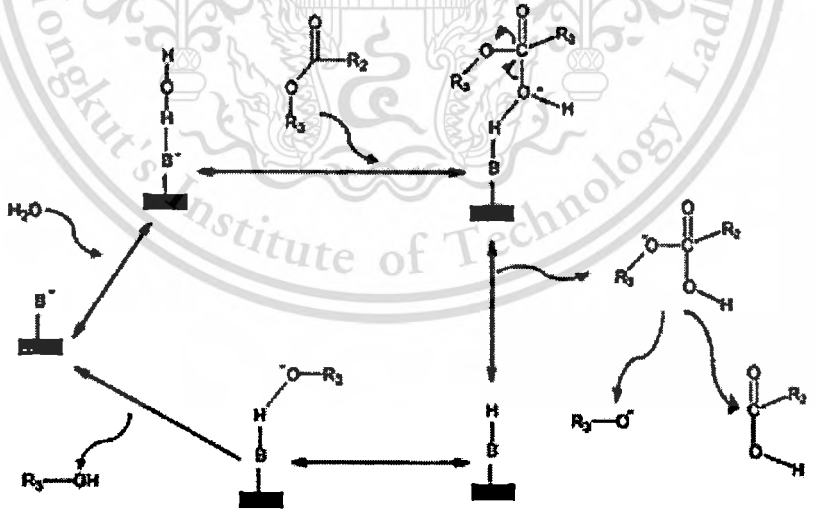

B: Base site on the catalyst surface

R2, R3: Carbon chain of fatty acid.

Figure 4.19 Schematic representation of possible mechanism for base catalysed hydrolysis of triglyceride.

The molar ratio of water to refined palm oil is one of the most important variables affecting the conversion of refined palm oil and the yield of fatty acids converted. The stoichiometric molar ratio of water to palm oil was 3:1. But when the mass transfer was limited due to problems of mixing, the mass transfer rate seemed to be much slower than the reaction rate, so the molar ratio of water to oil should be higher than that of stoichiometric ratio in order to drive the reaction towards completion and produce more fatty acids as product.

The effect of molar ratio of water to refined palm oil was varied within a range between 13:1 to 108:1. The reactions were carried out with 3.0 wt.% of both catalysts, reaction time of 60 minutes at 230 °C. The experimental results are shown in Table 4.6 and are plotted in Figures 4.20 which shows the relationships between the molar ratio of water to refined palm oil, and yield of fatty acids from non-catalytic and catalytic hydrolysis reaction. The fatty acids yield increased as the molar ratio increased. However, after the 54:1 molar ratio of water to refined palm oil was used, the yield increased slowly because the glycerine by product reach equilibrium conditions. At the point of equilibrium, the rates of hydrolysis and re-esterification are equal. The glycerine byproduct must be withdrawn continuously to force the reaction to completion [40]. The water to refined palm oil molar ratio of 54:1 clearly results in the best hydrolysis reaction in which the yields of 58.72 % and 77.74 % were reached using alumina and zinc aluminate within 60 minutes.

Kusdiana and Saka [14] has reported that, without a catalyst, the best hydrolysis reaction of rapeseed oil required the water to oil molar ratio of 54:1, a 80 % yield of fatty acids was observed in 20 minutes under a high reaction temperature (at 270 °C) and high pressure (above 70 bar), which are not viable in practice in industry. However, the results achieved in this research with the used of zinc aluminate showed that the water to refined palm oil molar ratio of 54:1 clearly results in the better hydrolysis reaction that occur under milder reaction conditions.

Table 4.6 The effect of the molar ratio of water to refined palm oil on % yield of fatty acids; reaction condition: reaction temperature = 230 °C, 3.0 wt.% of catalysts, reaction time = 60 minutes.

Catalyst / Water : oil	Non catalyst	Alumina	Zinc aluminate
	% yield of fatty acids	% yield of fatty acids	% yield of fatty acids
13:1	32.27	44.38	66.02
26:1	38.37	55.58	74.31
54:1	42.04	58.72	77.74
81:1	42.59	60.97	77.66
108:1	43.77	61.85	77.48

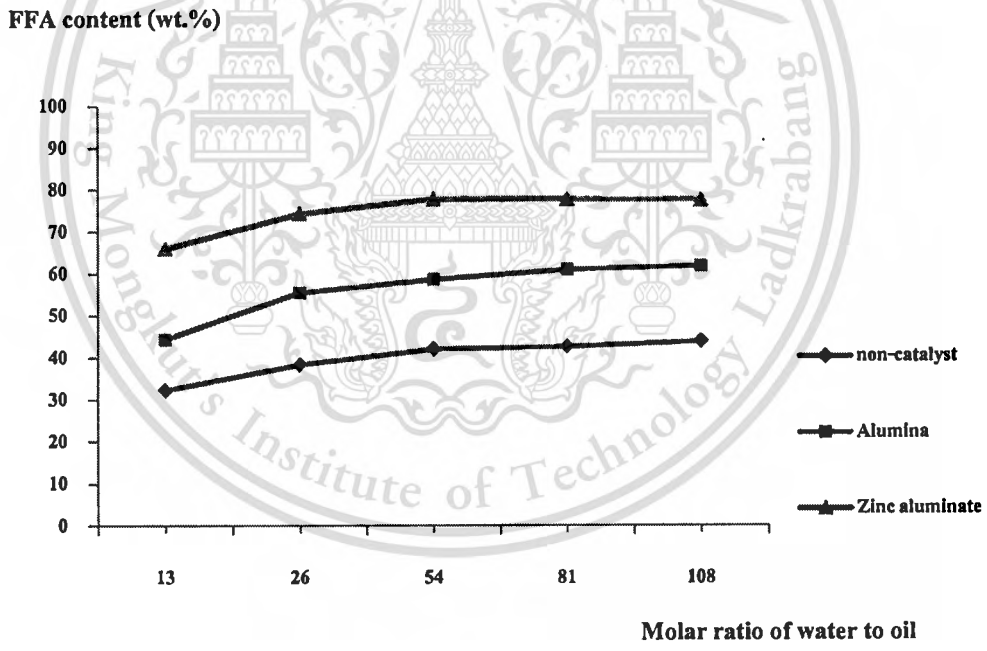

Figure 4.20 Effect of the molar ratio of water to refined palm oil on % yield of fatty acids; *reaction condition: reaction temperature= 230 °C, 3.0 wt.% of catalysts, reaction time = 60 minutes.*

The total surface area of catalyst has tremendous effect on the reaction rate. The rate of reaction increases when the surface area increased because the high surface area means many active sites per mass unit of the catalyst. Both catalysts in this thesis were determined by nitrogen physisorption. BET specific surface areas of zinc aluminate and alumina were 130.19 m^2/g and 21.17 m^2/g, respectively. Zinc aluminate had higher surface area than alumina, which gave high catalytic activity for hydrolysis.

The relationship between the surface hydrophobicity and the catalyst's activity are also very important. The mechanism of hydrophilic solid acid catalyzed hydrolysis showed in Figure 4.21 indicates that water does indeed have an inhibitory effect on hydrolysis on a solid acid surface by competing for active sites on the catalyst surface. Water molecules are well known to adsorb on hydrophilic solid acid sites [38]. As the zinc aluminate has hydrophobic nature, the triglycerides adsorption is improved. Therefore, the palm oil conversion is elevated.

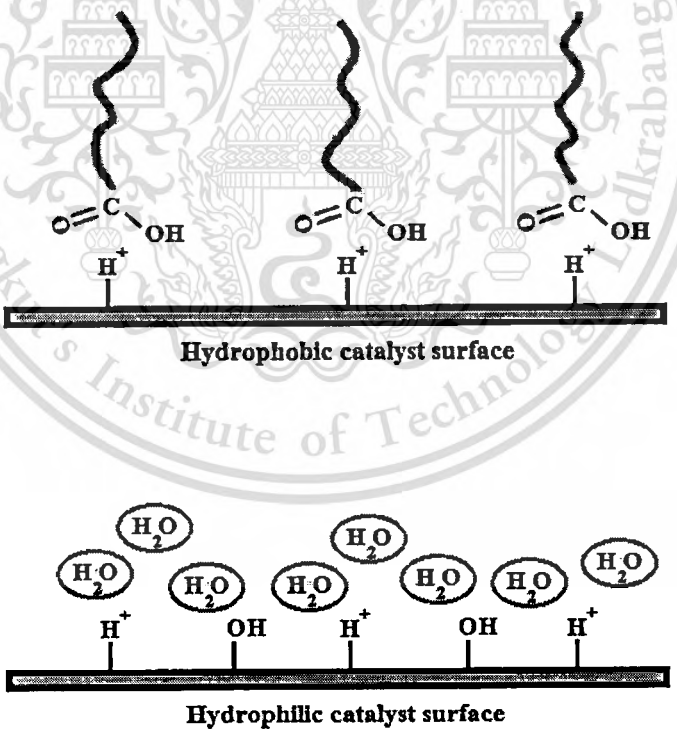

Figure 4.21 Influence of the surface hydrophobicity on the catalytic activity; (top) adsorption of a fatty acid on a hydrophobic catalyst; (bottom) formation of water layer on hydrophilic catalyst [38].

4.4.4 The effect of reaction temperature

To determine the effect of reaction temperature on the fatty acid formation, hydrolysis reactions of refined palm oil were carried out with a fixed water to refined palm oil molar ratio of 54:1. The reaction temperature was varied from 220 °C to 240 °C, using 3.0 wt.% of alumina, 3.0 wt.% of zinc aluminate and no catalyst, respectively. Table 4.7 and Figures 4.22 show the relationships between the temperature with fatty acids yield of non-catalytic and catalytic hydrolysis refined palm oil. Temperature plays an important role in the hydrolysis of fats and oils. Increasing reaction temperature can lead to better reaction kinetics and improved phase miscibility, important in a potentially diffusion-limited process. It was observed that increasing in the reaction temperature had a favorable influence on fatty acids yield. This is because liquid water is a polar solvent and has hydrogen bondings. As the fact that the degree of hydrogen bonding decreases with increasing temperature. This phenomenon with the high temperature conditions seems to be likely to promote hydrolysis reaction of refined palm oil [40].

As shown in Table 4.7 and Figures 4.22, the yields of fatty acids were relatively low even after a 60 minutes in non-catalytic reaction. At 220 °C with the use of catalysts, the yields of fatty acids were enormously improved, with alumina at 29.31 % and zinc aluminate at 48.64 %, respectively. As the temperature increased, the yield continued to improve markedly and zinc aluminate gave higher yield than alumina at the same reaction temperatures. The results indicated that when the reaction temperature was raised to 240 °C at pressure of 30 bar, the highest yields of fatty acids with alumina and zinc aluminate catalyst which were 86.02 % and 100.00 %, respectively, were achieved. This result is shown to be more commercially practical when compared to those from the previous researches. Alenezi, G.A. Leekea, R.C.D. Santos and A.R. Khan [44] studied the thermal non-catalytic hydrolysis of sunflower oil with subcritical water. A number of experimental runs were conducted in a tubular reactor over a range of temperatures from 270 °C to 350 °C and reaction times (up to 30 min) at 200 bar and was found to be an effective method for producing a fatty acid yield of greater than 90 % without any catalyst. Such high temperatures and pressures lead to high energy consumption.

Table 4.7 The effect of the reaction temperature on % yield of fatty acids; reaction condition; molar ratio of water to oil = 54, 3.0 wt.% of catalysts, reaction time = 60 minutes, reaction temperature 220 °C, 230 °C and 240 °C.

Catalyst / Reaction Temperature (°C)	Non catalyst	Alumina	Zinc aluminate
	% yield of fatty acids	% yield of fatty acids	% yield of fatty acids
220	16.18	29.31	48.64
230	42.04	58.72	77.74
240	73.86	86.02	100.00

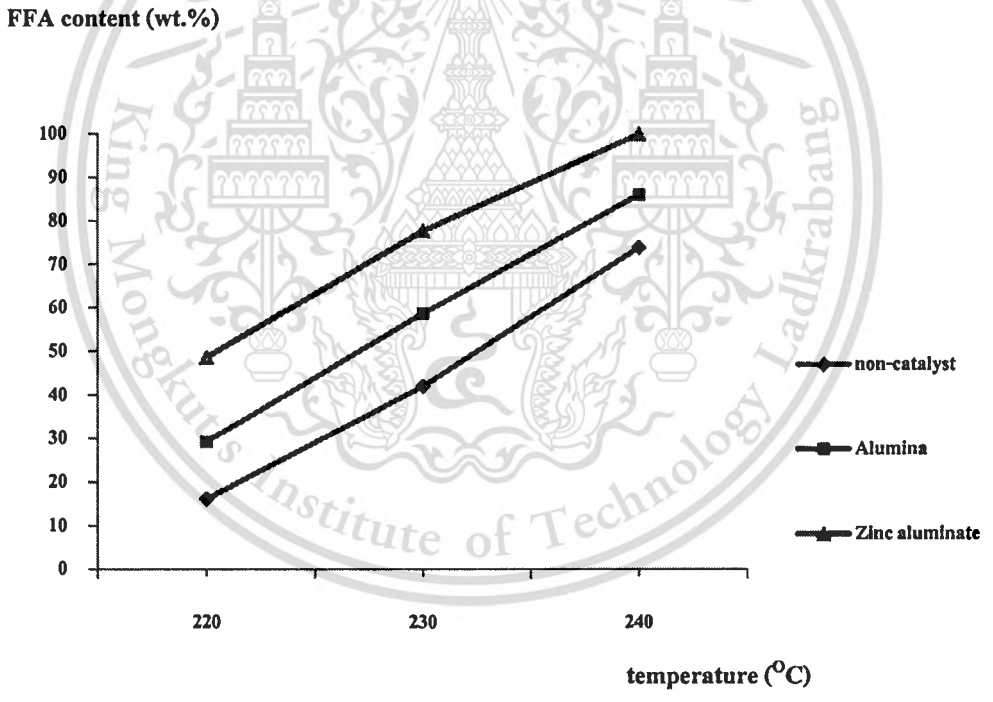

Figure 4.22 Effect of the reaction temperature on % yield of fatty acids; *reaction condition: molar ratio of water to oil = 54, 3.0 wt.% of catalysts, reaction time = 60 minutes, reaction temperature 220 °C, 230 °C and 240 °C.*

4.4.5 The effect of reaction time

The effect of reaction time on percent conversion and yield of fatty acids were investigated. The conditions were carried out with a fixed water molar ratio of 54:1, reaction time after the designated temperature was reached was varied from 30 minutes to 150 minutes, with 0.0 wt.% and 3.0 wt.% of alumina or zinc aluminate, respectively. The conversion and yield of the hydrolysis reaction at different reaction time are shown in Table 4.8, Figure 4.23 and Figure 4.24. After the reactor's temperature reached the pre-set temperature, the fatty acids conversion and yield increased with increasing in reaction time for both catalytic and non-catalytic reactions. Considering both alumina and zinc aluminate, it was found that the percent conversion and yield were boosted up in 60 minutes before finally became constant. This was due to the high reaction rate over the start of the reaction. Zinc aluminate gave higher conversion and yield than alumina over the same reaction time. Zinc aluminate gave 100.00 % yield within 60 minutes while alumina gave 86.02 % yield within 60 minutes of the reaction. At 240 $^{\circ}$C, a 60 minutes hydrolysis resulted in high conversion of triglyceride and yield of fatty acids.

J.K. Satyarthi, D. Srinivas and P. Ratnasamy [40] found that solid Fe-Zn double-metal cyanide (DMC) complexes exhibit high catalytic activity for hydrolysis of soybean oil. In a batch reaction, complete conversion of triglycerides and fatty acid yields greater than 73% were obtained at 463 K, autogenous pressure and with 5 wt.% of catalyst. The kinetics of hydrolysis of soybean oil was also monitored by ^{1}H NMR spectroscopy, it can be concluded that the conversion of triglycerides and rate of fatty acids formation was increased with time and remained nearly constant after 8 hours. From Figure 4.23 and 4.24, the results from this research were found to be in the same case that the conversion of triglycerides and reaction rate was increased by increased the reaction time during 0-60 minutes.

Table 4.8 The effect of reaction time on % conversion of refined palm oil and yield of fatty acids; reaction condition: molar ratio of water to oil = 54, 3.0 wt.% of catalysts, reaction temperature = 240 °C.

Catalyst / Time (minutes)	Non catalyst		Alumina		Zinc aluminate	
	% yield	%conversion	% yield	%conversion	% yield	%conversion
30	19.43	56.46	33.79	63.46	57.18	74.28
60	73.86	85.65	86.02	96.85	100.00	100.00
90	90.29	96.97	100.00	100.00	100.00	100.00
120	100.00	100.00	100.00	100.00	100.00	100.00
150	100.00	100.00	100.00	100.00	100.00	100.00

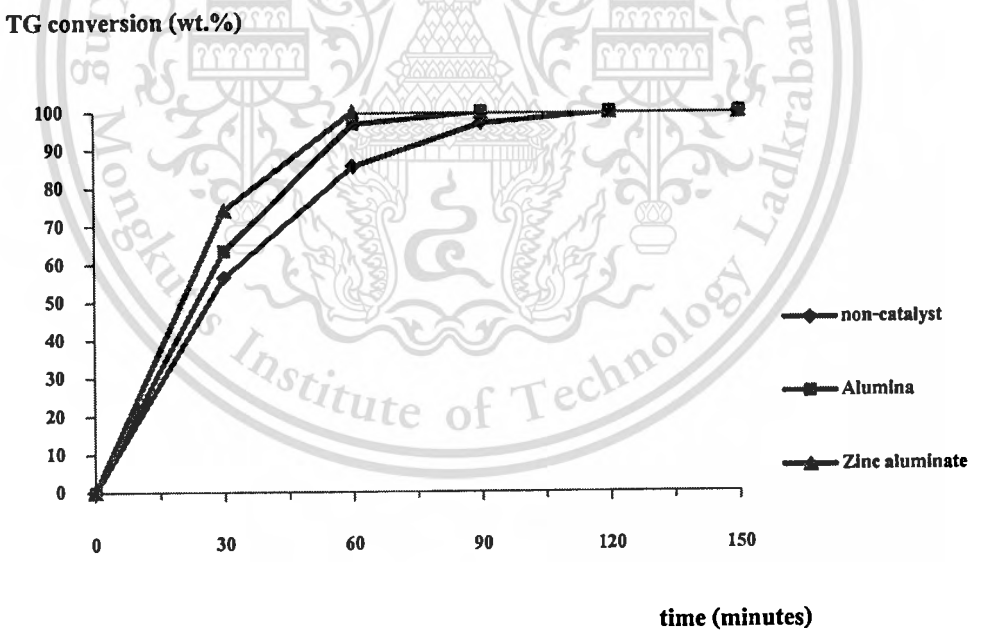

Figure 4.23 Effect of the reaction time on % conversion of refined palm oil; *reaction condition: molar ratio of water to oil = 54, 3.0 wt.% of catalysts, reaction temperature= 240 °C.*

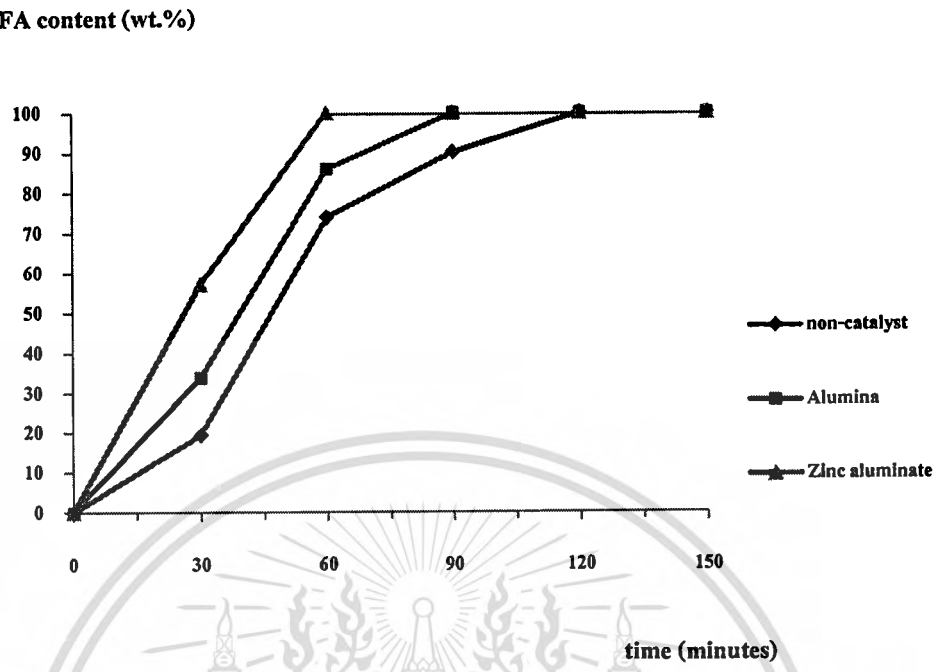

Figure 4.24 Effect of the reaction time on % yield of fatty acids; *reaction condition: molar ratio of water to oil = 54, 3.0 wt.% of catalysts, reaction temperature = 240 °C.*

4.4.6 The effect of the type of catalyst

The catalyst is an important factor in the hydrolysis reaction. The effect of the type of catalyst, alumina and zinc aluminate, was studied. The results are shown in Table 4.8 and are illustrated as shown in Figures 4.23 and 4.24. The reactions were carried out with a fixed water molar ratio of 54:1 with reaction time varied from 0 to 150 minutes at 240 °C using 3.0 wt.% of alumina and zinc aluminate, respectively. The results showed that, over the same reaction temperature, zinc aluminate gave higher conversion and yield than alumina. The reaction with zinc aluminate approached to 100.00 % conversion and 100.00 % yield after 60 minutes, while alumina gave 95.41 % conversion and 86.02 % yield after the same period. By considerating both solid oxides, it is clear that zinc aluminate has higher activity for hydrolysis than alumina because zinc aluminate higher surface area than alumina.

4.4.7 The reuse of catalysts

Alumina and zinc aluminate are representative heterogeneous solid catalysts for the hydrolysis of refined palm oils to fatty acids. The use of zinc aluminate catalyst in the transesterification of vegetable oil have been reported by Veronique Pugnet [5]. The experimental conditions of the reaction have been extensively studied. The leaching of active species has been thoroughly studied with zinc oxides and zinc aluminates at 200 °C in a stainless steel (SS) reactor. Zinc aluminate has been proven to be stable and active in the transesterification reaction of oil by methanol in a batch process. This study investigated and compared their stability and reusability in hydrolysis.

The reusability of the catalyst was investigated in the reactions with both used alumina and zinc aluminate which were attempted using fixed water molar ratio of 54 at 240 °C for 60 minutes with 3.0 wt.% of solid oxide catalysts. The collected alumina and zinc aluminate were then reused under the same reaction condition and were then called the reused catalysts. After the reaction was stopped, percent of fatty acids yield were determined. Both reused catalysts were washed with acetone to removed organic deposit. The alumina and zinc aluminate were then dried in oven at 120 °C for 12 hours. They were again reused as the catalyst in the next run under the same conditions. The conversion and yield of the hydrolysis reaction were presented in Table 4.9, Figure 4.25 and Figure 4.26. It showed that alumina and zinc aluminate catalyzed fatty acids yields were in excess of 80 % and 92 % at 240 °C for 60 minutes. It maintained sustained activity even after being used for 5 cycles and the fatty acids yield was only slightly decreased. These results suggested that the loss of hydrolysis activity in the present case mainly derived from the dissolution of active metal. Considering the weight of catalysts before and after used in hydrolysis reaction as shown in Table 4.10, it was found that used alumina and zinc aluminate was disappeared in significant quantity after filtration. In order to find the reason to disapperance of both used catalysts, they were subjected to X-ray powder diffractometer.

Table 4.9 Percent conversion of refined palm oil and yield of fatty acids by using fresh, reused alumina and reused zinc aluminate catalysts; reaction condition: 3.0 wt.% of solid oxide, reaction time = 60 minutes, molar ratio of water to oil = 54, temperature = 240 °C.

Catalyst / Repeated time	Alumina		Zinc alumiante	
	% yield	% conversion	% yield	% conversion
1	86.02	96.85	100.00	100.00
2	82.83	98.00	97.33	100.00
3	81.68	98.21	99.49	100.00
4	80.37	97.01	96.03	100.00
5	81.39	98.29	95.92	100.00

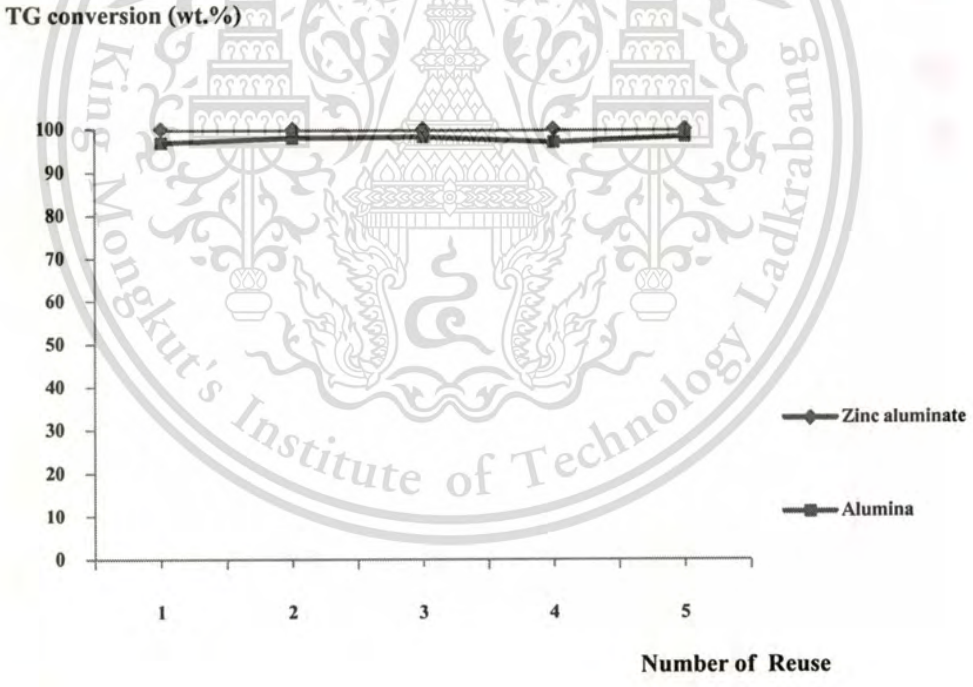

Figure 4.25 Effect of reuse of alumina and zinc aluminate catalysts on % conversion of refined palm oil; *reaction condition: molar ratio of water to oil = 54, 3.0 wt.% of catalysts, reaction time = 60 minutes, reaction temperature = 240 °C.*

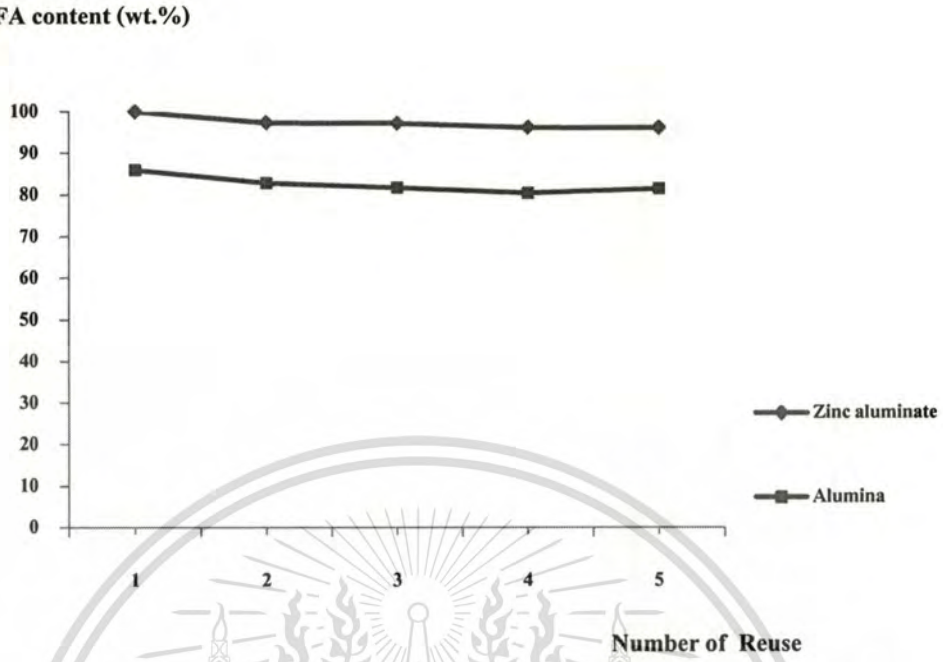

Figure 4.26 Effect of reuse of alumina and zinc aluminate catalysts on % yield of fatty acids; *reaction condition: molar ratio of water to oil = 54, 3.0 wt.% of catalysts, reaction time = 60 minutes, reaction temperature = 240 °C.*

Table 4.10 Weight of catalysts used in the reaction, weight of catalysts recovered after the reaction, and percent weight loss of catalysts; reaction condition: molar ratio of water to oil = 54, 3.0 wt.% of catalysts, reaction time = 60 minutes, reaction temperature = 240 °C.

Catalyst	Weight of catalyst (g)		Percent loss (%)
	Before	After	
Alumina	2.1020	2.0660	1.71
Zinc aluminate	2.1010	2.0680	1.57

Figures 4.27 and Figures 4.29 show X-ray diffraction patterns of both recycled solid oxides which did not show significant change after the fifth run in comparison with the fresh catalyst. This observation confirmed that the structure of both catalysts was stable under the reaction conditions and was not affected by the reactants.

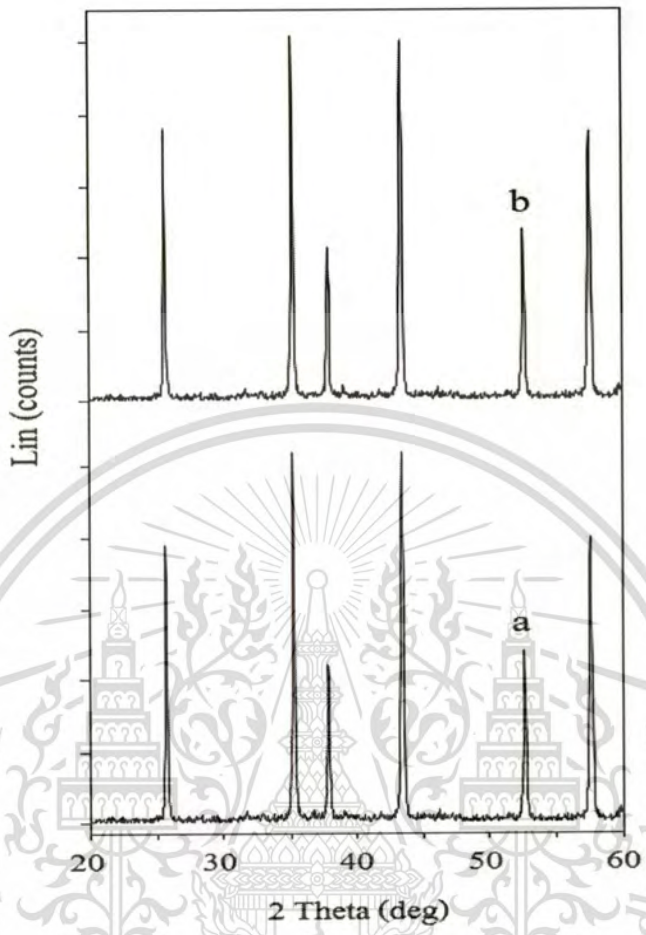

Figure 4.27 XRD diffraction patterns of alumina; (a) fresh catalyst; (b) fifth used catalyst.

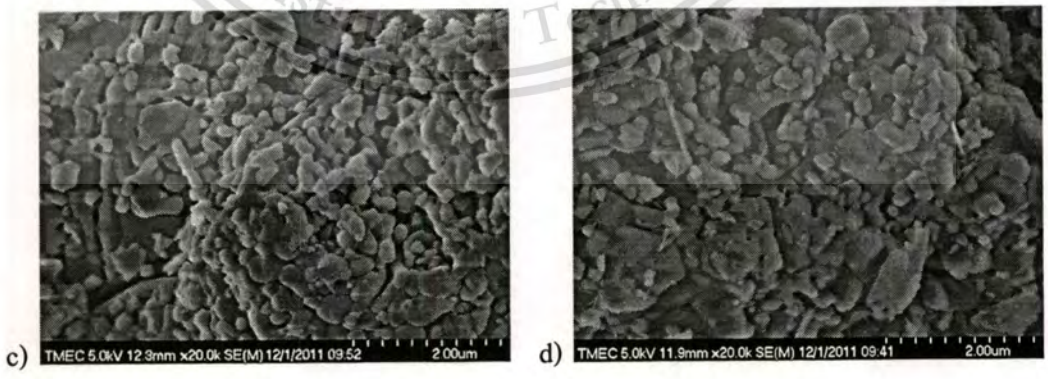

Figure 4.28 SEM images of alumina; (c) fresh catalyst; (d) fifth used catalyst.

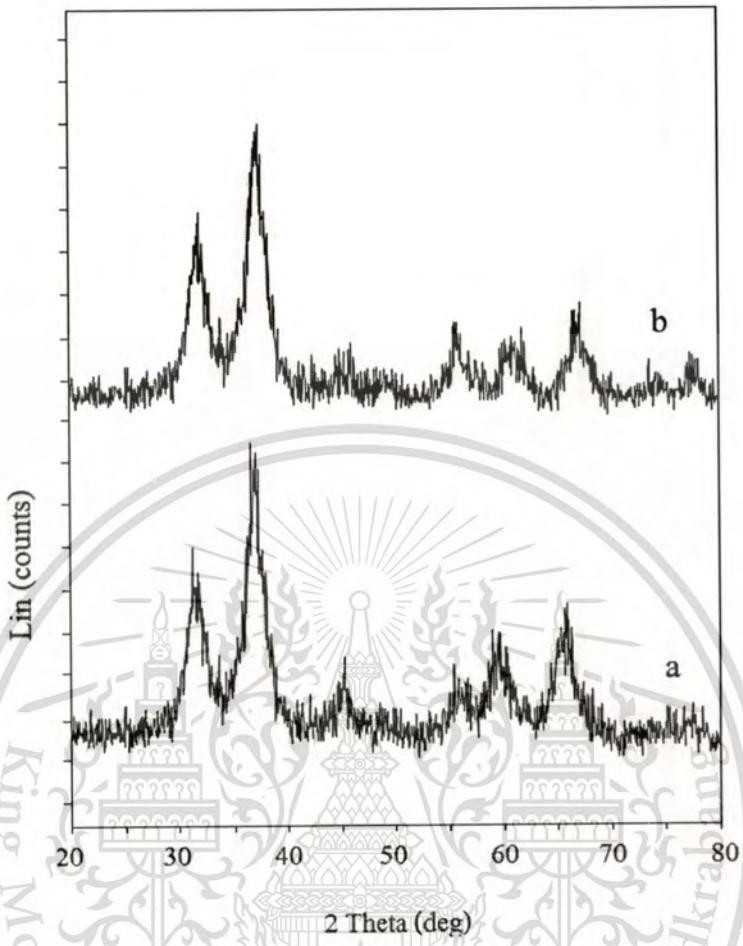

Figure 4.29 XRD diffraction patterns of zinc aluminate; (a) fresh catalyst; (b) fifth used catalyst.

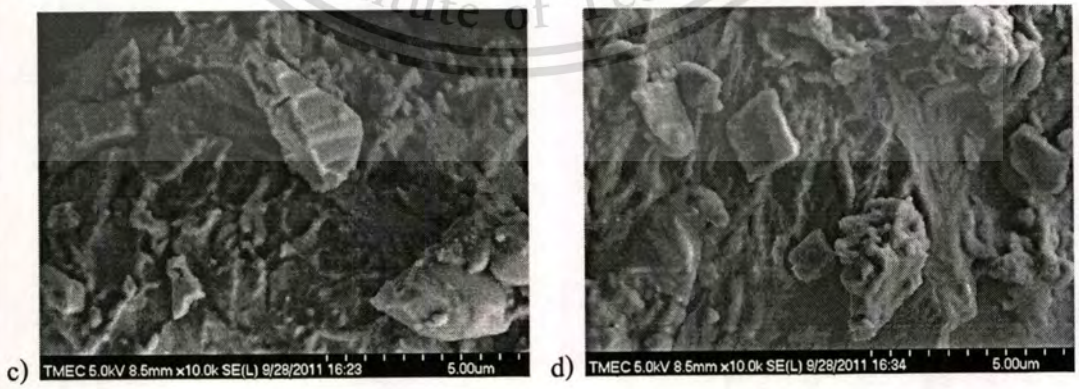

Figure 4.30 SEM images of zinc aluminate; (c) fresh catalyst; (d) fifth used catalyst.

Figures 4.28 and 4.30 presents SEM images of the fresh and fifth used catalyst of both solid oxides. Obviously, the surface morphology of these two catalysts did not change after the fifth run when compared with the fresh catalyst. The recycling of the both solid oxides (after rinsing with acetone) reveals that both catalysts can be reused at least fifth times without any loss of activity.

The AAS analysis was performed to study the leaching of zinc active phases for zinc aluminate catalysts. The result for the fresh and fifth used catalyst was depicted in Table 4.11. It is showed that the amount of Zn reaches 2.56 ppm in the water from fresh catalyst and 11.00 ppm in the water from the fifth used catalyst. V. Pugnet [5] reported that zinc aluminate is less soluble in the products of transesterification reaction than zinc oxide. With zinc aluminate catalyst, the Zn amount reaches 9 ppm in the polar phases. On the other hand, with zinc oxide powder, Zn amounts reach 259 ppm in the polar phases. However, it is well known that other solid oxides have a tendency to solubilise in the transesterification reaction medium than Zinc oxide. For example, Gryglewicz [56] reported a solubility of 1300 ppm for MgO and 350 ppm for CaO in methanol.

Table 4.11 AAS analysis of leached Zn in water; reaction condition: molar ratio of water to oil = 54, 3.0 wt.% of catalysts, reaction time = 60 minutes, reaction temperature = 240 °C.

Catalyst	Zn in water (ppm)
Fresh catalyst	2.56
Fifth used catalyst	11.00

Considering the ratio Al/Zn of catalysts before and after used in hydrolysis reaction as shown in Table 4.12, it was found that the Al/Zn ratio of 2.03 from fresh catalyst and 2.05 from the fifth used catalyst were detected. The ratio Al/Zn of the used catalyst after the fifth cycle increased slightly from that of the fresh catalyst and the activity of zinc aluminate was able to retain for the fifth run.

To conclude, zinc aluminate catalyst has little leaching effect occurs and it can be recycled up to 5 times without deactivation in the conditions used for the hydrolysis.

Table 4.12 AAS analysis of fresh and fifth used zinc aluminate; reaction condition: molar ratio of water to oil = 54, 3.0 wt.% of catalysts, reaction time = 60 minutes, reaction temperature = 240 °C.

Ratio of catalyst	Al/Zn
Fresh catalyst	2.03
Fifth used catalyst	2.05

CHAPTER 5

CONCLUSIONS AND SUGGESTIONS

5.1 Conclusions

Hydrolysis reaction of refined palm oil and water using solid oxide catalysts was investigated. Parameters that affect on percent yield of fatty acids i.e. the effect of calcinations temperature, type of catalyst, amounts of catalysts, reaction temperature, reaction time, water to oil ratio and the reused of catalysts were also investigated. The catalysts used in this study were characterized by X-ray powder diffractometer (XRD), Atomic Absorption Spectrophotometer (AAS), Gas Adsorption Analyzer (BET) and Scanning Electron Microscopy (SEM), and the products obtain from reaction were analyzed by Nuclear Magnetic Resonance Spectrometer (NMR) and High Performance Liquid Chromatography (HPLC), respectively.

The results showed that hydrolysis of refined palm oil using zinc aluminate synthesized by co-precipitation and calcining at 600 °C gave the higher catalytic activity than α-alumina (J.T.Baker) because zinc aluminate higher surface area than alumina. Zinc aluminate obtained from this work also possessed high acidity and basicity greater than alumina. Therefore, zinc aluminate catalyst is suitable catalyst in this study. The yield of fatty acids can be increased by increasing the amonts of catalysts, reaction temperature, reaction time, molar ratio of water to oil. The catalyst can be reused more than 5 cycles (with slightly decrease in yield). The reaction with the zinc aluminate catalyst achieved 100.00 % conversion and 100.00 % yield after 60 minutes under the optimized reaction condition: 240 °C, 3.0 wt.% catalyst dosage, water molar ratio of 54. It was considered as the best condition for fatty acids production in this research. Comparing with the non-catalysis reaction, less energy was needed for this condition. Furthermore, the reaction temperature and the reaction time required were significantly reduced, which gave the process the lower production costs. The relatively mild reaction conditions and high yield of fatty acids make it more viable for practical use in industry.

5.2 Suggestions

Water in hydrolysis of palm oil is a hydrophilic solvent. Oil and fat (TGs) are aprotic (hydrophobic) and are immiscible with water. Mono- and diglycerides are less hydrophobic than

the starting triglycerides and are more miscible with water. As a result, the mono-and diglycerides function as emulsifiers and enhance the mixing of the triglyceride layer with water. The miscibility of water and triglycerides can be boosted up by addition of suitable solvents, phase transfer agents and surfactants.

REFERENCES

[1] H.T. Khor, N.H. Tan and C.L. Chua, "Lipase catalysed hydrolysis of palm oil", JAOCS, Vol.63, pp. 538–540, 1986.

[2] A.N. Anozie and J.M. Dzobo, "Kinetics of the hydrolysis of palm oil and palm kernel oil", Ind. Eng. Chem. Res., Vol. 45, pp. 1604-1612, 2006.

[3] H. Hermansyah, M. Kubo, N. Shibasaki-Kitakawa and T. Yonemoto, "Mathematical model for stepwise hydrolysis of triolein using candida rugosa lipase in biphasic oil–water system", Biochemical Engineering Journal, Vol.31, pp.125-132, 2006.

[4] K.Jacobson, R.Gopinath, L.C.Meher and A. Kumar Dalai, "Solid acid catalyzed biodiesel production from waste cooking oil", Applied Catalysis B, Vol. 85, pp. 86-91, 2008.

[5] M.D.Serio, R.Tesser, L. Pengmei and E. Santacesaria, "Heterogeneous catalysts for biodiesel production", Pure and Applied Chemistry, Vol. 22, pp. 207-217, 2008.

[6] M.D.Serio, M. Cozzolino, M. Giordano, R. Tesser, P. Patrono and E. Santacesaria, "From homogeneous to heterogeneous catalysts in biodiesel production", Ind. Eng. Chem. Res., Vol. 46, pp. 6379-6384, 2007.

[7] E. Lotero, Y. Liu, D. E. Lopez, K. Suwannakarn, D. A. Bruce, and J. G. Goodwin Jr., "Synthesis of biodiesel via acid catalysis", Ind. Eng. Chem. Res., Vol. 44, pp. 5353-5363, 2005.

[8] A. Demirbas, "Comparison of transesterification methods for production of biodiesel from vegetable oils and fats", Energy Conversion and Management, Vol. 49, pp. 125-130, 2008.

[9] J. Yan and T. Lin,"Biofuels in Asia", Applied Energy, Vol. 86, pp. S1-S10, 2009.

[10] T. Thamsiriroj and J. D. Murphy, "Is it better to import palm oil from Thailand to produce biodiesel in Ireland than to produce biodiesel from indigenous Irish rapeseed", Applied Energy, Vol. 86, pp. 595-604, 2009.

[11] G.P. Hammond, S. Kallu and M.C. McManus, "Development of biofuels for the UK automotive market", Applied Energy, Vol. 85, pp. 506-515, 2008.

[12] M. Canakci, "The potential of restaurant waste lipids as biodiesel feedstocks", Bioresource Technology, Vol. 98, pp. 183-190, 2007.

[13] E. Minami and S. Saka, "Kinetics of hydrolysis and methyl esterification for biodiesel production in two-step supercritical methanol process", Fuel, Vol. 85, pp. 2479-2483, 2006.

[14] D. Kusdiana and S. Saka, "Two-Step Preparation for Catalyst-Free Biodiesel Fuel Production", Applied Biochemistry and Biotechnology, Vol. 113-116, pp. 781-791, 2004.

[15] H. Hermansyah, A. Wijanarko, M. Gozan, R. Arbianti, T. S. Utami, M. Kubo, N. Shibasaki-Kitakawa and T. Yonemoto, "Consecutive reaction model for triglyceride hydrolysis using lipase", Jurnal Teknologi, Vol. 2, pp. 151-157, 2007.

[16] I.M. Noor, M. Hasan and K. B. Ramachandran, "Effect of operating variables on the hydrolysis rate of palmoil by lipase", Process Biochemistry, Vol. 39, pp. 13-20, 2003.

[17] K. Ngaosuwan, E. Lotero, K. Suwannakarn, J.G. Goodwin, Jr. and P. Praserthdam, "Hydrolysis of triglycerides using solid acid catalysts", Process Biochemistry, Ind. Eng. Chem. Res., Vol. 48, pp. 4757-4767, 2009.

[18] J. Alander, A.C. Anderson, C. Bagge, K. bringsarve, M. Hjorth, M. Johansson, B.Granroth, S.norberg, M. Pedersen, M. Persson, B. Wennermark and M. Wennermark, "Handbook-vegetable oils and fats", Karlshamns AB, Karlshamn, Sweden, 2007.

[19] K. Hill, "Fats and oils as oleochemical raw materials", Pure and Applied Chemistry, Vol. 72, pp. 1255-1264, 2000.

[20] Hearsley, L. Bictor, V.J.Christinsen, Gene E. Hearsley, "Chemistry and life in the laboratory", Burgess Publishing Company, pp. 141-145, 1978.

[21] S.H. Hilal, S.W. Karickhoff, L.A. Carreira and B.P. Shrestha, "Estimation of carboxylic acid ester hydrolysis rate constants", QSAR. Comb. Sci., Vol. 22, pp. 917–925, 2004.

[22] V.Theodorou, K. Skobridis, A.G. Tzakosand, V. Ragoussis, "A simple method for the alkaline hydrolysis of esters", Tetrahedron Letters, Vol.48, pp. 8230-8233, 2007.

[23] M. Zayat and D. Levy, "Surface area study of high area cobalt aluminate particles prepared by the sol-gel method", Journal of Sol-Gel Science and Technology, Vol. 25, pp. 201–206, 2002.

[24] Y. Liu, Q. Jin, L. Shan, Y. Liu, W. Shen and X. Wang, "The effect of ultrasound on lipase Catalyzed hydrolysis of soy oil in solvent-free system", UltrasonicsSono chemistry, Vol. 15, pp. 402-407, 2008.

[25] R. Alenezi, G.A. Leeke, R.C.D. Santos and A.R. Khan, "Hydrolysis kinetics of sunflower oil under subcritical water conditions", Chemical Engineering Research and Design, Vol. 87, pp. 867-873, 2009.

[26] Barriga, F.J.A.S., Binns, R.A., Miller, D.J., and Herzig, "Proceedings of the ocean drilling program", Scientific Results, Vol. 193, 2002.

[27] B.C. Gates, "Catalytic Chemistry", John Wiley & Sons, pp. 371, 1992.

[28] B. Farhadiand and S. Panahandehjoo, "Spinel-type zinc aluminate ($ZnAl_2O_4$) nanoparticle sprepared by the co-precipitation method: A novel, greenand recyclable heterogeneous catalyst for the acetylation ofamines, alcohols and phenols under solvent-free conditions", Applied Catalysis A: General, Vol. 382, pp. 293-302, 2010.

[29] G. Aguilar-Rios, M. Valenzuela, P. Salas, H. Armendariz, P. Bosch, G. Del Toro, R. Silva, V. Bertin, S. Castillo, A. Ramirez-Solis and I. Schifter, "Hydrogen interactions and catalytic properties of platinumtin supported on zinc aluminate", Applied Catalysis A.: General, Vol. 127, pp. 65–75, 1995.

[30] O. S. Joo and K. D. Jung, "Stability of $ZnAl_2O_4$catalyst for reverse-water-gas-shift reaction (RWGSR)", Bull. Korean. Chem. Soc., Vol. 24, pp. 86-90, 2003.

[31] T. K. Parya, R. K. Bhattacharyya, S. Banerjee and U. B. Adhikari, "Co-precipitated $ZnAl_2O_4$ spinel precursor as potential sintering aid for pure alumina system", Ceramics International, Vol. 36, pp. 1211-1215, 2010.

[32] J. Wrzyszcz, M. Zawadzki, J. Trawczynski, H. Grabowska and W. Mista, "Some catalytic properties of hydrothermally synthesised zinc aluminate spinel", Applied Catalysis A: General, Vol. 210, pp. 236-269, 2001.

[33] M. Zawadzki, "Synthesis of nanosized and microporous zinc aluminate spinel by microwave assisted hydrothermal method (microwave–hydrothermal synthesis of $ZnAl_2O_4$)", Solid State Sciences, Vol. 8, pp. 14-18, 2006.

[34] X. Wei and D.Chen, "Synthesis and characterization of nanosized zinc aluminate spinel by sol–gel technique", Materials Letters, Vol. 60, pp. 823-827, 2006.

[35] A. R. Phani, M. Passacantando and S. Santucci, "Synthesis and characterization of zinc aluminum oxide thin films by sol–gel technique", Materials Chemistry and Physics, Vol. 68, pp. 66-71, 2001.

[36] Z. L. Wang, "Zinc oxide nanostructures: growth, properties and applications", J PHYS: CONDENSED MATTER, Vol. 16, pp. 829-858, 2004.

[37] K. Ngaosuwan, X. Mo, G. James, Jr. Goodwin and P. Praserthdam, "Effect of solvent on hydrolysis and transesterification reactions on tungstated zirconia", Applied Catalysis A: General, Vol. 380, pp. 81-86, 2010.

[38] K. Ngaosuwan, X. Mo, G. James, Jr. Goodwin and P. Praserthdam, "Reaction kinetics and mechanisms for hydrolysis and transesterification of triglycerides on tungstated zirconia", Top. Catal., Vol. 53, pp.783–794, 2010.

[39] P. S. Sreeprasanth, R. Srivastava, D. Srinivas and P. Ratnasamy, "Hydrophobic, solid acid catalysts for production of biofuels and lubricants", Applied Catalysis A: General, Vol. 314, pp. 148–159, 2006.

[40] J. K. Satyarthi, D. Srinivas and P. Ratnasamy, "Hydrolysis of vegetable oils and fats to fatty acids over solid acid catalysts", Applied Catalysis A: General, Vol. 391, pp. 437-435, 2010.

[41] S. Yan, S.O. Salley and K.Y. Simon Ng, "Simultaneous transesterification and esterification of unrefined or waste oils over ZnO-La_2O_3catalysts", Applied Catalysis A: General, Vol. 353, pp. 203–212, 2009.

[42] V. Pugnet, S. Maury, V. Coupard, A. Dandeu, AA. Quoineaud, JL. Bonneau, et al. "Stability, activity and selectivity study of a zinc aluminate heterogeneous catalyst for the transesterification of vegetable oil in batch reactor", Applied Catalysis A: General, Vol. 374, pp.71-78, 2010.

[43] R. L. Holliday, J. W. King, and G. R. List, "Hydrolysis of vegetable oils in sub and supercritical water", Ind. Eng. Chem. Res., Vol. 36, pp. 932–935, 1997.

[44] R. Sarkar, S. K. Das and G. Banerjee, "Effect of attritor milling on the densification of magnesium aluminatespinel", Ceramics International, Vol.25, pp.485-489, 1999.

[45] A. K. Anton, C. D. Alexandre, and R. Gadi, "Solid acid catalyst for biodiesel production–toward sustainable energy", Advanced Synthesis and Catalysis, Vol. 348, pp. 75-81, 2006.

[46] D. M. Alonso, R. Mariscal, R. Moreno-Tost, M. D. Z. Poves and M. L. P. Granados, "Potassium leaching during triglyceride transesterification using K/γ-Al_2O_3 catalysts", Catalysis Cominucations, Vol. 8, pp. 2074–2080, 2007.

[47] M. L. Granados, M. D. Z. Poves, D. M. Alonso, R. Mariscal, F. C. Galisteo, R. Moreno-Tost, J. Santamaria and J. L. G. Fierro, "Biodiesel from sunflower oil by using activated calcium oxide", Applied catalysis, Vol. 73, pp. 317–326, 2007.

[48] K. Masato, Y. Shin-ya, H. Jyu-sukeand T. Michito, "Heterogeneous catalysis of calcium oxide used for transesterification of soybean oil with refluxing methanol", Applied Catalysis A: General, Vol. 355, pp. 94-99, 2009.

[49] J. L. Ropero-Vega, A. Aldana-Perez, R. Gomez and M. E. Nino-Gomez, "Sulfated titania [TiO_2/SO_4^{2-}]: a very active solid acid catalyst for the esterification of free fatty acids with ethanol", Applied Catalysis A:General, Vol. 379, pp. 24-29, 2010.

[50] R. Qiu, S. Yin, X. Zhang, J. Xia, X. Xu and S. Luo, "Synthesis and structure of an air-stable cationic organobismuth complex and its use as a highly efficient catalyst for the direct diastereo selective Mannich reaction in water", Chemical Communications", Vol. 31, pp. 4759-476, 2009.

[51] J.K. Satyarthi, D. Srinivas and P. Ratnasamy, "Estimation of free fatty acid content in oils, fats, and biodiesel by ^{1}H NMR spectroscopy", Energy Fuels, Vol. 23, pp. 2273–2277, 2009.

[52] Gaita R, "A reversed phase HPLC method using evaporative light scattering detection(ELSD) for monitoring the reaction and quality of biodiesel fuels", Grace Davison discovery sciences: the application notebook, industrial 51, 2006. http://www.discoverysciences.com/WorkArea/downloadasset.aspx?id=5022

[53] H. C. Joshi, J. Toler and T. Walker, "Optimization of cottonseed oil ethanolysis to produce biodiesel high in gossypol content", Journal of the American Oil Chemists Society , Vol. 85, pp. 357-363, 2008.

[54] E. Minami, S. Saka, "Kinetics of hydrolysis and methyl esterification for biodiesel production in two-step supercritical methanol process", Fuel, Vol. 85, pp. 2479-2483, 2006.

[55] P. C. C. Faria, J. J. M. Orfao and M. F. R. Pereira, "Adsorption of anionic and cationic dyes on activated carbons with different surface chemistries", Water Research, Vol. 38, pp. 2043–2052, 2004.

[56] S. Gryglewicz, "Rapeseed oil methyl esters preparation using heterogeneous catalyst", Bioresource Technology, Vol. 70, pp. 249-253, 1999.

[57] M. Ghiaci, B. Aghabarari, A. Gil, "Production of biodiesel by esterification of natural fatty acids over modified organoclay catalysts", Fuel, Vol. 90, pp. 3382-3389, 2011.

[58] T. Witshuta, 2007, "Synthesis of biodiesel from palm oil using alkali earth metal oxides as catalysts under critical temperature and pressure", M.Sc. Thesis of Science in Petrochemicals and Hydrocarbon Chemistry school of graduate studies King Mongkut's Institute of Technology Ladkrabang.

APPENDIX

APPENDIX A

PRODUCT CALCULATION

1. Percent conversion of triglycerides calculated from HPLC chromatogram

Example 1. Determination of percent conversion of triglycerides from the hydrolysis of refined palm oil using 54:1 triglyceride/water, 3.0 % zinc aluminate at 240 °C for 30 minutes (sample 1, Figure A-1).

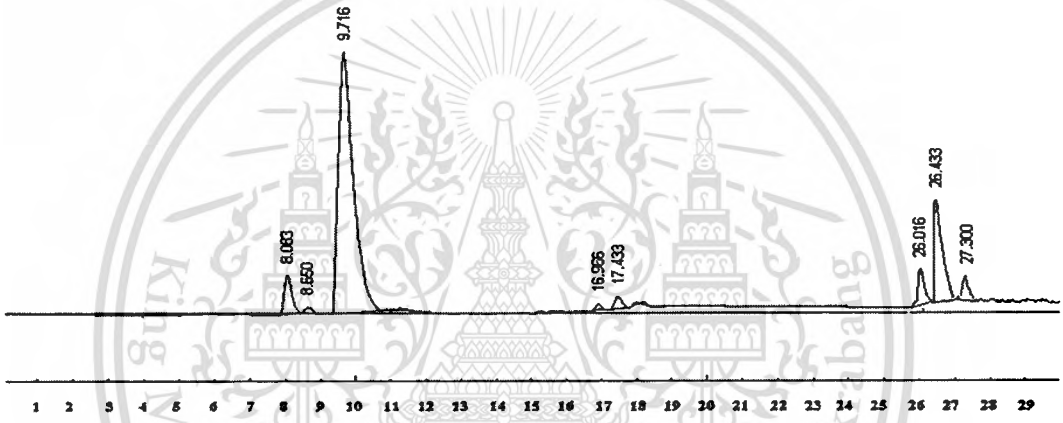

Figure A-1 HPLC chromatogram of sample 1.

Table A-1 Intensity histogram from HPLC spectrum of sample 1.

Component	Retention	Area	Area %	Units
	8.083	1120.1720	4.4982	
	8.650	181.7585	0.7299	
	9.716	15601.3550	62.6499	
	16.966	142.3525	0.5716	
	17.433	344.8590	1.3848	
	26.016	1182.7100	4.7494	
	26.433	4704.4260	18.8914	
	27.300	1101.1940	4.4220	

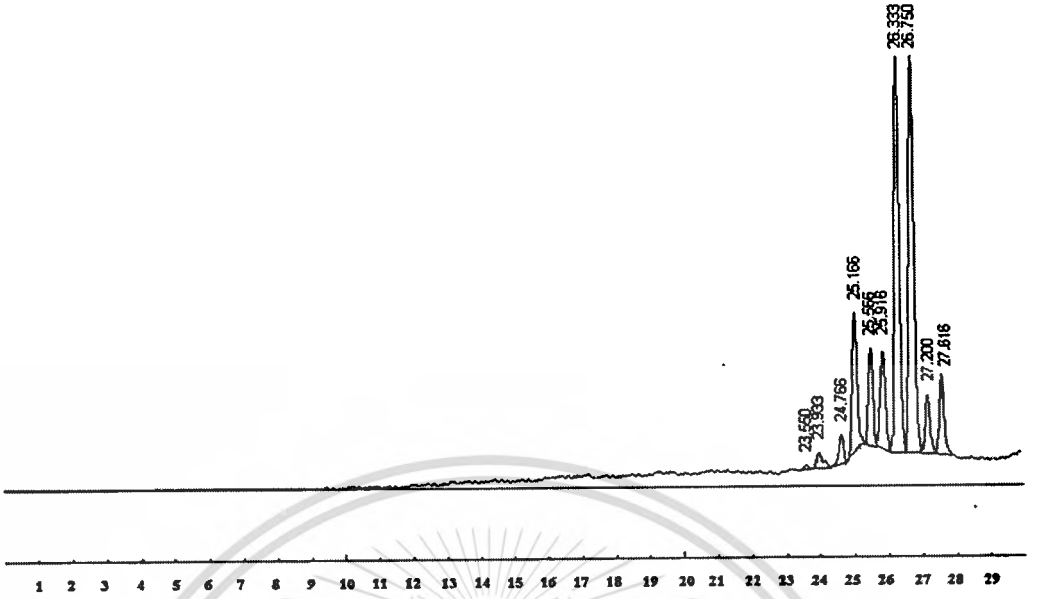

Figure A-2 HPLC chromatogram of refined palm oil.

From Figure A-2, the signals of triglycerides separated by the high performance liquid chromatography appear at the retention time between 23-28 minutes in chromatograms

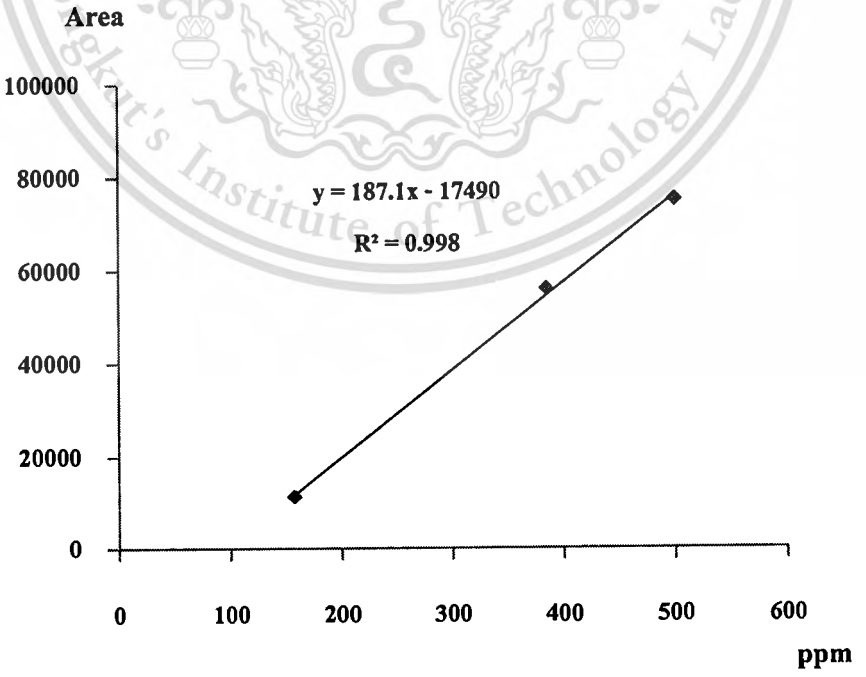

Figure A-3 Calibration curve for refined palm oil.

Table A-2 Concentration of triglycerides in sample 2 from the calibration curve.

Retention time (minutes)	Component	Area
26.016	Triglyceride	1182.7100
26.433	Triglyceride	4704.4260
27.300	Triglyceride	1101.1940
	Sum area =	7651.751
	Concentration of triglycerides =	134.347 ppm

$$\frac{\text{Concentration of triglycerides from HPLC chromatogram (g/ml)}}{\text{Concentration of product mixture used for HPLC (g/ml)}} = \frac{\text{weight of triglyceride in product mixture (g)}}{\text{weight of product mixture from reaction (g)}}$$

$$\frac{134.347\times10^{-6}\ \text{g/ml}}{0.0005\ \text{g/ml}} = \frac{A}{67}$$

$$A = \text{weight of triglyceride in product mixture (g)}$$

$$A = 18.00\ \text{g}$$

$$\%\ \text{conversion} = \frac{\text{weight of palm oil (g)} - \text{weight of triglyceride in product (g)}}{\text{weight of palm oil (g)}} \times 100$$

$$= \frac{70 - 18.00}{70} \times 100$$

$$= 74.28\%$$

2. Percent yield of fatty acids calculated from ^{1}H-NMR spectrum

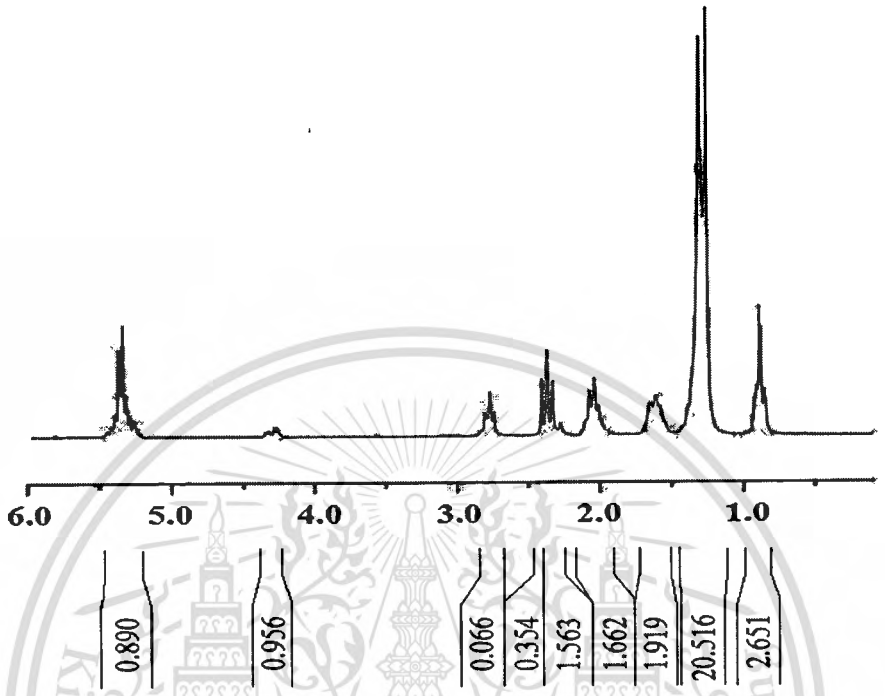

Figure A-4 ^{1}H-NMR spectrum in $CDCl_3$ of non-catalytic reaction of refined palm oil with water; *reaction condition: molar ratio of water to oil = 54, reaction time = 60 minutes, reaction temperature 240 °C* (sample 2).

The triplet peaks appear with an intensity ratio of 1:2:1. The total area corresponding to α-CH_2 of both FFA and ester can be determined by integrating the spectral region at 2.20-2.41 ppm. The area of the unmerged peak of the FFA triplet can be determined by integration of the spectral region at 2.37-2.41 ppm. The weight percentage of FFA in oil is thus

$$\text{Free fatty acids (FFA), \%} = \frac{4 \times \text{area of umerged peak of } \alpha\text{-CH}_2 \text{ of FFA}}{\text{total area of } \alpha\text{-CH}_2 \text{ of both FFA and ester}} \times 100$$

$$\text{Free fatty acids (FFA), \%} = \frac{4 \times 0.354}{(0.354+1.563)} \times 100$$

$$\text{Free fatty acids (FFA), \%} = 73.86$$

APPENDIX B

HPLC CHROMATOGRAM OF GLYCERIDES

Figure B-1 HPLC chromatogram of triglycerides.

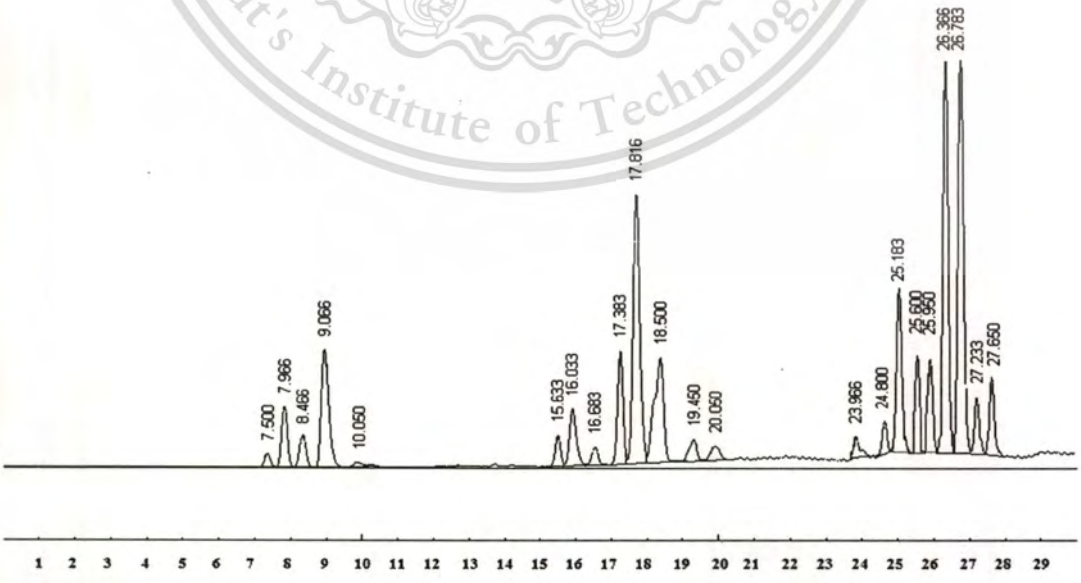

Figure B-2 HPLC chromatogram of free fatty acids, mono-, di- and triglycerides.

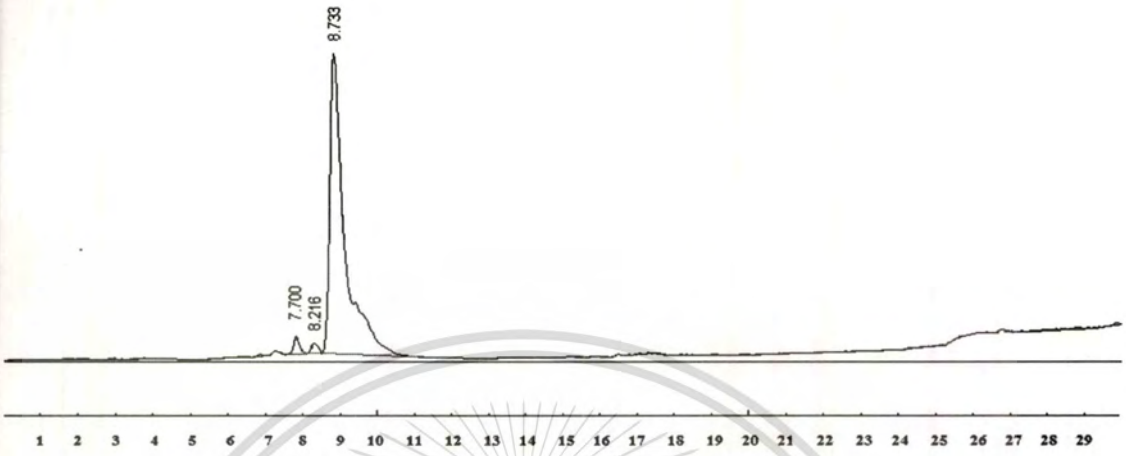

Figure B-3 HPLC chromatogram of free fatty acids.

APPENDIX C

CHARACTERIZATION DATA

1. Surface Area and BET Plot from Gas Adsorption Analyzer

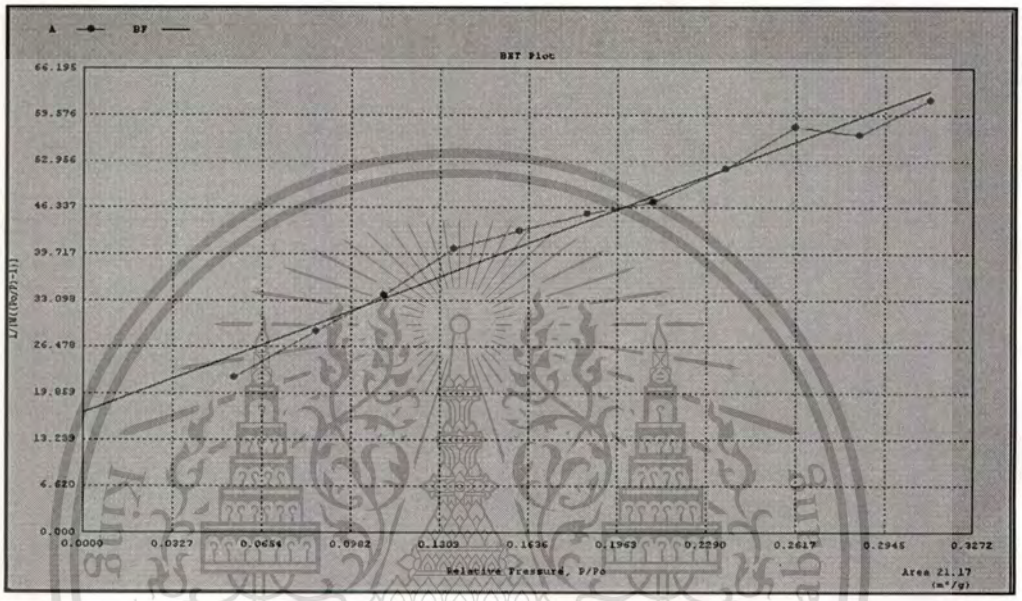

Figure C-1 BET plot of alumina calcined at 500 ^{o} C.

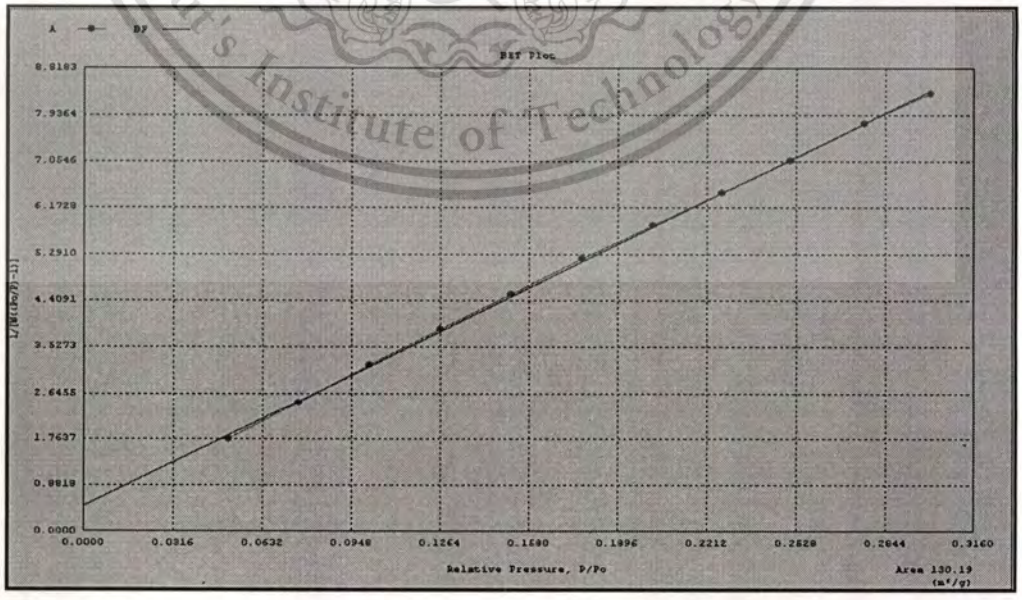

Figure C-2 BET plot of zinc aluminate calcined at 600 ^{o} C.

2. X-Ray Diffraction Patterns of catalyst

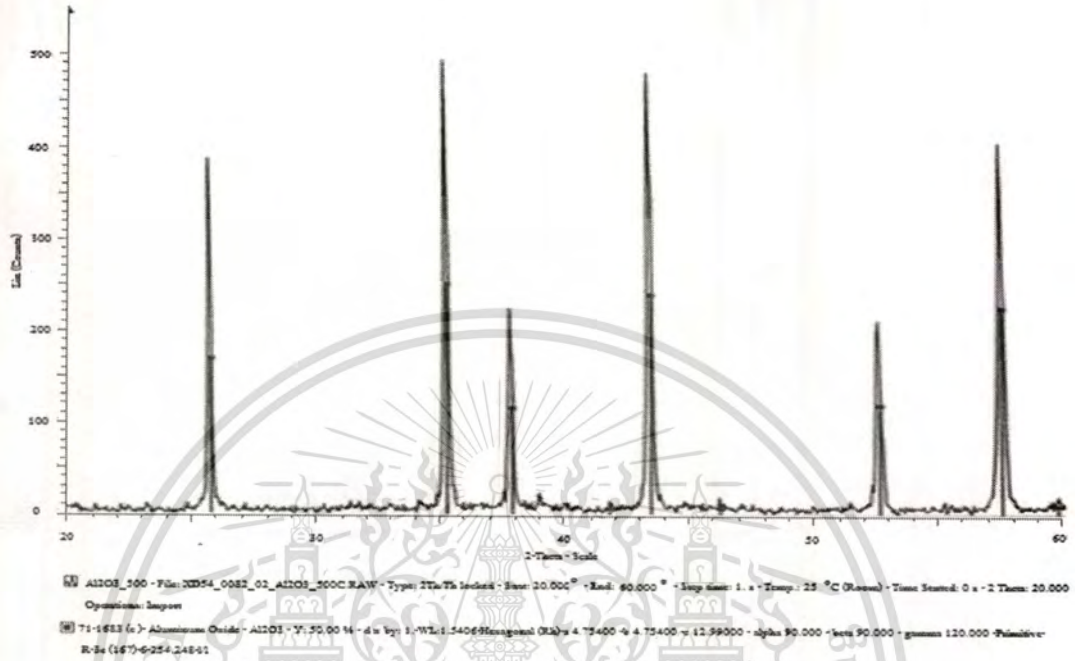

Figure C-3 XRD pattern of alumina calcined at 500 ^{o}C.

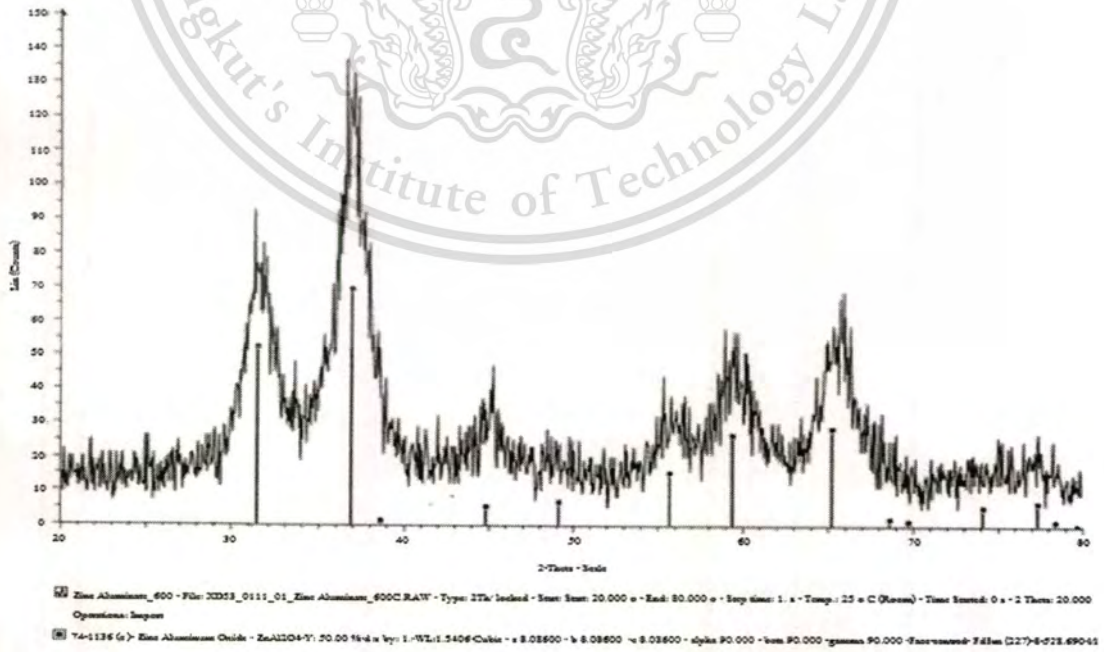

Figure C-4 XRD pattern of zinc aluminate calcined at 600 ^{o}C.

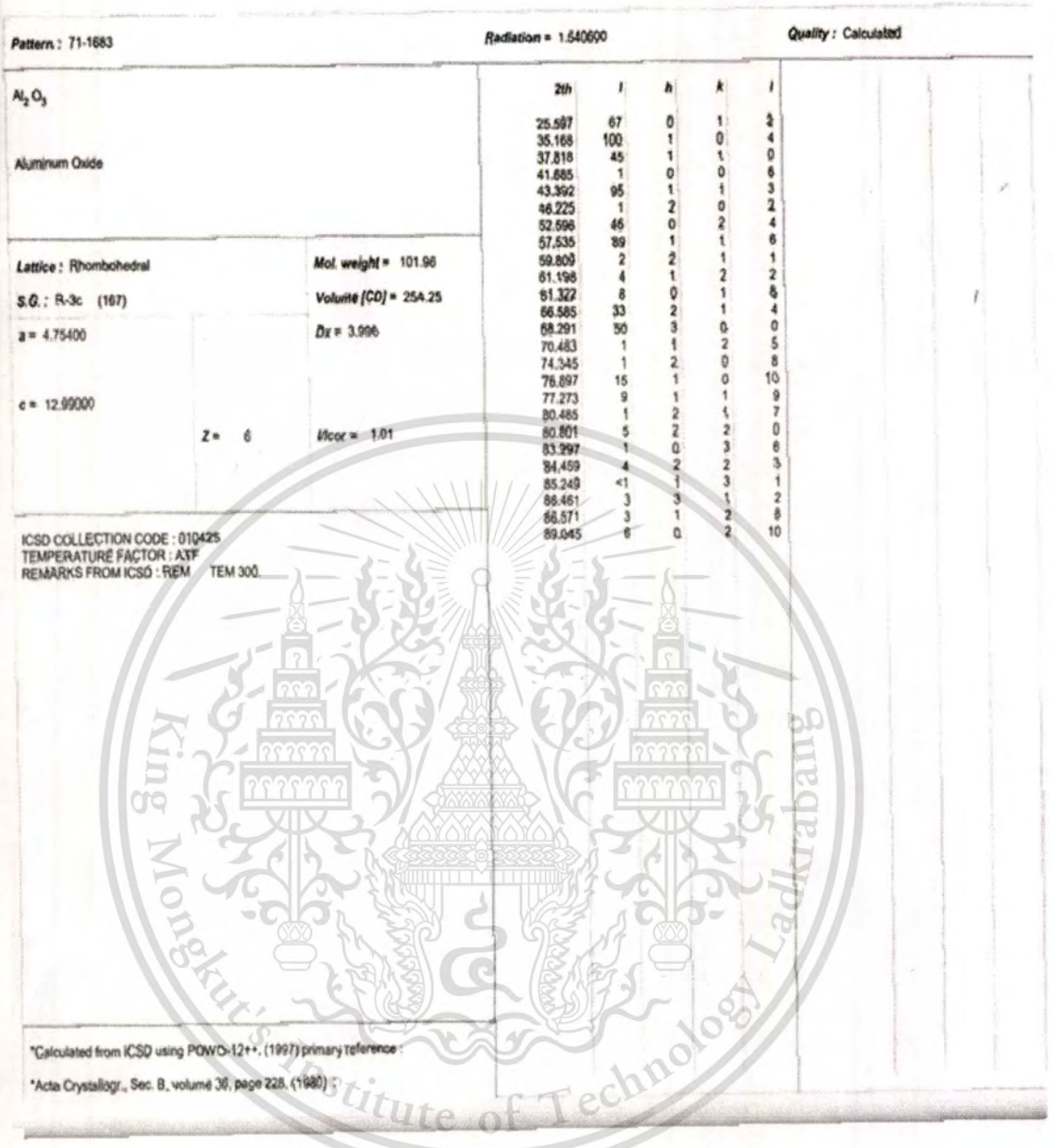

Pattern : 71-1683 Radiation = 1.540600 Quality : Calculated

Al_2O_3

Aluminum Oxide

Lattice : Rhombohedral Mol. weight = 101.96

S.G. : R-3c (167) Volume [CD] = 254.25

a = 4.75400 Dx = 3.996

c = 12.99000

Z = 6 I/Icor = 1.01

ICSD COLLECTION CODE : 010425
TEMPERATURE FACTOR : ATF
REMARKS FROM ICSD : REM TEM 300.

2th	I	h	k	l
25.587	67	0	1	2
35.168	100	1	0	4
37.818	45	1	1	0
41.685	1	0	0	6
43.392	95	1	1	3
46.225	1	2	0	2
52.596	46	0	2	4
57.535	89	1	1	6
59.809	2	2	1	1
61.198	4	1	2	2
61.322	8	0	1	8
66.585	33	2	1	4
68.291	30	3	0	0
70.483	1	1	2	5
74.345	1	2	0	8
76.897	15	1	0	10
77.273	9	1	1	9
80.485	1	2	1	7
80.801	5	2	2	0
83.297	1	0	3	6
84.459	4	2	2	3
85.249	<1	1	3	1
86.461	3	3	1	2
86.571	3	1	2	8
89.045	6	0	2	10

*Calculated from ICSD using POWD-12++, (1997) primary reference :

*Acta Crystallogr., Sec. B, volume 36, page 228, (1980) ;

Figure C-5 X-ray diffraction pattern of alumina.

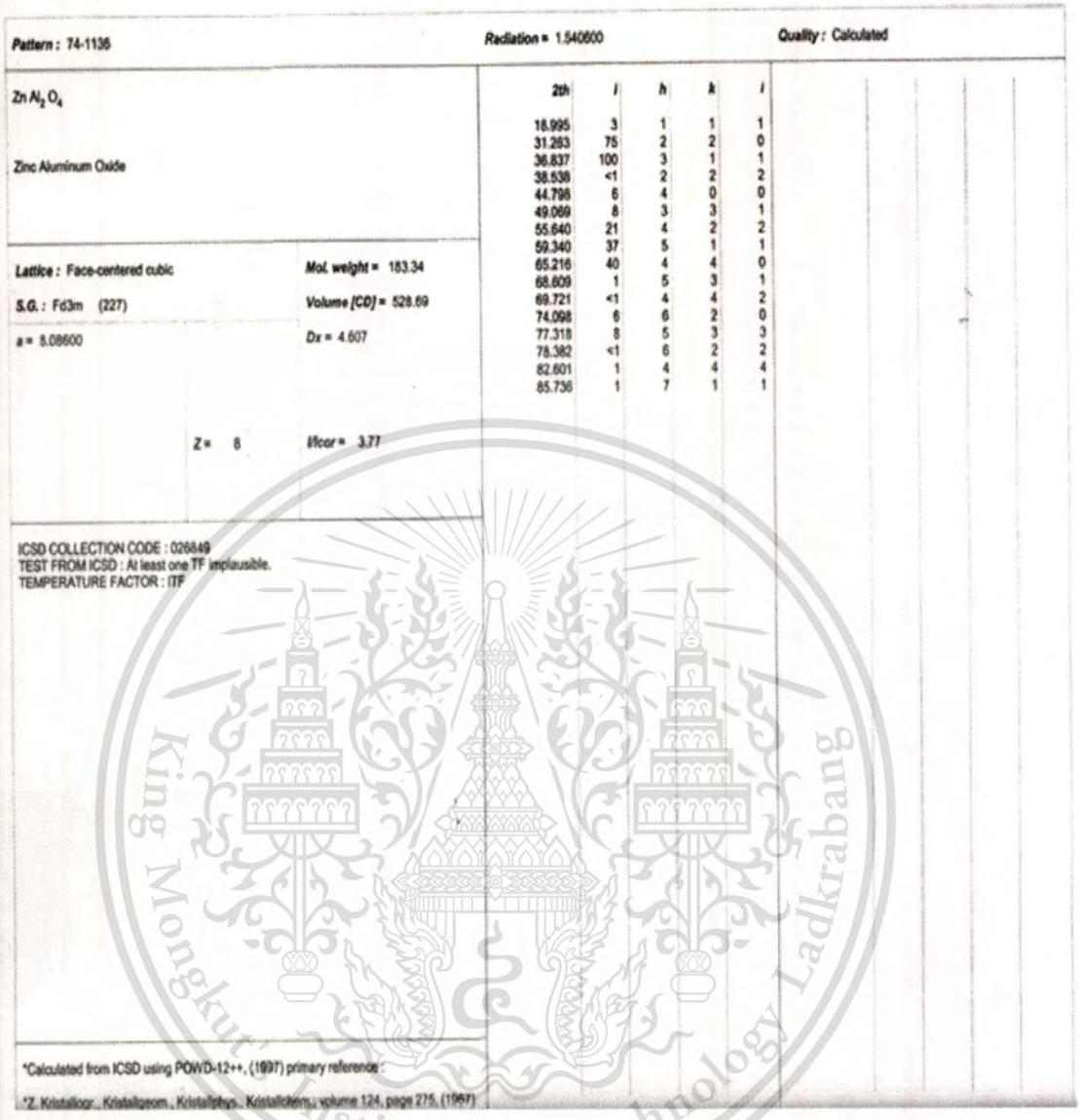

Pattern : 74-1136 Radiation = 1.540600 Quality : Calculated

$Zn Al_2 O_4$

Zinc Aluminum Oxide

Lattice : Face-centered cubic Mol. weight = 183.34

S.G. : Fd3m (227) Volume [CD] = 528.69

a = 8.08600 Dx = 4.607

Z = 8 I/Icor = 3.77

ICSD COLLECTION CODE : 026849
TEST FROM ICSD : At least one TF implausible.
TEMPERATURE FACTOR : ITF

*Calculated from ICSD using POWD-12++, (1997) primary reference :

*Z. Kristallogr., Kristallgeom., Kristallphys., Kristallchem., volume 124, page 275, (1967)

2th	I	h	k	l
18.995	3	1	1	1
31.283	75	2	2	0
36.837	100	3	1	1
38.538	<1	2	2	2
44.798	6	4	0	0
49.069	8	3	3	1
55.640	21	4	2	2
59.340	37	5	1	1
65.216	40	4	4	0
68.609	1	5	3	1
69.721	<1	4	4	2
74.098	6	6	2	0
77.318	8	5	3	3
78.382	<1	6	2	2
82.601	1	4	4	4
85.736	1	7	1	1

Figure C-6 X-ray diffraction pattern of zinc aluminate.

3. Molar ratio of zinc aluminate calculated from AAS

Preparation of sample was done by diluted digestion 0.5830 g of $ZnAl_2O_4$ in 50 ml distilled water and then diluted it for AAS analysis.

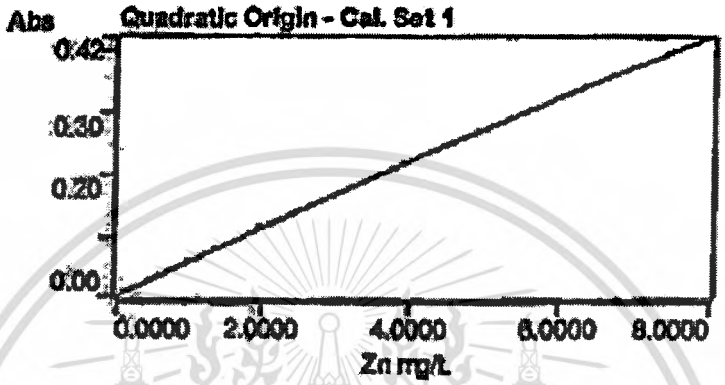

Figure C-7 Calibration curve of zinc from fresh catalyst

Curve Fit	= Quadratic Origin
Characteristic Conc	= 0.0762 mg/L
r	= 1.0000
Calculated Conc	= -0.0037 1.0137 2.0078 4.9863 4.9863
Residuals	= 0.0037 -0.0137 -0.0078 0.0137 7.9863

Abs = - 0.00059 x C x C + 0.05722 x C

check std	4.9629		0.3	0.2695
	Readings			
	0.2696	0.2703		0.2685
ZnAl2O4 1 [Dil: 700]	5.8652		0.6	0.3184
	Readings			
	0.3169	0.3159		0.3134
ZnAl2O4 2 [Dil:700]	5.7012		0.4	0.3071
	Readings			
	0.3074	0.3056		0.3081
check std	5.0117		0.4	0.2719
	Readings			
	0.2706	0.2729		0.2723

The Zn, Al concentration from calibration curve is thus

Detection limit (ppm) = s × dilution factor

(s = standard deviation of instrument "readings" in ppm.)

3.1 Zn concentration in sample1 ($ZnAl_2O_4$ 1) ; s = 5.8652, dilution factor = 700

Detection limit (ppm) = 5.8652 × 700

= 4,105.64 mg/l

From AAS analysis, the concentration of Zn is 4,105.64 mg/l from stock solution.

Stock solution 1000 ml has Zn concentration = 4,105.64 mg

Stock solution 50 ml has Zn concentration $= \frac{4{,}105.64 \text{ mg}}{1000 \text{ ml}} \times 50 \text{ ml}$

= 205.28 mg

0.583 g of sample 1 has Zn concentration = 205.28 mg

1000 g of sample 1 has Zn concentration $= \frac{205.28 \text{ mg} \times 1000 \text{ g}}{0.583 \text{ g}}$

= 352,113.21 mg/kg

Covert of mg/kg to mol/kg $= \frac{352{,}113.21 \text{ mg}}{1 \text{ kg}} \times \frac{1 \text{ g}}{1000 \text{ mg}} \times \frac{1 \text{ mol}}{MW}$

= 5.39 mol/kg

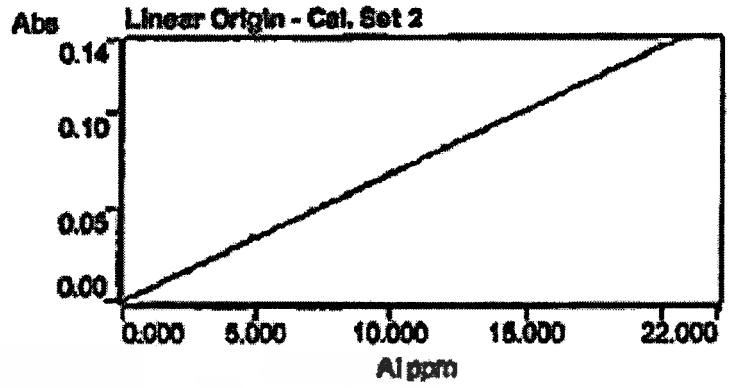

Figure C-8 Calibration curve of aluminium from fresh catalyst

QC Test: Correlation coefficient 1.0000 within 0.9950 limit
QC Test: Correlation coefficient 1.0000 within 0.9950 limit
Curve Fit = Linear Origin
Characteristic Conc = 0.652 ppm
r = 1.0000
Calculated Conc = -0.231 4.999 10.001 20.000
Residuals = 0.231 0.001 -0.001 0.000

Abs = 0.00674 x C

check std	19.988		0.6	0.1348
	Readings			
	0.1356	0.1348		0.1340
ZnAl2O4 1 [Dil 1:200]	17.249		0.1	0.1163
	Readings			
	0.1165	0.1164		0.1162
ZnAl2O4 2 [Dil 1:200]	16.353		0.3	0.1103
	Readings			
	0.1104	0.1106		0.1099
check std	19.826		0.2	0.1337
	Readings			
	0.1338	0.1340		0.1335

3.2 Al concentration in sample1 ($ZnAl_2O_4$ 1) ; s = 17.249, dilution factor = 200

Detection limit (ppm) = 17.249 × 200

= 3,449.80 mg/l

From AAS analysis, the concentration of Al is 3,449.80 mg/l from stock solution.

Stock solution 1000 ml has Al concentration = 3,449.80 mg

Stock solution 50 ml has Al concentration $= \frac{3{,}449.80\ \text{mg}}{1000\ \text{ml}} \times 50\ \text{ml}$

$= 172.49\ \text{mg}$

0.583 g of sample 1 has Al concentration = 172.49 mg

1000 g of sample 1 has Al concentration $= \frac{172.49\ \text{mg} \times 1000\ \text{g}}{0.583\ \text{g}}$

$= 295{,}866.21\ \text{mg/kg}$

Covert of mg/kg to mol/kg $= \frac{295{,}866.21\ \text{mg}}{1\ \text{kg}} \times \frac{1\ \text{g}}{1000\ \text{mg}} \times \frac{1\ \text{mol}}{\text{MW}}$

$= 10.96\ \text{mol/kg}$

3.3 Ratio of zinc aluminate

Ratio Al : Zn (sample 1) = Al/Zn

$= \frac{10.96\ \text{mol/kg}}{5.39\ \text{mol/kg}}$

$= 2.03$

AUTHOR BIOGRAPHY

First Name-Last Name	Miss Kamonwan Sitanon
Birthdate	2 February 1981
Birthplace	Phitsanulok Thailand
Address	77/47 Moo 5 Saimai Road Kwnag Saimai Khet Saimai Bangkok. 10220
Previous Cerificate/Degree	Bachelor degree of Science in Chemistry from Naresuan University, Thailand in 2005. She has been a graduated student of the program of Petrochemicals and Hydrocarbon Chemistry, Graduate School, King Mongkut's Institute of Technology Ladkrabang, since 2007